CHARACTERIZATION OF TRICHLOROETHYLENE DEGRADATION BY RECOMBINANT PHENOL HYDROXYLASE IN AN *ALCALIGENES EUTROPHUS* JMP134 DERIVATIVE

By

PATRICIA J. AYOUBI

Bachelor of Science
Oklahoma State University
Stillwater, Oklahoma
1986

Master of Science
Oklahoma State University
Stillwater, Oklahoma
1990

Submitted to the Faculty of the
Graduate College of the
Oklahoma State University
in partial fulfillment of
the requirements for
the Degree of
DOCTOR OF PHILOSOPHY
July, 1997

OKLAHOMA STATE UNIVERSITY

CHARACTERIZATION OF TRICHLOROETHYLENE DEGRADATION BY RECOMBINANT PHENOL HYDROXYLASE IN AN *ALCALIGENES EUTROPHUS* JMP134 DERIVATIVE

Thesis Approved:

Thesis Advisor

Dean of the Graduate College

ACKNOWLEDGMENTS

I wish to express my sincere appreciation to my major advisor, Dr. Alan Harker, for his intelligent supervision, constructive guidance, inspiration, and patience. My appreciation extends to my committee members Dr. Robert Burnap, Dr. Will Clarkson, Dr. Jeff Hadwiger and Dr. Robert Miller whose guidance, assistance, and encouragement were also invaluable. I also wish to extend my sincere and heartfelt gratitude to Dr. Rolf Prade for his invaluable guidance, assistance, encouragement and friendship which contributed greatly to the successful completion of this work. My appreciation extends to Dr. Gilbert John and Dr. Greg Wilber for the use of their equipment and laboratory. I would also like to thank the Department of Microbiology and Molecular Genetics for providing me with their support. And a special thanks to my coworkers, friends and fellow students for their support and sympathy, especially during the more difficult times.

I would also like to thank the Oklahoma State University Recombinant DNA/Protein Resource Facility for their support and assistance with DNA sequence analysis and synthetic oligonucleotide synthesis. A special thanks to Janet Rogers and Sueann Hudiburg for their prompt and efficient attention which enable rapid data collection and analysis.

I would also like to express my deepest appreciation to my family for their love and support. I especially thank my husband, Amjad, who always encouraged me to move forward with my education. I would also like to thank my daughter, Samia, for her incredible patience and understanding.

TABLE OF CONTENTS

LIST OF TABLES

LIST OF FIGURES

CHAPTER I

INTRODUCTION

The widespread use and application of various chemicals and synthetic compounds has resulted in extensive release of pollutants into the environment. The accidental or intended release of pollutants from industry and agriculture causes serious environmental and health problems in the United States and throughout the rest of the world. Compounds of greatest concern include herbicides, pesticides, plastics, solvents and degreasers (12). Of growing concern is the release of pollutants into soils and waters including ground water aquifers used for drinking. Various regulatory agencies, such as the Environmental Protection Agency (EPA), have designated many of these compounds as toxic and priority pollutants requiring their removal from the contaminated sites (46).

A recent survey of public ground water supplies in the United States identified and prioritized contaminants relative to their frequency of occurrence and adverse health effects. This studied revealed that approximately 200 different contaminants have been detected in the US public ground water supplies. Of these, the contaminant of the greatest concern is trichloroethylene (TCE) (52). TCE is a low molecular weight, volatile chlorinated hydrocarbon. This compound is commonly used as a solvent and degreasing agent in the drycleaning industry and semiconductor manufacturing. With a density greater

than water, TCE has been shown to migrate down through soils from disposal sites where it leaches into the water stream to contaminate the ground water aquifers (24). The degree and ubiquity of TCE contamination suggests that existing environmental conditions are not conducive for TCE degradation. In fact, the anoxic and anaerobic conditions of ground water most often result in reductive declorination of TCE and the accumulation of vinyl chloride (112). Although TCE is readily removed by air stripping or sorption, these methods merely transfer the pollutant to other media. The high cost of chemical or catalytic oxidation make biological degradation of TCE the best alternative for permanent and cost-effective removal of TCE from the environment.

Microorganisms play a major role in the degradation and mineralization of many pollutants and contaminants. The diverse habitats and metabolic capabilities of microorganisms make them excellent candidates for assisting in the degradation of pollutants. Many pollutants are degraded by bacteria, fungi and consortia of diverse microbial populations (2). While the natural biodegradative capabilities of microorganisms are diverse and can produce desirable results, the process is often much too slow to satisfy growing public health and environmental concerns. Unfortunately, many factors such as temperature, pH, oxygenation, nutrient availability, salinity, and toxicity of the compound itself have considerable effect on biodegradation rates. Further, many pollutants contain novel chemical structures which are rarely or never found in nature and are often resistant to microbial degradation. Some compounds are degraded by native microorganisms to generate metabolites more toxic than the parent substrate. This can, in some cases, result in toxicity effecting entire microbial communities (106).

The removal of natural or synthetic organic compounds from contamination sites has been accomplished through a variety of treatments

including chemical, physical or biological approaches. The ability of some microorganisms to degrade and mineralize pollutants and contaminants has resulted in extensive research to elucidate the mechanisms involved in this metabolism. Understanding the pathways may allow for the construction of novel pathways with greater substrate diversity and effectiveness against compounds previously thought to be recalcitrant. Approaches to these challenges have resulted in modifications of various microorganisms to increase the substrate range, degradation rates and improve survivability under environmental stresses. For example, a starvation promoter has been coupled with TCE and phenol degradation genes to limit the nutrients required and the biomass produced in transformation of these compounds and enhance their overall removal (64). Increased knowledge of metabolic pathways involved in biodegradation of recalcitrant compounds and their regulation may enable us to produce genetically engineered microorganisms capable of efficient degradation of novel or more complex compounds.

Alcaligenes eutrophus JMP134 is a soil bacterium with diverse metabolic capabilities. JMP134 is capable of utilizing several non-chlorinated and chlorinated aromatic compounds such as phenol, benzoate and 2,4-dichlorophenoxy acetic acid as the sole carbon source (84, 85). JMP134 is also capable of co-metabolizing TCE through a chromosomally encoded, phenol-induced phenol hydroxylase pathway. In contrast to reductive dechlorination, the oxidation of TCE by phenol hydroxylase in JMP134 results in products which are less toxic than TCE. Using Tn5 transposon mutagenesis of JMP134, AEK301 was isolated and found to be deficient in phenol metabolism and TCE degradation. The genes responsible for phenol metabolism in JMP134 were then cloned by complementation of AEK301, uncoupled from a regulatory gene and subcloned into the pMMB67EH vector. This plasmid, termed pYK3021, when

introduced back into *A. eutrophus* AEK301 resulted in constitutive phenol hydroxylase activity and TCE degradation under non-induced conditions; that is, it does not require any aromatic inducers to degrade TCE. Preliminary studies using this construct have shown a high capacity for TCE removal with limited sensitivity to TCE-mediated toxicity (49). This construct has excellent potential for use in the biological remediation of TCE-contaminated aquifers.

The purpose of this study is to characterize the degradation of TCE by constitutively expressed phenol hydroxylase in *A. eutrophus* AEK301/ pYK3021. Initially, the conditions for TCE degradation were optimized and the whole-cell rates of degradation by this construct were examined. Optimization of the conditions and establishment of a time course for TCE degradation by *A. eutrophus* AEK301/pYK3021 were conducted in small reactor vials with batch cultures. Parameters such as incubation time, reactor volume, sample volume, temperature and carbon and energy source were investigated to determine which conditions provide optimal TCE removal. Once established, TCE degradation over a period of 3 hours was examined to produce a progress curve of TCE degradation. The whole-cell kinetics of constitutive TCE degradation by AEK301/pYK3021 was determined using whole-cells in batch cultures, and assays at 5-minute intervals over 20 to 30 minutes were conducted at several different concentrations of TCE to determine the rates of TCE degradation. These rates were then be plotted as Lineweaver-Burk plots to determine the whole-cell K_s and V_{max} for TCE degradation by this construct under the conditions previously established.

DNA sequence analysis of the genes involved in TCE degradation was determined and comparisons with similar, related genes were made. From the nucleotide sequence, the deduced amino acid sequence of each putative open reading frame of the phenol degradation genes from pYK3021 was compared to

GenBank and SwissProt databases for further comparisons with homologous peptides.

Finally, the stability and overall usefulness of AEK301/pYK3021 could be improved through the formation of a stable genomic insertion of the constitutive phenol hydroxylase genes. Using a mini-Tn*5* transposon vector, the genes responsible for constitutive TCE degradation located on pYK3021 were fused at random with the AEK301 genome to generate a strain which is able to degrade TCE constitutively in the absence of any recombinant plasmid vectors. The elimination of a plasmid vector in the constitutive degradation of TCE should enhance the overall stability and usefulness of this strain.

CHAPTER II

LITERATURE REVIEW

Microbial degradation of trichloroethylene. Trichloroethylene (TCE) is a low-molecular-weight, volatile chlorinated aliphatic hydrocarbon with a density greater than H_2O. While aliphatic hydrocarbons are widespread contaminants of ground water and soil, TCE is the most frequently reported contaminant at hazardous waste cited on the National Priorities List of the US EPA (58) and it threatens or contaminates the potable water supply of many communities (60).

There are no reports of microbial growth on TCE as a sole carbon and energy source, but TCE has been found to be fortuitously degraded (co-metabolized) by organisms growing on a variety of substrates. In general, anaerobic degradation of TCE results in the formation of undesirable metabolites, such as dichloroethylene and vinyl chloride. Aerobic conditions do not appear to support the formation of such products (112). Co-metabolic conversion of TCE relies on nonspecific enzymes, usually mono- and dioxygenases to oxidize TCE, resulting in the production of an unstable epoxide intermediate that releases chlorides by spontaneous chemical decomposition. In aqueous solution under neutral or basic conditions, the TCE epoxide decomposes to form carbon monoxide and formate while glyoxylic acid and dichloroacetic acid are formed under acidic conditions (38, 66). Four major groups of TCE oxidizers have been identified: (1) aromatic compound-degrading bacteria, (2) methanotrophic microorganisms, (3) propane/propene/isoprene-oxidizers and (4) ammonia-

oxidizing bacteria. The enzymes implicated in the oxidation of TCE include phenol hydroxylase, toluene mono- and dioxygenase, methane monooxygenase, propane and propene monooxygenase and ammonia monooxygenase (Table 1). Of these, the largest and best studied group are those induced by aromatic compounds such as phenol, toluene, cresol, benzene and 2,4-D (Table 1). These enzymes tend to be rather promiscuous in their catabolism and induction schemes and often are capable of induction and subsequent degradation of numerous chloro- and methyl-substituted substrates. For example, toluene-3-monooxygenase (Tbu) from *Burkholderia* (formerly *Pseudomonas*) *pickettii* has a rather broad substrate range that includes toluene, benzene and TCE. Using a *lacZ*-gene fusion system to report gene expression, activation of the *tbu* operon was observed in response to a variety of hydrocarbons including benzene, toluene, ethylbenzene, *o*-, *m*-, and *p*-xylene, phenol, *o*-, *m*-, and *p*-cresol, benzyl alcohol, benzaldehyde and even TCE although the degree of responsiveness varied tremendously (9).

Kinetics of bacterial TCE oxidation. Most studies on the kinetics of aerobic TCE degradation have been conducted with methane- and toluene-utilizing mixed and pure cultures (26, 37, 54, 62, 74, 79, 80, 113). In fact, limited data on the kinetics of aerobic TCE degradation by phenol hydroxylases is available. The highest observed rate of toluene dioxygenase-mediated TCE removal from batch cultures of *P. putida* F1 was 1.8 nmol/min/mg total protein at a TCE concentration of 80 μM. This rate decreased rapidly with time and dropped to undetectable levels at concentrations greater than 300 μM TCE (113). In the case of toluene dioxygenase of wild type *P. putida*, TCE was removed at a maximum rate of 5.2 nmol/min/mg total protein (37). In wild type *P. putida* and *P. putida* F1, TCE removal leads to the formation of toxic oxidation products

Table1. Microbial aerobic degradation of trichloroethylene

Microorganism	Enzyme	Inducer(s)	References
Aromatic induction			
Alcaligenes eutrophus JMP134	phenol hydroxylase	phenol	48, 49
Alcaligenes eutrophus JMP134	TfdA or TfdB	2,4-dichlorophenoxyacetic acid	48, 49
Burkholderia pickettii PKO1	toluene-3-monooxygenase	toluene, benzene, ethylbenzene, cresols,xylenes, trichloroethylene	30
Pseudomonas cepacia G4	toluene 2-monooxygenase	toluene, phenol, cresol	74
Pseudomonas medocina KR1	toluene-4-monoxygenase	toluene, phenol, trichloroethylene	65
Pseudomonas putida BH	phenol hydroxylase	phenol, cresols	109, 110
Pseudomonas putida F1	toluene dioxygenase	toluene, phenol	113
Pseudomonas putida KN1	phenol hydroxylase	phenol	69
Pseudomonas putida NCIMB 11767	toluene dioxygenase	toluene, phenol, trichloroethylene	37
Pseudomonas sp. strain JS150	toluene dioxygenase	toluene	33
Pseudomonas sp. strain JS150	toluene monooxygenase	NR	44
Methanotrophs			
Methylosinus trichosporium OB3b	methane monooxygenase	methane	79, 111
Strain 46-1	methane monoxygenase	methane, methanol	58
Aliphatic induction			
Alcaligenes denitrificans	propene monooxygenase	isoprene	22
Mycobacterium vaccae JOB5	propane monooxygenase	propane	114
Xanthobacter sp strain Py2	alkene monooxygenase	propene	92
Ammonia oxidizing bacteria			
Nitrosomonas europaea	ammonia monoxygenase	ammonia	3, 91

NR Not Reported

which causes oxidation toxicity and even cell death (37, 113). Following phenol induction of toluene-2-monooxygenase, *Burkholderia cepacia* G4 cells degrade TCE at concentrations of at least 300 μM. The rate of TCE removal has been measured at 8 nmol/min/mg total protein, but Folsom *et al* note that TCE transiently inhibited its own degradation at concentrations higher than 50 μM (26). Although the methanotroph *Methylosinus trichosporium* OB3b appears to have a more sustained rate of TCE degradation activity compared to *P. putida* F1, neither strain is able to completely remove relatively low concentrations of TCE from reactor vials even after 6 hours of incubation (113). Similar to *P. putida* F1, acute toxicity was apparent at 70 μM TCE resulting in inactivity of *M. trichosporium* OB3b cells at a rate of 0.48 mg of cells inactivated per μmol of TCE converted (79).

Microbial degradation of phenol. Phenol and its derivatives are widely distributed environmental pollutants. Phenol and phenolic compounds are common constituents of effluents from many industrial processes including oil refineries, petrochemical plants, coal conversion plants and phenolic resin industries (23). Phenolic compounds can be highly toxic to microorganisms and even in low concentration can often result in the breakdown of wastewater treatment plants by the inhibition of microbial growth (56). Accordingly, phenols are frequently used as antimicrobial agents.

However, a number of microorganisms have been found to degrade phenol, including bacteria such as *Acinetobacter calcoaceticus* (70), *Alcaligenes eutrophus* (84), *Bacillus* sp. (18, 47) *Burkholderia pickettii* (53), *Pseudomonas* sp. (28, 33, 40, 44, 71, 100, 119) and yeasts such as *Candida tropicalis* (73) and *Trichosporon cutaneum* (72) (Table 2). In oxygenated environments, the first step in phenol metabolism is a phenol hydroxylase-catalyzed hydroxylation to catechol.

Table 2. Microbial degradation of phenol.

Microorganism	Gene(s)	Enzyme	Pathway	References
Single-component enzymes				
Bacillus stearothermophilus BR219	*pheA*	phenol hydroxylase	*meta-* cleavage	47
Burkholderia pickettii PKO1	*tbuD*	phenol hydroxylase	*meta-* cleavage	30
Pseudomonas sp EST1001 (pEST1226)	*pheA*	phenol-2-monooxygenase	*ortho-* cleavage	78
Trichosporon cutaneum	*phyA*	phenol hydroxylase	*ortho-* cleavage	45
Multi-component enzymes				
Acinetobacter calcoaceticus NCIB 8250	*mopKLMNOP*	phenol hydroxylase	*ortho-* cleavage	20
Pseudomonas putida BH	*pheA1A2A3A4A5A6*	phenol hydroxylase	*meta-* cleavage	109, 110
Pseudomonas putida H (pPGH1)	*ph1ABCDEF*	phenol hydroxylase	*meta-* cleavage	40
Pseudomonas putida KN1	NR	phenol hydroxylase	*meta-* cleavage	69
Pseudomonas putida P35X	*phhKLMNOP*	phenol hydroxylase	*meta-* cleavage	76
Pseudomonas sp. CF600 (pVI150)	*dmpKLMNOP*	phenol hydroxylase	*meta-* cleavage	77
Pseudomonas mendocina KR1	*tmoABCDEF*	toluene-4-monooxygenase	*ortho-* cleavage	116
Pseudomonas putida F1	*todABCDE*	toluene dioxygenase	*meta-* cleavage	105
Sequence not determined				
Bacillus stearothermophilus FDTP-3	phenol hydroxylase	phenol hydroxylase	*meta-* cleavage	18
Candida tropicalis	NR	NR	*ortho-* cleavage	73
Pseudomonas cepacia G4	NR	toluene-2-monooxygenase	*meta-* cleavage	97
Pseudomonas putida MCIMB 11767	NR	toluene dioxygenase	*meta-* cleavage	37

NR Not Reported

These enzymes incorporate one atom of molecular oxygen into the aromatic phenol substrate while the second oxygen atom is reduced to H_2O by an appropriate electron donor such as NAD(P)H or $FADH_2$. Catechol is a substrate for ring-cleavage enzymes following modified *ortho*-cleavage or *meta*-cleavage pathways and these products enter into central metabolism (Figure 1). Most phenol-degrading bacteria metabolize catechol through the *meta*-cleavage pathway.

Phenol hydroxylase. Two different types of phenol hydroxylases have been identified. Single-chain flavoproteins with phenol hydroxylase activity have been isolated and characterized from *Trichosporon cutaneum* (PhyA) (45), *Pseudomonas* sp. EST1001 (PheA) (78) and *Pseudomonas pickettii* PKO1 (TbuD) (53). These bright-yellow flavoproteins have molecular weights ranging from 70 to 75 kDal, appear to exist as dimers in their functional form and contain 2 mol of FAD per mol of enzyme. In addition, each require NADPH as an electron donor in the oxidation of phenol (53). Another single-chain phenol hydroxylase has been isolated and characterized from *Bacillus stearothermophilus* BR219 (PheA) (47). This 43 kDa protein appears to bind FAD and demonstrates an NADH rather than NADPH cofactor requirement.

In contrast, numerous multicomponent enzymes with phenol hydroxylase activity have been isolated and characterized. The first multicomponent phenol hydroxylase to be sequenced was isolated from *Pseudomonas* sp. CF600 where it is encoded on a plasmid designated pVI150. This enzyme consists of six polypeptides ranging in size from 10 to 58 kDal and is encoded by six open reading frames arranged in an operon on a 5.5 kb DNA fragment (77). Various types of experimental evidence indicate that this enzyme consists of three protein components: a hetero-dimeric ($(\alpha\beta\gamma)_2$) oxygenase component containing nonheme

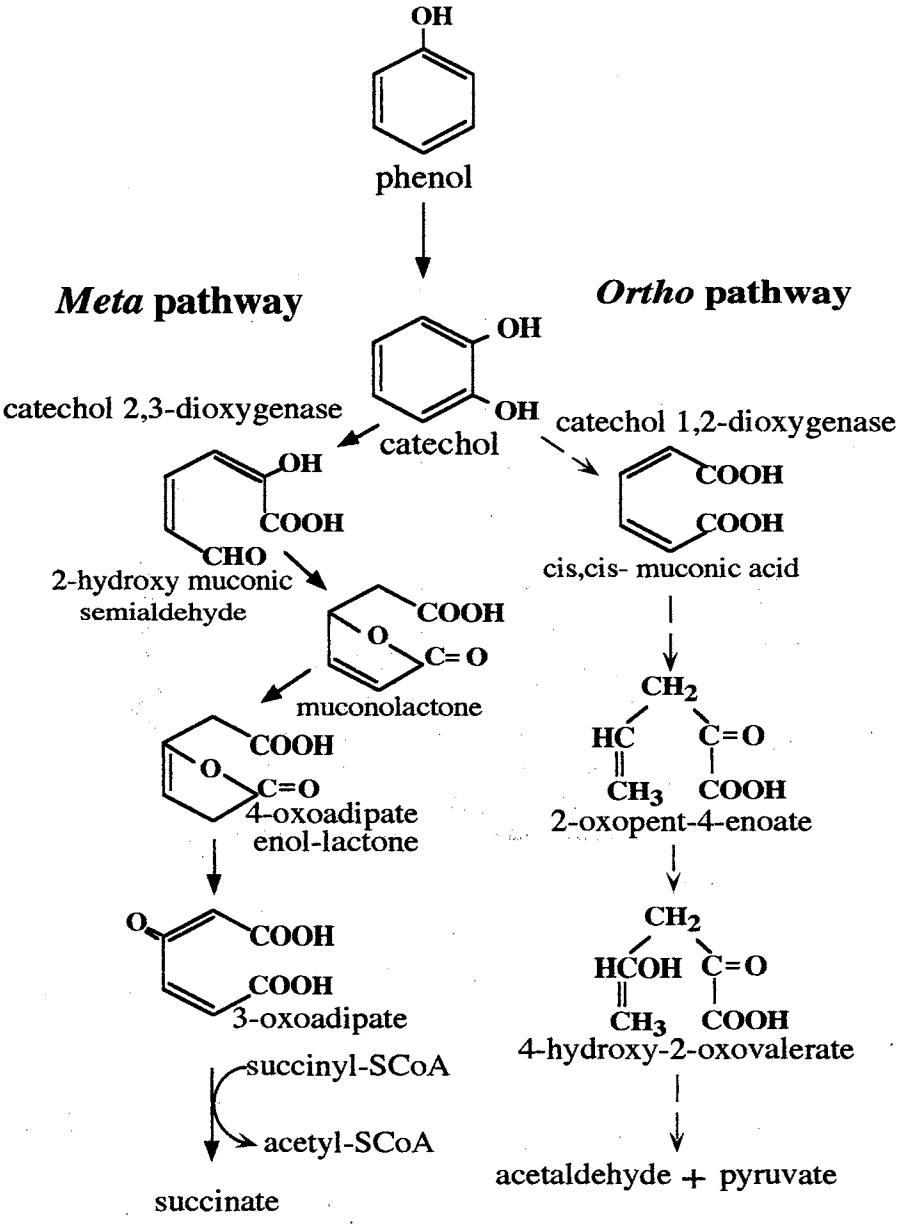

Figure 1. Ortho- and meta- pathways of catechol ring-cleavage by bacteria.

iron (encoded by *dpm*LNO), a monomeric FAD dependent reductase component (encoded by *dpm*P), and a monomeric component associated with no cofactors (encoded by *dpm*M). This arrangement is very similar to that of the well characterized binuclear iron center-containing methane monooxygenase (57). The reductase component is an FAD flavoprotein that contains a ferredoxin-type [Fe_2-S_2] center. Further, *in vitro* studies have shown the reductase component of this enzyme requires NADH as an electron donor in the hydroxylation of phenol (77, 87, 103). The protein encoded by *dmpM* (DmpM) is an accessory protein which interacts directly with the reductase and oxygenase components and is required for optimal turnover of the hydroxylase. The first open reading frame of this operon encodes for a 10.5 kDal gene product, DmpK, which is involved in an iron-dependent assembly of active phenol hydroxylase. Powlowski *et al.* (87) suggested that DmpK plays a role in post-translational incorporation of iron into the apo-oxygenase. In addition, two more open reading frames within the same operon exist downstream from the phenol hydroxylase structural genes. One (*dmpB*) encodes catechol-2,3-dioxygenase, another (*dmpQ*) encodes a ferredoxin-like protein which is probably involved in reactivation of catechol-2,3-dioxygenase, and both are required in meta-cleavage of the catechol product from phenol hydroxylase (76, 103). The later genes are not required for phenol hydroxylase activity but are required for growth on phenol as a sole carbon source.

Since the characterization of this multicomponent phenol hydroxylase, four other multicomponent phenol hydroxylase nucleotide sequences have been reported (20, 40, 76, 110). In each case, the phenol hydroxylase consists of six proteins arranged within an operon and shows high homology to the enzymes encoded by pVI150 of *Pseudomonas* sp. CF600. In addition, downstream from the phenol hydroxylase genes but within the same operon, exist two more open

reading frames which are homologous to *dmpB* and *dmpQ* and are required for *meta*-cleavage of catechol. Even the relative order of all eight homologues of these operons is conserved between these strains. A notable exception to this arrangement is *Acinetobacter calcoaceticus* NCIB 8250 in which catechol follows an ortho-cleavage pathway. In this case, genes homologous to *dmpB* and *dmpQ* are notably absent but a seventh and final open reading frame of the phenol hydroxylase operon encoding catechol-1,2-dioxygenase (20) is present. The sequences of these characterized multicomponent phenol hydroxylases show little homology to the characterized single component phenol hydroxylases.

Microbial degradation of toluene. Bacterial oxidation of toluene is catalyzed by at least five distinctly different pathways whose products are shown in Figure 2. Based on the currently available biochemical and sequence data of these complexes, these enzymes can be divided into three distinct groups (Table 3). One of these enzyme groups includes toluene dioxygenases. Three toluene dioxygenase complexes have been reported. The DNA sequence analysis of toluene dioxygenase from *Pseudomonas putida* F1 (termed Tod) revealed that it is composed of four distinct peptides whose genes are clustered together in a single operon. Tod catalyses the incorporation of both atoms of oxygen from the same molecule of O_2 into toluene to produce (+)-*cis*-1(S),2(R)-dihydroxylcyclohexa3,5-diene. Similar to phenol hydroxylases, this enzyme consists of three protein components, however several differences exist. Tod is composed of (1) a monomeric FAD-dependent flavoprotein reductase component (TodA) which utilizes NADH as an electron donor but, in contrast to the reductase component of phenol hydroxylase, lacks an iron or iron-sulfur cluster, (2) a monomeric ferredoxin-like peptide (TodB) which contains a Rieske-type [Fe_2-S_2] cluster and (3) a terminal oxygenase component which also contains a Rieske-type [Fe_2-S_2]

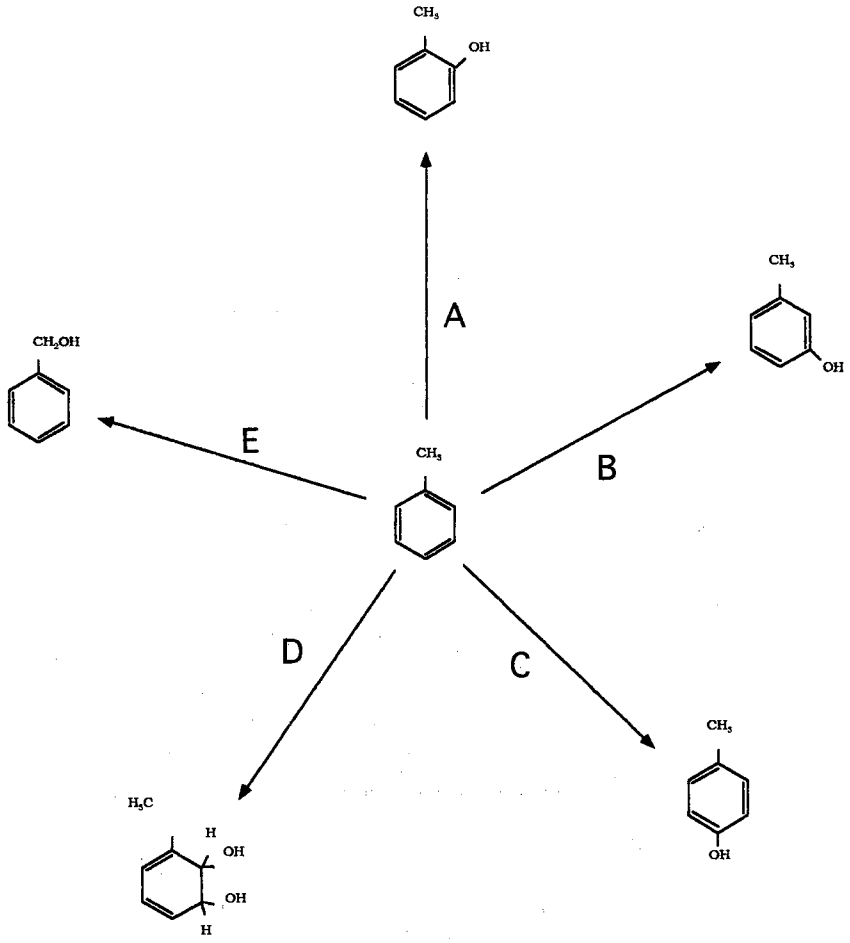

Figure 2. Pathway diversity of bacterial oxidation of toluene. (A) toluene-2-monooxygenase from *Burkholderia cepacia* G4 (97), (B) toluene-3-monooxygenase from *B. pickettii* PKO1 (8), (C) toluene-4-monooxygenase from *Pseudomonas mendocina* KR1 (119), (D) toluene dioxygenase from *P. putida* F1 (113) and (E) xylene monooxygenase from *P. putida* mt-2 (117).

Table 3. Microbial degradation of toluene

Microorganism	Gene(s)	Enzyme	Pathway	References
Burkholderia cepacia G4	NR	toluene-2-monooxygenase	NR	97
Pseudomonas sp. strain JS150	*tbmABCDEF*	toluene/benzene-2-monooxygenase	*ortho* - and *meta* -cleavage	44
Burkholderia pickettii PKO1	*tbuA1UBVA2C*	toluene-3-monooxygenase	*meta* -cleavage	8
Pseudomonas mendocina KR1	*tmoABCDEF*	toluene-4-monooxygenase	*ortho* -cleavage	118, 119
Pseudomonas putida F1	*todABC1C2*	toluene dioxygenase	*meta* -cleavage	113
Pseudomonas putida NCIMB 11767	NR	toluene dioxygenase	*meta* -cleavage	37
Pseudomonas sp. strain JS150	NR	toluene dioxygenase	NR	33
Pseudomonas putida mt-2 (pWWO)	*xylMA*	xylene monooxygenase	*meta* -cleavage	117

NR not reported

cluster in an $\alpha_2\beta_2$ subunit conformation (encoded by *tod*C1 and *tod*C2, respectively) (43). A protein component homologous to the accessory proteins found in phenol hydroxylases (e.g. DmpM) has not been identified in Tod. A second group of toluene oxygenases includes xylene monooxygenase from *Pseudomonas putida* mt-2 (pWWO) which catalyses the monooxidation of the methyl substituent of toluene and xylenes rather than the aromatic ring (108). This enzyme is a member of the iron-containing integral membrane proteins, consists of two peptide components (XylM and XylA) and bears little resemblance to other known toluene oxidases or phenol hydroxylases (96).

A third group of toluene oxidizing enzymes consists of toluene monooxygenases. As a group, these soluble enzyme complexes catalyze hydroxylation of the toluene aromatic ring to form cresols. Three different toluene monooxygenases have been characterized. These include toluene-2-monooxygenase (T2MO) (97), toluene-3-monooxygenase (Tbu) (30) and toluene-4-monooxygenase (Tmo) (116) which produce *o*-cresol, *m*-cresol and *p*-cresol, respectively. The first toluene monooxygenase to be sequenced was Tmo isolated from *Pseudomonas mendocina* KR1 (119). This enzyme is encoded by six tightly clustered open reading frames arranged within an operon on a 4.8 kb DNA fragment (118, 119). On the basis of deduced amino acid sequence determination and database comparisons coupled with extensive biochemical analysis, toluene-4-monooxygenase (Tmo) has been characterized as a unique four-component oxygenase (86, 119). These components are as follows: (1) hetero-dimeric ($(\alpha\beta\varepsilon)_2$) hydroxylase component (encoded by *tmoABE*) containing nonheme iron, (2) a monomeric effector protein (encoded by *tmoD*) associated with no known cofactors or metals, (3) a ferredoxin component containing a Rieske-type [Fe_2-S_2] center (encoded by *tmoC*), and (4) an NADH dependent flavoprotein containing a ferredoxin [Fe_2-S_2] center (encoded by *tmoF*). A

comparison between this novel composite structure and other oxygenases reflects a combination of elements from multicomponent phenol hydroxylases, toluene dioxygenases and soluble methane monooxygenase complex (Mmo) (57).

More recently, the nucleotide sequence of the genes encoding Tbu from *Burkholderia pickettii* PKO1 has been determined (8). Again, this enzyme is encoded by six tightly clustered genes arranged within a single operon. Database comparisons of the deduced amino acid sequences from toluene-3-monooxygenase (Tbu) revealed significant homology to Tmo. In addition, comparisons of the open reading frames from the *tmo* and *tbu* operons reveal a conservation in the gene number and the relative gene order. Biochemical studies of toluene-2-monooxygenase from *Burkholderia* (formerly *Pseudomonas*) *cepacia* G4 have determined it is composed of three components which are similar in function to the components of Tmo with the notable absence of a fourth ferredoxin-like component. However, in the absence of nucleotide sequence data, the existence of such a subunit cannot be excluded. A comparison of the deduced composition of representative phenol hydroxylases, toluene oxygenases and soluble methane monooxygenase is provided in Figure 3.

Transcriptional regulation of phenol and toluene metabolism. Examination of the promoter regions of several characterized multicomponent phenol hydroxylase operons (*dmp*, *mop*, *phe*, *phh*, and *phl*) indicates transcription from a σ^{54} RNA polymerase-dependent promoter sharing sequence similarity with the σ^{54} consensus promoter sequence. In each case, transcription of the phenol hydroxylase operon is regulated by a phenol-inducible transcriptional activator located in divergent orientation immediately upstream from the regulated operon. These transcriptional activators belong to the NtrC-family of transcriptional activators (99), are constitutively expressed at low levels

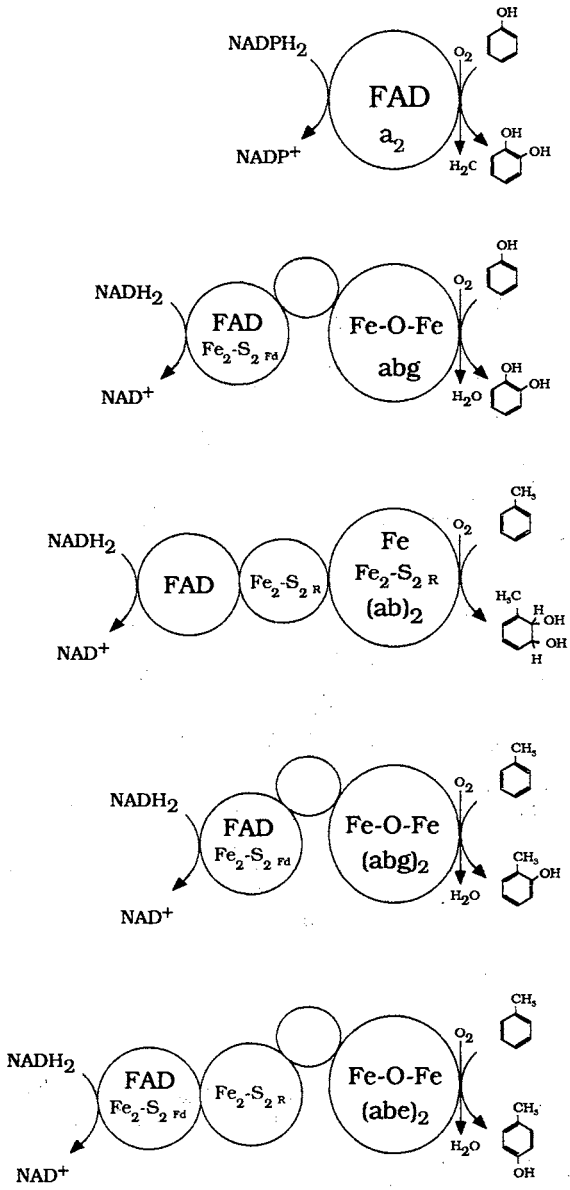

phenol hydroxylase (Phy)
(*T. cutaneum*) (45)

phenol hydroxylase (Dmp)
(*Pseudomonas* CF600) (77)

toluene dioxygenase (Tod)
(*Pseudomonas putida* F1) (120))

toluene-2-monooxygenase (T2MO)
(*Burkholderia cepacia* G4) (97)

toluene-4-monooxygenase (Tmo)
(*Pseudomonas mendocina* KR1) (119)

Figure 3. Deduced composition of representative hydroxylating mono- and di-oxygenases involved in microbial metabolism of aromatic compounds. (Fd) denotes ferredoxin-type [Fe_2-S_2] center. (R) denotes Rieske-type [Fe_2-S_2] center.

from a separate promoter and are self modulated by the presence of phenol to allow expression of the catabolic enzymes only when substrate is present (68, 75, 95, 101, 109). Expression of the toluene-3-monooxygenase operon (*tbuA1UBVA2C*) is activated by a similar regulator, termed TbuR, in the presence of toluene and other inducing compounds. In contrast, the TbuT coding region is located downstream of the catabolic genes and within the same operon. The *tbuT* gene is driven by read-through transcription from the σ^{54}-dependent *tbu* promoter located upstream from the catabolic genes. Basal levels of expression from the *tbu* promoter appear to promote *tbuT* read-through transcription and expression of low levels of TbuT in the absence of inducing substrate (9). When an appropriate inducing compound (or effector) is present, transcription of the entire *tbu* operon (including *tbuT*) is elevated as long as effector is present. A diagram of the genetic organization of these operons and their respective transcriptional activators is provided in Figure 4.

Transcription by σ^{54} dependent RNA polymerase is regulated by a distinct class of positive activators. The transcription of these regulators is self-modulated in response to environmental or metabolic signals. This group of activators regulate a variety of physiological processes including nitrogen assimilation and fixation, hydrogen oxidation, alginate utilization, dicarboxylic acid transport, pilus formation and degradation of aromatic compounds. One common feature of all these processes is that none are strictly essential for cell survival. The σ^{54} dependent regulators usually exert their regulatory effect 100 to 200 bp or more upstream from promoters they regulate most often through binding to a conserved nucleotide sequence composed of perfect or imperfect inverted repeats within this region. Environmental or metabolic signals (which can be accomplished through phosphorylation, protein:protein interactions or direct effector interaction with the DNA bound regulator) result in modulation of

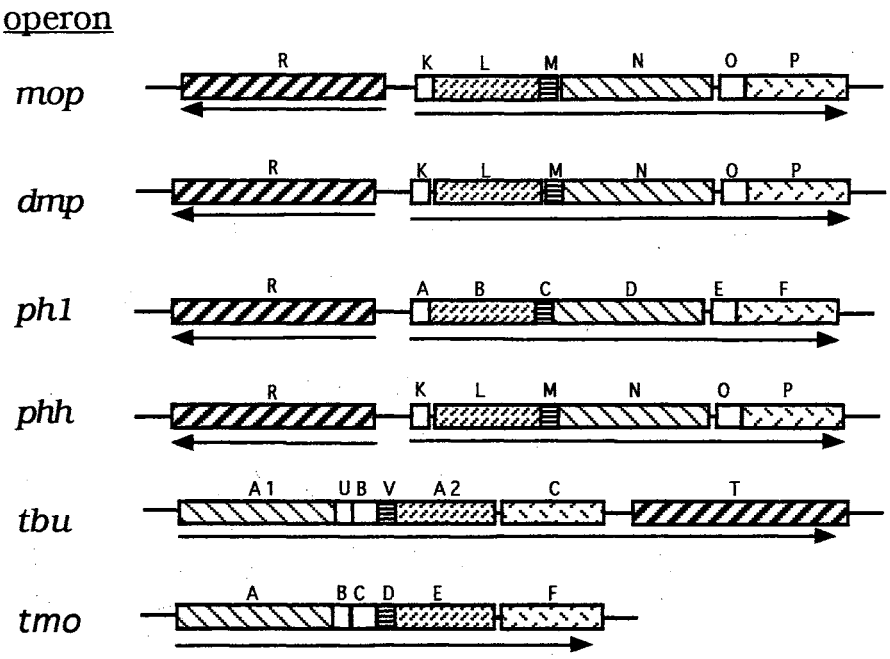

Figure 4. Genetic organization of representative phenol and toluene degradation genes and their respective transcription activators. The operon designations are as follows: *mop*, phenol hydroxylase (20); *dmp*, phenol hydroxylase (99); *phl*, phenol hydroxylase (68); *phh*, phenol hydroxylase (75); *tbu*, toluene-3-monooxygenase (9) and *tmo*, toluene-4-monooxygenase (119). Homologous genes common to each operon are indicated by similar shading and the deduced peptide functions are as follows: (▨), oxygenase component; (▤), effector/activator peptide; (▧), oxygenase component; (▨), oxidoreductase component; (▨), transcriptional activator.

the regulator to an active form. The DNA bound activator protein contacts the promoter bound inactive σ^{54}-RNA polymerase to form a loop of the intervening DNA. In some cases, loop formation appears to be facilitated by integration host factor (IHF). In a still unclear mechanism, the activated regulator leads to ATP hydrolysis which provides the energy required for activation of σ^{54}-RNA polymerase to form open transcriptional complexes. Transcription is then initiated from a -24/-12 promoter that differs considerably from the more typical -35/-10 type of promoters recognized by σ^{70}-RNA polymerase. This alternate promoter is defined by conserved -24 GG motif and -12 GC or -12 GG motif in the consensus sequence of TGGCAC-N5-TTGC upstream from the transcriptional start site (67, 98).

The σ^{54}-dependent regulator proteins are composed of three functional domains. These domains are involved in signal reception, σ^{54}-RNA polymerase activation and DNA binding. Each domain is separated by linkers which vary in length. The COOH-terminal domain is the shortest and contains a helix-turn-helix DNA-binding motif typical of those found in other transcriptional activators and repressors. The central activation domain is about 240 amino acids long and is highly conserved among this class of transcription regulators. The activation domain can be subdivided into functional regions which include motifs implicated in ATP binding and hydrolysis. The amino-terminal signal reception domain is the least conserved domain in the entire family of σ^{54}-dependent regulators. However, homologies of aligned signal domains appear to fall into subgroups which reflect the mechanisms by which activation is modulated (i.e. phosphorylation, protein:protein interactions or direct effector interaction). Those which are activated directly by the effector include those genes involved in degradation of aromatic compounds such as multicomponent phenol hydroxylase and toluene-3-monooxygenase. These regulators are activated directly by their

respective aromatic substrates, some intermediates and/or structural analogues (9, 75, 95, 101).

At least in the case of DmpR, direct binding of the effector molecule with the activator protein appears to stimulate ATPase activity and subsequent activation of transcription (102). Thus, the specificity of effector recognition by the regulator is intimately involved in determining the range of compounds that can activate the subsequently modulated operon. Given the promiscuous substrate range of phenol hydroxylases and toluene monooxygenases in general, changes in effector recognition and subsequent induction of catabolic genes lends itself to metabolic diversity. This has been demonstrated in the manipulations of the pWWO-encoded benzoate metabolism pathway (1, 90). Here, the substrate range of the pathway was expanded through selective mutation of the effector protein (XylS) of the benzoate operon. This effector protein (XylR) also belongs to the NtrC-family and is homologous to DmpR of *Pseudomonas* sp. CF600 (pVI150) (98).

CHAPTER III

WHOLE CELL KINETICS OF TRICHLOROETHYLENE DEGRADATION BY PHENOL HYDROXYLASE IN AN *ALCALIGENES EUTROPHUS* JMP134 DERIVATIVE

Introduction

Like many other chlorinated hydrocarbons, trichloroethylene (TCE) has become a significant and important environmental pollutant because of its toxic properties and widespread occurrence in ground water. TCE, a U. S. Environmental Protection Agency priority pollutant, is the most commonly reported volatile organic pollutant of ground water in the United States (89). While there are no reports of bacterial growth on TCE as a sole carbon and energy source, co-metabolic oxidation of TCE by nonspecific catabolic oxygenases has been described for several types of microorganisms (21) and is perhaps the best studied compound subject to aerobic co-metabolism.

The application of bacteria for the aerobic bioremediation of TCE has been proposed and investigated for a wide variety of microorganisms. The most critical factors in consideration for such studies are the specific activity of the cells for TCE and the possible formation of toxic intermediates. For example, in wild type *Ps. putida* and *Ps. putida* F1, in which TCE oxidation is mediated by toluene dioxygenase, observed inhibition of growth has been attributed to covalent modification of cellular molecules through reactive products from TCE degradation (37 , 114). In each case, the rate of TCE removal declines rapidly in

batch cultures when it is supplied at initial concentrations greater than 10 μM or 80 μM, respectively. Furthermore, it has been shown that growth substrate added to induce the catabolic genes involved in oxidation of TCE can be competitive inhibitors of TCE conversion (25,

Most studies on the kinetics of aerobic TCE degradation have been done with methane- and toluene-utilizing mixed and pure cultures (54, 79, 37, 113, 62, 74, 26, 80). In fact, limited data on the kinetics of aerobic TCE degradation by phenol induced monooxygenases and possible toxic effects of TCE oxidation metabolites are available.

Alcaligenes eutrophus JMP134 is able to degrade TCE by an inducible chromosomally encoded phenol hydroxylase (35). We have previously reported isolation of the chromosomally encoded phenol hydroxylase genes through complementation of a mutant deficient in phenol degradation with a JMP134 genomic cosmid library (48). Subcloning restriction fragments from this cosmid resulted in a recombinant plasmid conferring phenol hydroxylase activity and TCE degradation in the absence of phenol induction. Preliminary studies using this construct have shown a high capacity for TCE removal in the absence of aromatic induction with limited sensitivity to TCE-mediated toxicity (49) and excellent potential for use in the biological remediation of TCE contaminated aquifers.

The purpose of the work presented here was to determine the whole-cell kinetics of constitutive TCE degradation by suspended batch cultures of AEK301 containing the recombinant plasmid, pYK3021. We also wished to examine the degree of TCE degradation using a variety of non-inducing carbon sources in an effort to optimize TCE removal.

Materials and Methods

Bacterial strains, plasmids, media, growth conditions and chemicals. *Alcaligenes eutrophus* AEK301 is an *A. eutrophus* JMP134 derivative deficient in phenol metabolism by the generation of a Tn*5*-induced mutation and is resistant to rifampin and kanamycin. The recombinant plasmid pYK3021 contains an 8.6 kb *Xho*I-*Bam*HI fragment in the pMMB67EH vector and confers TCE degradation in the absence of phenol induction and resistance to carbenicillin when placed in AEK301 (48). Cultures of *A. eutrophus* AEK301 with and without pYK3021 were maintained at 30°C on minimal salts medium (MMO) (107) supplemented with 20 mM sodium citrate or tryptone-yeast extract-glucose medium (TNB) (81). Unless otherwise indicated, MMO was also supplemented with benzoate (2.5 mM), citrate (20 mM), sodium citrate (20 mM), gluconate (20 mM), lactate (20 mM), malate (20 mM), or 0.3 % casamino acids. Concentrated stock solutions of each carbon source were prepared and adjusted to a pH of 7.0 with NaOH where necessary. When required, 50 μg/ ml of carbenicillin, 150 μg/ml of rifampin or 100 μg/ml of kanamycin were added to the growth medium. Yeast extract, tryptone and agar were purchased from Difco. Other media additives, bovine serum albumin and chromatography quality *n*-pentane were all purchased from Sigma. Chromatography quality trichloroethylene (TCE) and 1,2-dibromoethane (EDB) were purchased from Aldrich. Teflon/butyl septa and reactor vials were purchased from Fisher Scientific.

Analytical methods. TCE was measured by gas chromatography analysis with a Hewlett-Packard 5890 gas chromatograph equipped with a 25 m cross-linked methyl silicone gum capillary column (Hewlett-Packard) and electron capture detection system. Peak integrations were obtained with a Hewlett-Packard 3390A integrator. The following operating conditions were used: injector temperature, 150°C; detector temperature, 250°C; column temperature

40°C to 100°C at 20°C/min; helium carrier gas flow 6 ml/min. Under these conditions TCE and EDB (internal standard) in pentane extracts had retention times of 2.2 and 2.9 minutes, respectively.

Standard TCE degradation kinetics assay. AEK301/pYK3021 was grown in MMO containing 10 mM sodium citrate, kanamycin and carbenicillin at 30°C shaking at 180 RPM to mid-log phase at an optical density of 0.6 to 0.8 at 425 nm. Cells were harvested by centrifugation at 8000 x g for 10 minutes. Cell pellets were then suspended in fresh MMO containing 10 mM sodium citrate to an optical density of 1.0 at 425 nm. The cultures were then returned to 30°C shaking at 180 RPM. After one hour, 2 ml samples were dispensed into 20 ml glass vials and crimp-sealed with Teflon/butyl septa. The appropriate volume of an 8 mM TCE stock was added by injection through the septum with a gas-tight syringe (Hamilton, Reno, Nev.). The vials were inverted and returned to 30°C shaking at 180 RPM. At the appropriate time, the reactions were stopped by the addition of 2 ml of *n*-pentane containing 1 ppm EDB. EDB was added as an internal standard to correct for GC sampling imprecision. The vials were placed at room temperature on a shaker platform for 15 minutes and then centrifuged at 4000 x g for 10 minutes to aid in the separation of the organic phase. Following centrifugation, approximately 0.5 ml was transferred with a gas-tight syringe to a Teflon/butyl septum-sealed vial. A 1 µL sample was then removed and analyzed on the GC for TCE concentrations. Control samples of sterile medium gave TCE recoveries of 95-97% under these conditions. The data represent an average of two or more samples. TCE stocks of 8 mM were prepared by completely filling a 20 ml glass vial containing eight 3-mm diameter glass beads (to facilitate mixing) with sterile water. Once crimp-sealed with a Teflon/butyl septum with no trapped air, the appropriate volume of pure TCE was added by injection through

the septum which was then allowed to dissolve completely overnight at room temperature with constant mixing.

No-headspace assay. Cultures were incubated and prepared as described above. Following the 1 hour pre-incubation, approximately 2 ml of cell suspensions and a glass bead (3-mm diameter) were placed in a 2-ml crimp-seal vial were sealed with Teflon/butyl septa with no trapped air. The glass bead was added to facilitate thorough mixing of the contents. The appropriate volume of an 8 mM TCE stock was added by injection through the septum with a gas-tight syringe and the vials were incubated at 30°C with constant mixing. At the appropriate time, the reactions were stopped by the transfer of 0.5 ml of TCE-cell suspensions to sealed vials containing 0.5 ml of *n*-pentane and 1 ppm EDB. The vials were placed at room temperature for extraction as described above and 1 µL of the organic phase was analyzed on the GC for TCE concentrations.

Protein determinations. Cell suspensions were solubilized by the addition of 0.2 volumes of 5 M NaOH and heating at 85°C for 10 minutes. Following the addition of 0.2 volumes of 4 M HCl, the total protein concentrations were determined by the Lowry assay (59). Bovine serum albumin which had been treated with NaOH, heat and HCl in parallel was used as a standard in these assays.

Calculations and equations. The doubling time (dt) in hours of batch cultures was determined during the logarithmic phase of growth according to :

$$dt = \frac{T_1 - T_0}{[\log_2(N_1) - \log_2(N_0)]}$$

where T_1 = the time at the end of logarithmic phase, T_0 = the time at the beginning of logarithmic phase, N_1 = the optical density of the culture at 425 nm at the end

of logarithmic phase, N_0 = the optical density of the culture at 425 nm at the beginning of logarithmic phase.

The air-water partitioning behavior of TCE was expressed by using a modified Equilibrium Partitioning In Closed Systems (EPICS) equation developed for predicting the partitioning of volatile C_1 and C_2 chlorinated hydrocarbons with a dimensionless Henry's law constant which has been adapted for studies conducted at different temperatures (31). The total moles (M) of a volatile solute added to a sealed reactor vial will be partitioned at equilibrium according to the following:

$$M = C_g [(V_w / H_c) + V_g]$$

where C_g = concentration (μM) of TCE in the gas phase or headspace, V_w = the volume of the aqueous phase in the reactor, V_g = the volume of the headspace in the reactor and H_c = dimensionless Henry's constant for TCE which was previously determined to be 0.492 at 30°C. The K_s, which is the Michaelis constant for cellular kinetics and is analogous to K_m for enzymatic reactions, and V_{max} were determined from the axis intercepts from a Lineweaver-Burk double-reciprocal plot.

Results and Discussion

Effects of substrate on TCE removal by AEK301/pYK3021. While TCE degradation by AEK301/pYK3021 occurs in the absence of phenol induction, the apparent rate of TCE co-metabolism varies depending on the carbon and energy source provided (48, 49). To further characterize this observation and optimize TCE removal by AEK301/pYK3021, the degree of TCE oxidation was examined with a variety of non-inducing carbon sources.

AEK301/pYK3021 was grown to mid-log phase in MMO supplemented with different substrates or enriched medium (TNB) and subjected to a standard TCE degradation assay at an initial concentration of 40 μM TCE. After two hours the reactions were stopped by the addition of pentane and the remaining concentration of TCE was determined by GC analysis. While measurable amounts of TCE were removed from all reaction mixtures within two hours, the degree of removal varied greatly between substrates. MMO containing citrate, sodium citrate or gluconate provided the highest degree of TCE removal while MMO containing malate or enriched medium (TNB) provided relatively poor TCE removal capacity within two hours (Table 4). The doubling time for AEK301/pYK3021 in MMO supplemented with these different substrates or enriched medium (TNB) was also determined (Table 5). Examination of the doubling time showed a wide range from 1.2 hours in enriched medium to 2.6 hours in MMO supplemented with citrate. Comparison of the observed doubling time and TCE removal capacities in the various media shows some interesting correlations. MMO containing citrate, sodium citrate or gluconate had the slowest doubling times (2.6, 2.5 and 2.4 hours, respectively) yet provided the greatest TCE removal capacity of the carbon sources tested. Similarly, MMO supplemented with malate or TNB had the fastest doubling times (1.6 and 1.2 hours, respectively) while providing relatively poor TCE removal capacities. No significant effect on doubling time was observed in the presence of 40 μM TCE (Table 5). These data indicate the existence of carbon catabolite repression affecting the metabolism of TCE by phenol hydroxylase in AEK301/pYK3021. The addition of citrate or sodium citrate to the growth medium appeared the least repressive. Additional testing revealed no significant difference between the addition of 10 mM or 20 mM sodium citrate (data not shown). Therefore, sodium citrate at a concentration of 10 mM was selected as the carbon source in MMO

Table 4. Effect of carbon source on TCE degradation by AEK301/pYK3021

Carbon Source	Concentration	TCE Remaining (μM)[b]	Decrease (%)
benzoate	2.5 mM	23.4	41.5
casamino acids	0.30%	12.3	69.3
citrate	20 mM	1.2	97.0
gluconate	20 mM	6.5	83.8
lactate	20 mM	23.0	42.5
malate	20 mM	37.4	6.5
sodium citrate	20 mM	ND[c]	>99.9
TNB[a]	-	38.5	3.8

[a]TNB, tryptone-yeast extract glucose medium

[b]following two hours of incubation at 30°C and an initial concentration of 40 μM TCE

[c]ND, not detected

Table 5. Doubling times of AEK301/pYK3021 in minimal medium supplemented with various carbon sources or enriched medium

		Doubling time (hours/generation)	
Carbon Source	Concentration	Without TCE	40 μM TCE[a]
benzoate	2.5 mM	2.0	2.1
casamino acids	0.30%	1.8	1.8
citrate	20 mM	2.6	2.5
gluconate	20 mM	2.4	2.5
lactate	20 mM	1.7	1.8
malate	20 mM	1.6	1.7
sodium citrate	20 mM	2.5	2.4
TNB	-	1.2	1.2

[a]TCE was added by injection to sealed cultures during early exponential phase.

for all TCE degradation assays.

For bacterial genes encoding catabolic enzymes, regulation depends on the availability of the respective carbon source. However, if one carbon source is more rapidly metabolized than another, function of the catabolic enzymes for the less rapidly metabolized carbon source can be decreased by a regulator process commonly referred to as carbon catabolite repression (CCR). CCR of the phenol hydroxylase catabolic genes has been shown in *Ps. putida* H and is mediated by inhibition of a phenol hydroxylase-specific transcriptional activator and subsequent reduction in transcription of the phenol hydroxylase catabolic genes, thus interfering with phenol induction of this catabolic enzyme (68). CCR was observed with the addition of glucose, succinate, lactate or acetate. Phenol hydroxylase in *Ps. putida* H was least affected by the addition of pyruvate or citrate. Pyruvate was the least repressive of all carbon sources tested and it would be interesting to test TCE degradation by AEK301/pYK3021 in MMO with pyruvate as the carbon and energy source.

Time course of TCE degradation by AEK301/pYK3021. In previous studies of AEK301/pYK3021, TCE degradation was monitored over a period of many hours or even days (48, 49). For the purpose of determining the whole-cell kinetics of TCE degradation by AEK301/pYK3021, TCE degradation was instead monitored for three hours at 15 minute intervals at two different initial concentrations of TCE (16 μM and 80 μM). The negative control (AEK301 alone) was unable to degrade detectable amounts of TCE. For each initial TCE concentration tested, an initial lag period of approximately 40 minutes was observed prior to the onset of TCE degradation by AEK301/pYK3021 (Figure 5). Following the initial lag, the rate of TCE degradation by AEK301/pYK3021 at an initial concentration of 80 μM TCE was sustained and remained essentially

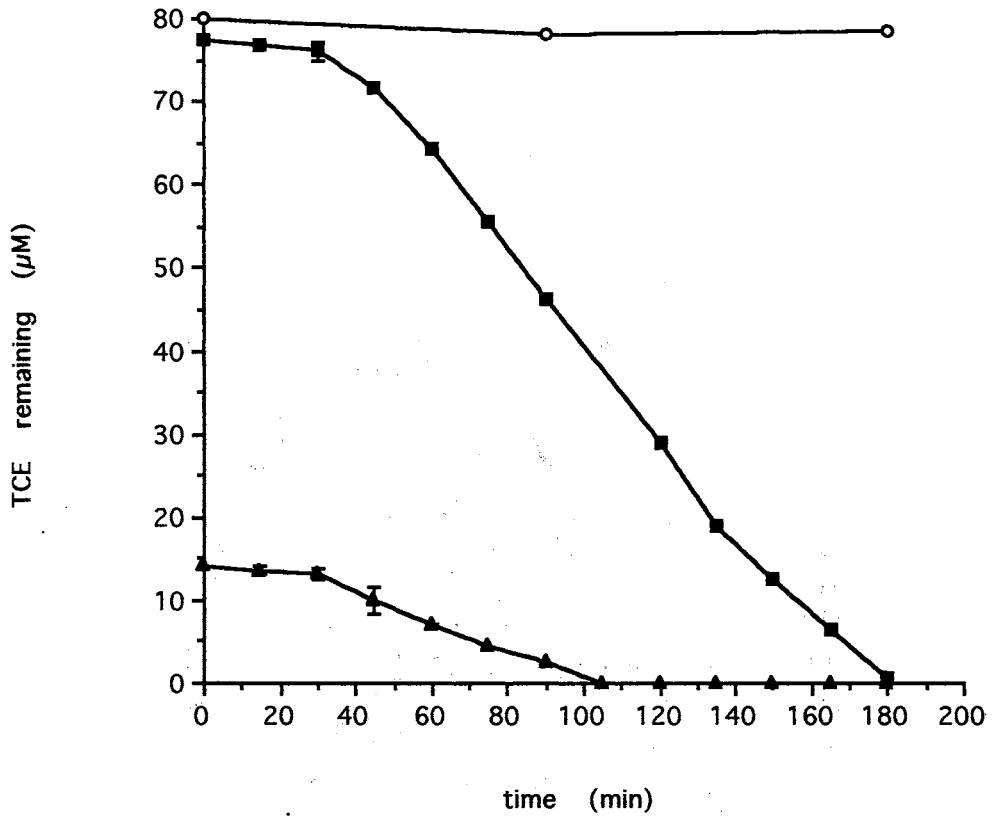

Figure 5. Degradation of TCE by AEK301/pYK3021. (▲) AEK301/pYK3021 at an initial concentration of 16 μM TCE, (■) AEK301/pYK3021 at an initial concentration of 80 μM TCE, (0) negative control AEK301, at an initial concentration of 80 μM TCE. Cultures where grown in MMO supplemented with 10 mM sodium citrate to mid-log phase, harvested by centrifugation and suspended in fresh medium to an optical density of 1.0 at 425 nm. After one hour at 30°C, 2 ml samples of each strain were then distributed into vials and sealed. Reactions were initiated by the injection of TCE through the septum. Samples were collected in duplicate every 15 minutes for a total of three hours. Each data point represents the average of two or more samples and error bars are provided where visible.

constant for a period of almost two hours until TCE was no longer detectable. This differs significantly from TCE degradation by *Ps. putida* F1 or *Methylosinus trichosporium* where the rate of TCE degradation is sustained only 20 to 60 minutes, respectively (113). Following an initial burst of TCE degradation, the rates declined rapidly and even at initial concentrations of 15 μM TCE added to induced cultures of *Ps. putida* F1, significant quantities of TCE remained in reactor vials even after 6 hours of incubation (113). These studies suggest that TCE may be toxic to *Ps. putida* F1 or *Methylosinus trichosporium* through the formation of toxic intermediates. The sustained rates of TCE degradation by AEK301/pYK3021 suggest that the degradation of TCE by this construct is not affected by the formation of toxic intermediates at the levels tested.

Whole-cell kinetics of TCE degradation by AEK301/pYK3021. To gain insight into the kinetics of TCE degradation by whole cells of AEK301/pYK3021, 5-minute assays (beginning 50 minutes following the addition of TCE to reactor vials) were conducted at various initial concentrations of TCE. For seven different initial TCE concentrations ranging from 16 μM to 1600 μM, TCE degradation rates and total protein determinations were made. These results, illustrated in Figure 6 and summarized in Table 6, represent the averages of at least two different samples. The velocity or rate of degradation for each concentration was determined (nmoles/min/mg total protein) and these values were plotted as a function of the initial TCE concentration (Figure 7) to generate a Michaelis-Menten plot for whole-cell kinetics. The rate of TCE degradation by AEK301/pYK3021 was linear from 16 μM to 800 μM TCE. The rate observed at 1600 μM TCE was similar to that observed at 800μM TCE indicating saturation or inhibition of the catabolic enzymes at this point. It is interesting to note that the rate of TCE degradation continues to increase at concentrations that are known to inhibit other enzymatic systems (113). At 320

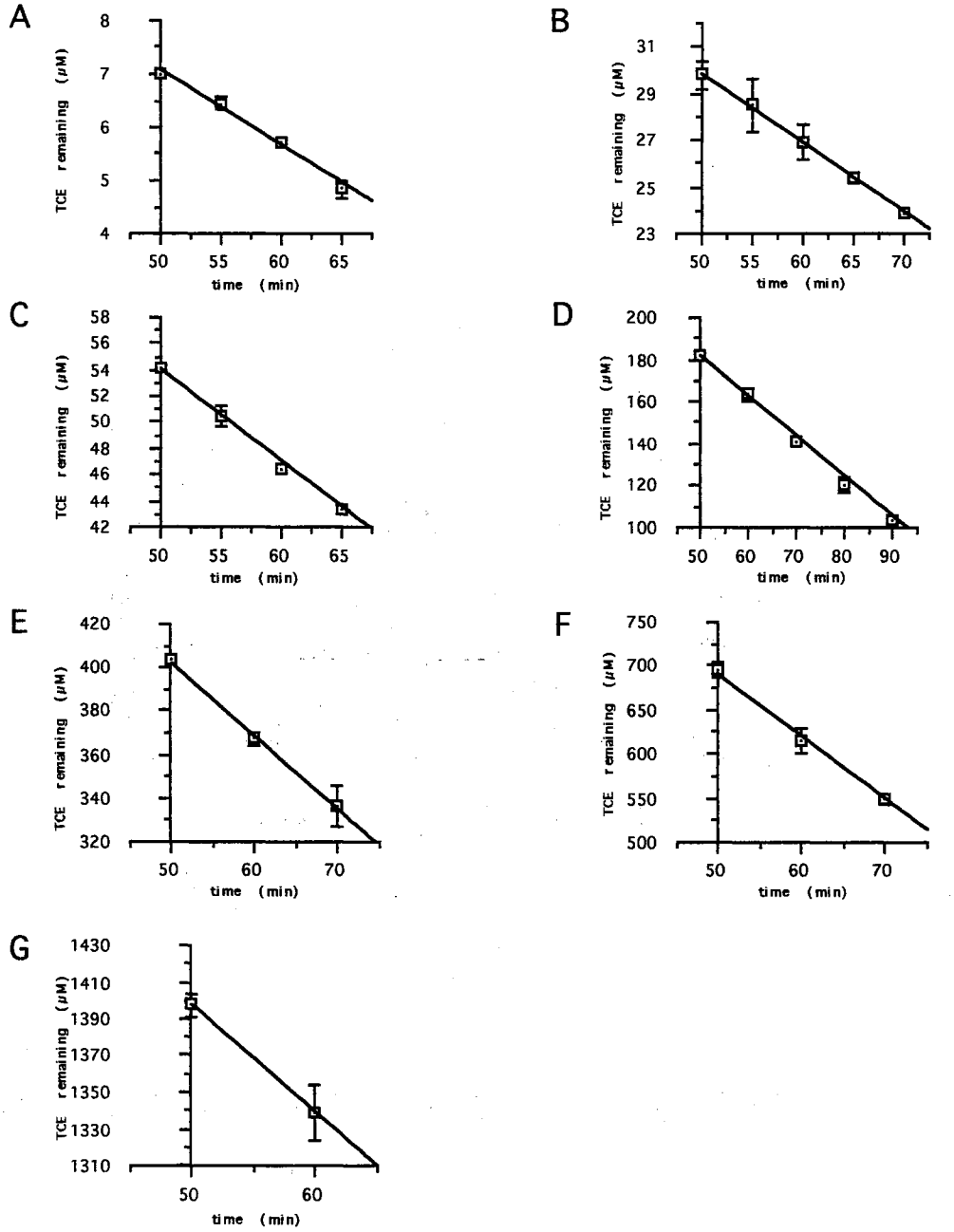

Figure 6. Rate of TCE degradation by AEK301/pYK3021 at initial substrate concentrations of (A) 16 μM, (B) 40 μM, (C) 80 μM, (D) 200 μM, (E) 400 μM, (F) 800 μM and (G) 1600 μM. Cultures where grown in MMO supplemented with 10 mM sodium citrate to mid-log phase, harvested by centrifugation and suspended in fresh medium to an optical density of 1.0 at 425 nm. Following 1 hour pre-incubation, 2 ml samples were then distributed into vials and sealed. In each case, sample collection began 50 minutes after the addition of TCE. Each data point represents the average of two or more samples and error bars are shown.

Table 6. Whole cell kinetics of TCE degradation by AEK301/pYK3021

Initial [TCE] (μM)	TCE Consumed (nmoles/min)	Total Protein (TP) (mg/ml)	Rate (nmoles/min/mg TP)
16	0.144	0.253 ± 0.006	0.57
40	0.299	0.238 ± 0.026	1.26
80	0.724	0.321 ± 0.016	2.26
200	2.010	0.342 ± 0.013	5.88
400	3.355	0.297 ± 0.010	11.30
800	7.240	0.312 ± 0.008	23.21
1600	5.890	0.273 ± 0.004	21.58

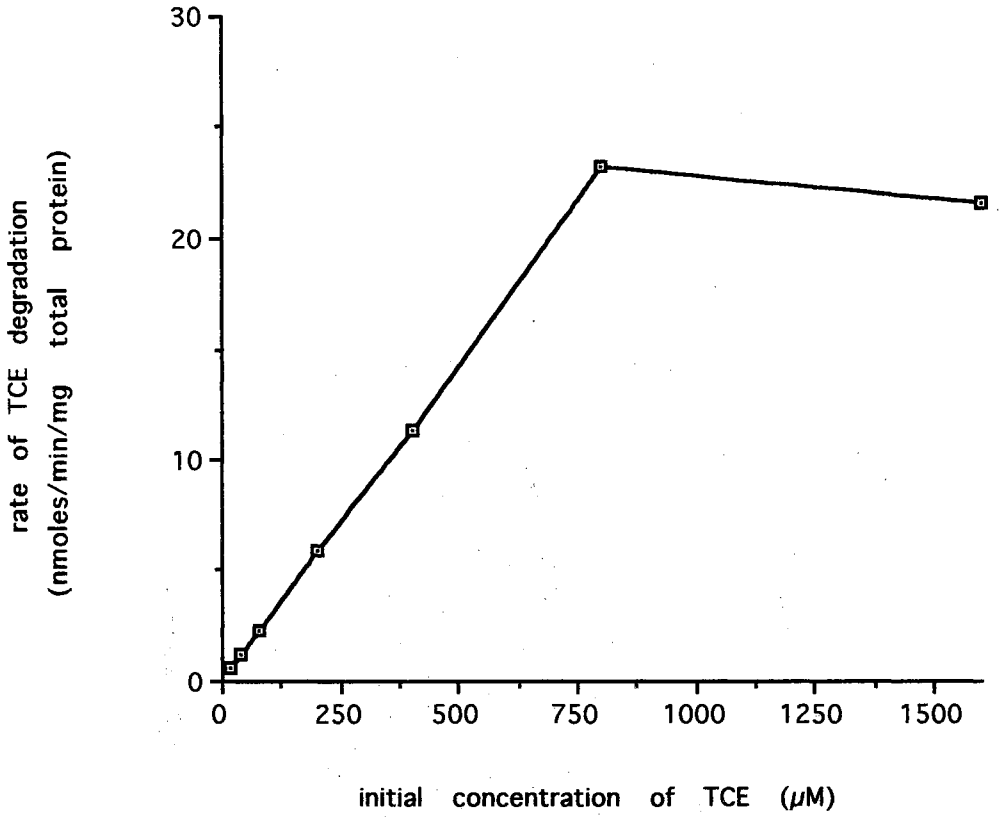

Figure 7. Whole cell kinetics of TCE degradation by AEK301/pYK3021. The initial rates of TCE degradation were determined and are plotted as a function of initial TCE concentration.

μM TCE, TCE degradation by *Ps. putida* F1 no longer occurred. In methane induced *Methylosinus trichosporium* OB3b, toxicity was apparent at concentration of 70 μM TCE and cell suspensions were not able to degrade higher concentrations of TCE (79). These studies suggest that TCE may be toxic to *Ps. putida* F1 and/or *Methylosinus trichosporium* OB3b by direct disruption of catabolic activity or by general toxicity during the degradation of TCE resulting in the loss of activity. The linear rate of TCE degradation by AEK301/pYK3021 up to a concentration of 800 μM TCE would suggest these effects are limited during the degradation of TCE.

Kinetics parameters were estimated by transforming the data (Table 6) to produce a Lineweaver-Burk plot (Figure 8). The apparent K_s and V_{max} were then estimated to be 630 μM and 22.6 nmoles/min/mg total protein. The rate of TCE degradation by AEK301/pYK3021 is much higher than those reported for similar systems. For example, the highest observed rate of TCE degradation by *P. putida* F1 was 1.8 nmoles/min/mg total protein at 80 μM TCE and dropped rapidly at concentrations higher than 300 μM TCE (113). Further, the observed rates of TCE degradation by AEK301/pYK3021 were sustained for long periods of time compared to the initial burst followed by rapid decline of TCE removal rates reported in *P. putida* F1 and wild type (37, 113).

No-headspace assay. Although TCE is highly volatile, for convenience it is often reported as an aqueous concentration in closed systems containing both air and water phases. This could be considered misleading when reporting kinetics data. To determine the effects, if any, of TCE volatility and phase partitioning on the before mentioned kinetics, a no-headspace assay was developed for comparison. Degradation of TCE by AEK301/pYK3021 is an aerobic process and dependent on available oxygen. In such a closed system with no headspace to replenish the consumed dissolved oxygen, it is likely that oxygen would

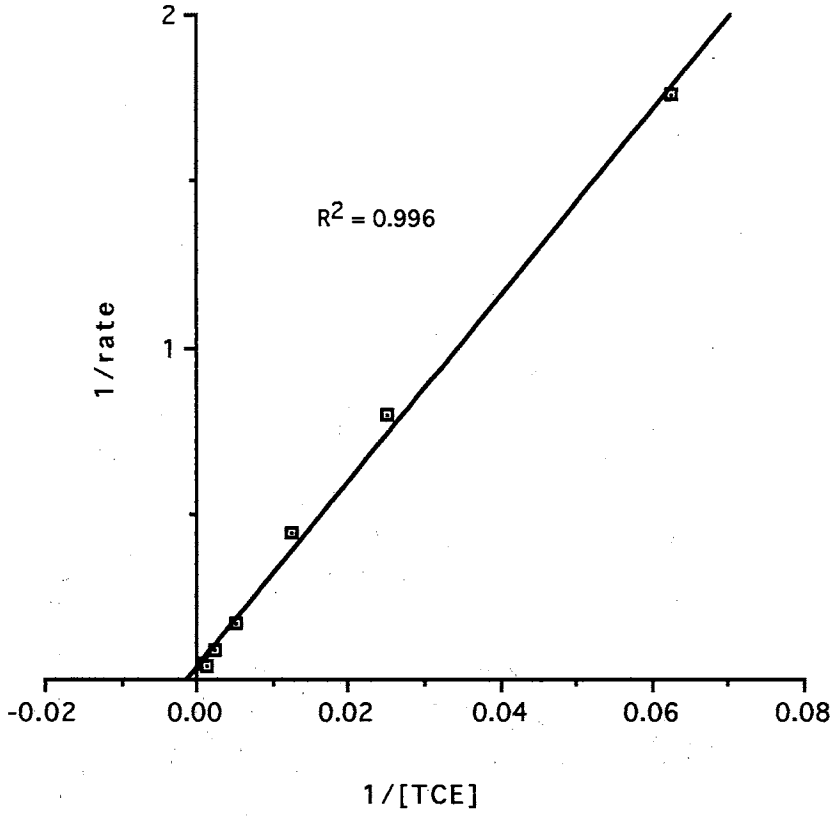

Figure 8. A double-reciprocal or Lineweaver-Burk plot of TCE degradation kinetics data by whole-cells of AEK301/pYK3021 for determination of V_{max} and K_s. K_s is the Michaelis constant for cellular kinetics and is analogous to K_m for enzymatic reactions.

become a limiting factor in such an assay. Accordingly, the degradation of TCE in a no-headspace assay was examined at a low concentration of TCE (initial concentration). The rate of TCE degradation was determined to be 0.538 nmoles/min/mg total protein at an initial TCE concentration of 21.6 μM in a no-headspace assay and compared to the rates observed at 16 μM and 80 μM TCE (uncorrected) (Table 7). This rate is comparable to the rate observed in the standard assay at 16 μM even though the aqueous concentrations are different. When compared to the rates observed at 80 μM in the standard assay where the aqueous concentration of TCE (17.7 μM) is more similar, the rate of TCE degradation in the no-headspace assay was significantly lower. These results suggest that the redistribution of TCE from the gas phase into the aqueous phase occurred faster than the rate of degradation and was not a limiting factor in the well-mixed standard assay. Similar observations have been reported by Folsom, *et al* (26).

Conclusions

In this study, the kinetics of TCE degradation by AEK301/pYK3021 whole cells were examined in the absence of aromatic induction. TCE degradation by this construct is subject to carbon catabolite repression. The most repressive carbon sources (malate and enriched medium) were also the most rapidly metabolized as determined from the rate of growth. The least repressive carbon source of those assayed, citrate or sodium citrate, was selected as the carbon source of choice for optimal TCE degradation. TCE degradation by AEK301/pYK3021 is preceded by a lag time of 40 minutes followed by rapid, sustained TCE degradation. This lag was not observed in TCE degradation of phenol induced wildtype JMP134 (49) and is likely the result of TCE-mediated induction of the catabolic genes. The K_s and V_{max} for TCE degradation by

Table 7 Comparison of the standard TCE degradation assay with a no-headspace TCE degradation assay

Assay Method	Total TCE (nmoles/vial)	Uncorrected [TCE] (μM)	Aqueous [TCE] (μM)[a]	Relative Rate (nmoles/min)	Rate (nmoles/min/mg TP)
90 % headspace	32	16	3.53	0.144	0.568
90 % headspace	160	80	17.70	0.724	2.255
no-headspace	40	21.6	21.60	0.112	0.538

[a]determined using a dimentionless Henry's law constant adjusted for the assay temperature and accounting for the reactor volume and sample volume according to the equation provided in Materials and Methods.

AEK301/pYK3021 whole cells were determined to be 630 μM and 22.6 nmoles/min/mg total protein, respectively. This construct is an ideal candidate for *in situ* remediation studies based on the following attributes: (1) AEK301/pYK3021 is able to degrade significant quantities of TCE at relatively high and sustained rates in the absence of aromatic induction and (2) sensitivity to TCE-mediated toxicity and metabolite toxicity is limited and high concentrations of TCE appear to be well tolerated by the system. Bench-scale studies involving continuous culture and substrate challenge to characterize the effectiveness of this construct would provide valuable insight into the remediation capacity of this genetically engineered microorganism.

CHAPTER IV

COMPLETE NUCLEOTIDE SEQUENCE AND ANALYSIS OF THE PHENOL HYDROXYLASE GENE CLUSTER FROM *ALCALIGENES EUTROPHUS* JMP134

Introduction

Alcaligenes eutrophus JMP134 utilizes phenol as a sole carbon and energy source. Phenol is oxidized in this bacterial strain to catechol, which is further oxidized through *meta* ring cleavage to form substrates of the tricarboxylic acid cycle (84, 85). The initial step in this pathway is catalyzed by an inducible, chromosomally encoded phenol hydroxylase which can also co-metabolize trichloroethylene (TCE), a common ground water pollutant.

The locus for phenol hydroxylase has been identified in a JMP134-derived Tn5-induced mutant (termed AEK301) that lacks both phenol hydroxylase and catechol 2,3-dioxygenase activities by complementation with a genomic cosmid clone (termed pYK301) (48, 49). The genes for phenol hydroxylase and catechol 2,3-dioxygenase activity were mapped, subcloned, and expressed independently in the pMMB67EH expression vector. One such subclone, termed pYK3021, expressing phenol hydroxylase activity is able to degrade TCE in the absence of aromatic induction. To further characterize the region encoding phenol hydroxylase activity, the complete nucleotide sequence of this region has been determined and is presented in this chapter. Analysis of the nucleotide sequence and the putative polypepetide products of the phenol hydroxylase gene cluster from pYK3021 is also presented.

Materials and Methods

Bacterial strains and plasmids. The bacterial strains and plasmids used in this study are listed in Table 8. Strains of *Escherichia coli* were grown with aeration at 37°C in Luria-Bertani (LB) medium (61). Cultures of *Alcaligenes eutrophus* were grown with aeration at 30°C in minimal salts medium (MMO) (107) supplemented with 10 mM sodium citrate. Antibiotics were used at the following concentrations: ampicillin, 100 μg/ml (*E. coli*) and carbenicillin, 50 μg/ml (*A. eutrophus*).

General DNA protocols. Preparation of competent *E. coli* cells and plasmid transformation were performed as described by Inoue, *et al.* (41). Plasmid DNA was isolated by rapid alkaline-sodium dodecyl sulfate extraction (5). For highly purified plasmid DNA, extraction was followed by sedimentation on cesium chloride-ethidium bromide density gradients. Purified plasmid DNA dissolved in sterile TE (10 mM Tris, pH 8.0 and 1 mM EDTA, pH 8.0) was quantified by measuring the absorbance at 260 nm. Restriction enzyme mapping, agarose gel electrophoresis and electroelution of DNA fragments from agarose gels were performed using standard procedures (4, 61). Restriction endonucleases and T4 DNA ligase were purchased from Bethesda Research Laboratories (BRL) while shrimp alkaline phosphatase was purchased from United States Biochemical Company (USBC), and each were used according to the directions of the suppliers. RnaseA and X-gal were purchased from Sigma. Nested deletions were performed using the exonuclease III Erase-a-Base kit (Promega) as directed by the manufacturer.

Nucleotide sequence determinations. Various restriction fragments from pYK3021 were separated by agarose gel electrophoresis, isolated by electroelution and subcloned into the multiple-cloning site of the pBSIIKS+

Table 8. Bacterial strains and plasmids relevant to this study.

Strain or plasmid	Relevant characteristics[a]	Reference or source
Strains		
A. eutrophus JMP134	Prototroph, Phl^+, Tfd^+, Hg^r	17
A. eutrophus AEO106	Prototroph, Phl^+, Tfd^-, Hg^- derivative of JMP134	39
A. eutrophus AEK301	Rif^r, Phl^-, $C23O^-$, Km^r derivative of AEK106	48, 49
E. coli DH5α	*rec*A1, Φ80ΔM15m Δ(*lac*ZYA-*arg*F)U169	BRL
E. coli STBL2	*recA1merA*Δ(*mcr*BC-*hsd*RMS-*mrr*) Δ(*lac*AYA-*pro*AB)	BRL
Plasmids		
pBSIIKS+	Amp^r, *lacZ'*	Stratagene
pVK102	IncP, cos^+, Km^r, Tc^r	51
pMMB67EH	Amp^r, Tac expression cloning vector	29
pYK301	Tc^r, 16.8 kb *Hind*III fragment of AEO106 DNA in pVK102	48, 49
pYK3021	Amp^r, 8.6 kb *XhoI/BamHI* fragment from pYK301 containing the *phl*KLMNOPRX genes cloned into pMMB67EH	48, 49

[a]Abbreviations: Amp, ampicillin; Hg, mercury; Km, kanamycin; Rif, rifampin; Tc, tetracycline; Phl, phenol hydroxylase; C23O, catechol 2,3-dioxygenase;

sequencing vector (Stratagene). Unidirectional deletion libraries of the resulting plasmids were generated and the nucleotide sequence of both strands was determined by the dideoxy method (94) aided by an Applied Biosystems automated sequencer. Gaps in the sequences obtained from deletion libraries were determined by using custom-designed synthetic oligonucleotides.

Computer analysis. The sequences were entered, aligned, edited and analyzed using the Sequencher sequence assembly/analysis software version 3.0.1 (Gene Codes Corporation) and MacDNASIS pro DNA and protein sequence analysis system software version 3.0 (Hitachi). The nucleotide and deduced amino acid sequences were compared with GenBank and SwissProt databases using the BLASTX and BLASTP programs. The nucleotide and deduced amino acid sequences were also analyzed by the University of Wisconsin Genetics Computer Group (GCG) software package; Motif Finder program at the University of Kyoto, Japan; Pfam program at the Sanger Centre, UK and the TMPred program at ISREC, Switzerland.

Results and Discussion

Nucleotide sequence analysis. The nucleotide sequence of the 8.6 kb *Xho*I/*Bam*HI insert in pYK3021 was determined. Examination of the nucleotide sequence from the phenol hydroxylase-encoding region revealed eight tightly clustered open reading frames (ORF's) that were designated *phlK*, *phlL*, *phlM*, *phlN*, *phlO*, *phlP*, *phlR* and *phlX* (Figure 9). The *phlKLMNOPR* gene cluster appears to comprise an operon and is preceeded by two regions which show significant homology to σ^{54}-dependent operator/promoter regions. Upstream of *phlK* a σ^{54}-dependent -24/-12 consensus promoter sequence of TGGCAc-N5 -TTGC was identified (Figure 10, nucleotides 194 to 208) (98). Comparison of the putative *phlKLMNOPR* promoter region with the -24/-12 promoter sequences of

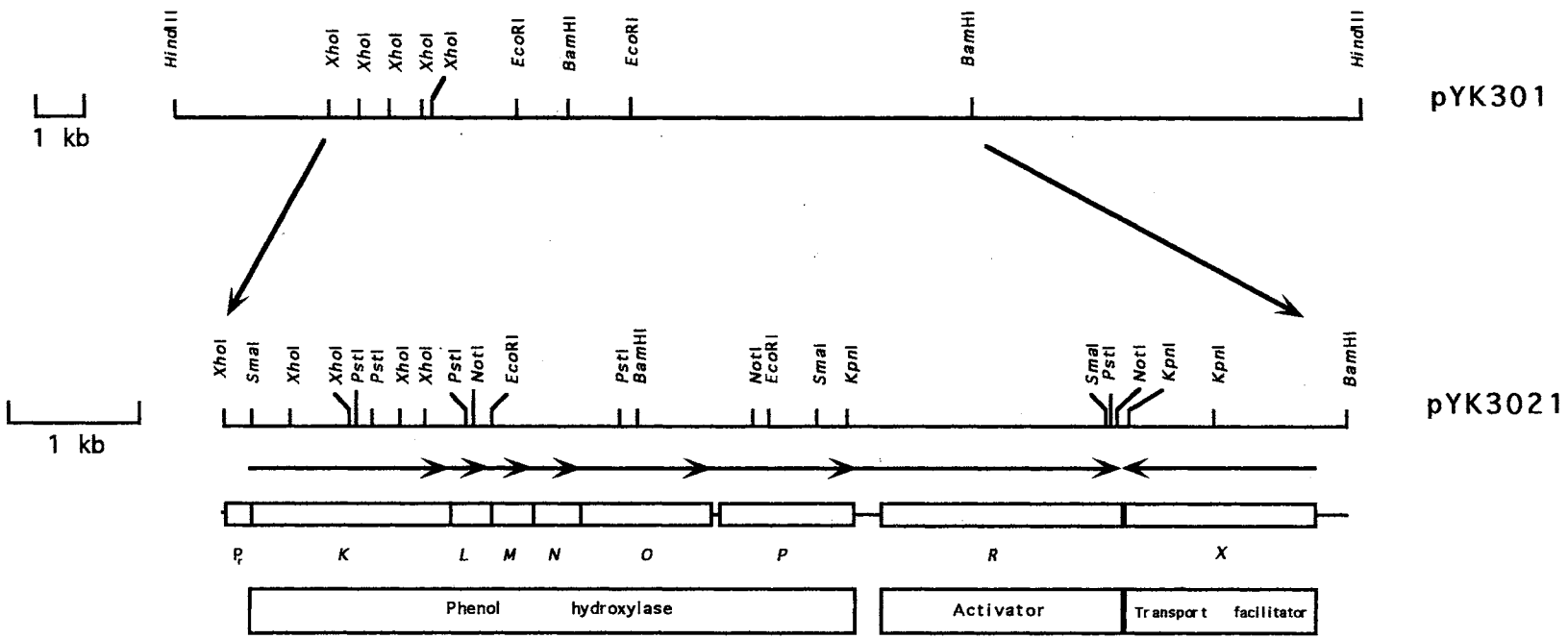

Figure 9. Physical and genetic map. The plasmid pYK301, a cosmid clone expressing inducible phenol hydroxylase activty, was previously subcloned into the pMMB67EH vector (48, 49) to generate the plasmid pYK3021 which, when placed in AEK301, expresses TCE degradation in the absence of aromatic induction. DNA sequence analysis of the 8.6 kb *Xho*I/*Bam*HI fragment from the plasmid pYK3021 required for phenol hydroxylase activity in AEK301 has revealed eight open reading frames. Database searches of the deduced amino acid sequences revealed the putative gene products indicated above. The arrows indicate the divergent transcription of the *phlX* transport facilitator gene and the phenol hydroxylase operon which is composed of the *phlKLMNOP* phenol hydroxylase genes and the *phlR* positive regulator. Examination of the nucleotide sequence upstream of the phenol hydroxylase operon has revealed σ^{54}-dependent promoter-like sequences (designated P_r). A DNA region exhibiting homology with the TbuT, XylR and DmpR-binding sites and an overlapping region homologous to the binding site for the integration host factor (IHF) were also identified in this promoter region. *phlX* appears to be transcribed constitutively from the vector-encoded promoter.

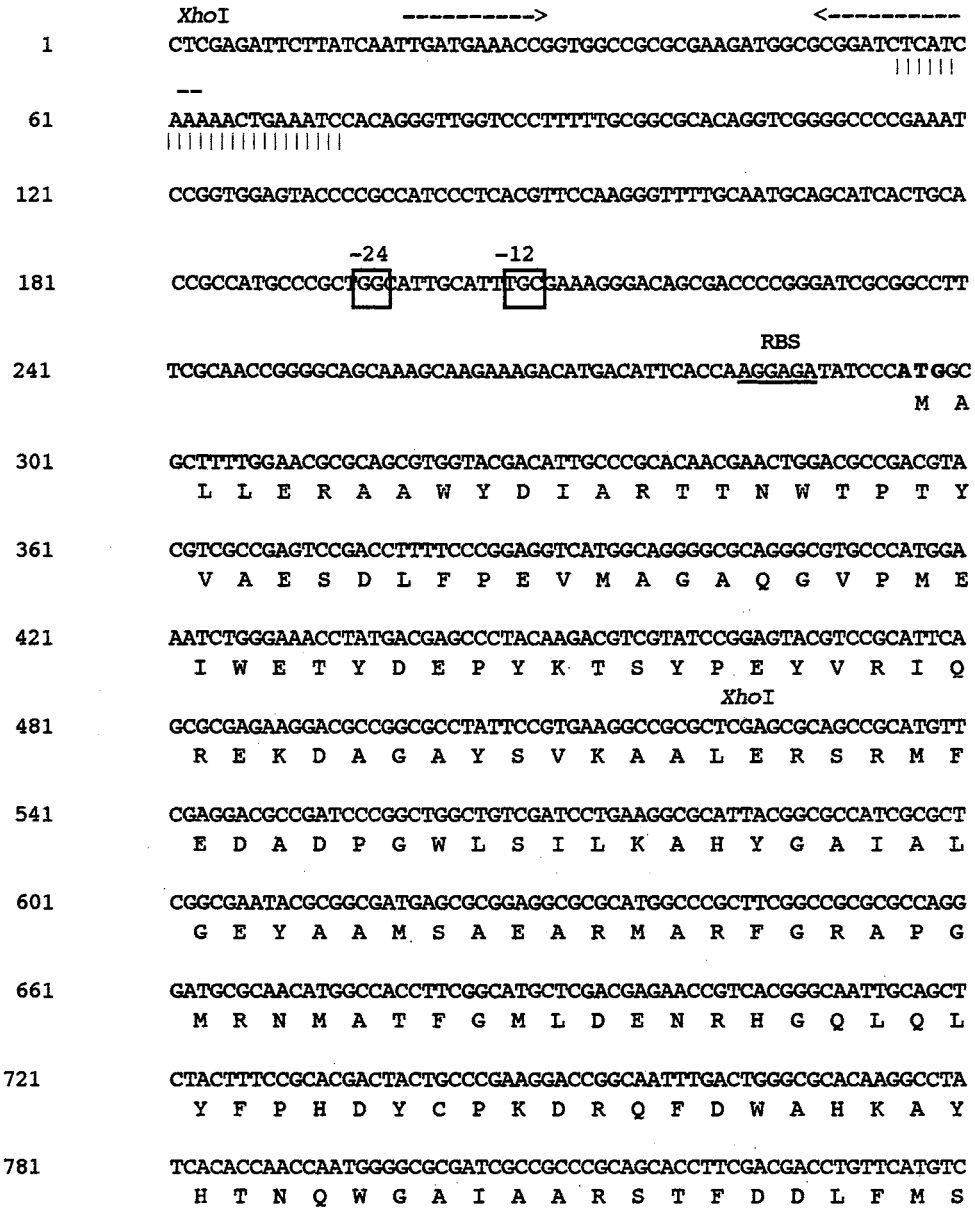

Figure 10. Complete nucloetide sequence of the phenol hydroxylase gene cluster from JMP134. Nucleotide sequence of the 8620 bp region required by AEK301 for TCE degradation in the absence of aromatic induction. Some restriction sites are shown for comparison with Figure 8. The coding strand is given for the first seven putative open reading frames (ORFs). The eighth ORF is divergently encoded and the nucleotide sequence of the non-coding strand is given. The region similar to the consensus σ^{54}-dependent promoter is boxed and labeled -24 and -12. Putative Shine-Delgarno (RBS) sequences are underlined and translation start signals are shown in boldface type. The deduced amino acid sequences of the first seven ORFs are displayed in single-letter code below the respective codons and above the eighth ORF. The DNA region containing the 13 bp imperfect inverted repeats and with homology to the TbuT, XylR and DmpR-binding sites is indicated by arrows. The location of a putative IHF-binding site is indicated by the horizontal hatched bar located below the respective sequence.

```
841   GCGAAGCGCGATCGAGATCGCCGTGATGCTTACGTTTGCCTTCGAAACGGGTTTCACCAA
        R  S  A  I  E  I  A  V  M  L  T  F  A  F  E  T  G  F  T  N

901   CATGCAGTTCCTCGGGCTGGCGGCCGATGCGGCGGAAGCCGGCGATTTCACCTTCGCCAG
        M  Q  F  L  G  L  A  A  D  A  A  E  A  G  D  F  T  F  A  S
              XhoI
961   CCTCATCTCGAGCATCCAGACGGACGAGTCGCGACACGCGCAGATCGGCGGCCCGGCACT
        L  I  S  S  I  Q  T  D  E  S  R  H  A  Q  I  G  G  P  A  L

1021  GCAGATCCTGATCGCCAACGGGCGCAAGGAGCAGGCGCAGCAGCTCGTGGACGTCGCCAT
        Q  I  L  I  A  N  G  R  K  E  Q  A  Q  Q  L  V  D  V  A  I

1081  TGCACGCGCATGGCGCCTGTTCTCCCTGCTGACTGGCACGTCGATGGACTACGCCACGCC
        A  R  A  W  R  L  F  S  L  L  T  G  T  S  M  D  Y  A  T  P
        PstI
1141  GCTGCAGCATCGCAAGGAGTCATTCAAGGAGTTCATGACGGAATGGATCGTCGGCCAGTT
        L  Q  H  R  K  E  S  F  K  E  F  M  T  E  W  I  V  G  Q  F

1201  CGAGCGCACGCTGATCGACCTCGGTCTCGACCTGCCCTGGTACTGGGACCAGATGATCAA
        E  R  T  L  I  D  L  G  L  D  L  P  W  Y  W  D  Q  M  I  N

1261  TGAGTTCGACTACCAGCACCATGCCTATCAGATGGGCATCTGGTTCTGGCGGCCGACCGT
        E  F  D  Y  Q  H  H  A  Y  Q  M  G  I  W  F  W  R  P  T  V
                                                    XhoI
1321  CTGGTGGAACCCGGCCGCCGGCATGACGCCGGACTGCCGTGACTGGCTCGAGGAAAAGTA
        W  W  N  P  A  A  G  M  T  P  D  C  R  D  W  L  E  E  K  Y

1381  TCCCGGCTGGAACGACACGTTCGGCAAGGCCTGGGACGTCATCATCGACAACCTGCTTGC
        P  G  W  N  D  T  F  G  K  A  W  D  V  I  I  D  N  L  L  A

1441  GGGCAGGAAGGAATTGACCGTCCCCGAGACCCTGCCCATCGTCTGCAACATGAGCCAGTT
        G  R  K  E  L  T  V  P  E  T  L  P  I  V  C  N  M  S  Q  L
                                                          XhoI
1501  GCCAATCTGCGCGGTGCCCGGCAACGGCTGGAACGTCAGGGACTATCCGCTCGAGTACAA
        P  I  C  A  V  P  G  N  G  W  N  V  R  D  Y  P  L  E  Y  N

1561  CGGCCGCACGTACCACTTCAACTCCGAGATCGACCGCTGGGTCTTCCAGCAGGACCCGGT
        G  R  T  Y  H  F  N  S  E  I  D  R  W  V  F  Q  Q  D  P  V

1621  GCGCTACCGCGACCACCTGACCCTGGTCGACCGTTTCCTCGCCGGGCACATCCAGCCGCC
        R  Y  R  D  H  L  T  L  V  D  R  F  L  A  G  H  I  Q  P  P

1681  CGACCTGGGGGGCGCACTCCGGTACATGAACCTCGCCCCCGGCGAGATTGGCGACGACGC
        D  L  G  G  A  L  R  Y  M  N  L  A  P  G  E  I  G  D  D  A

1741  ACACCAGTACGCGTGGGTAGAGGCCTACCGCCGCCAGCGCGAACAGAACAAGGCCGCCTG
        H  Q  Y  A  W  V  E  A  Y  R  R  Q  R  E  Q  N  K  A  A stop

                    RBS
1801  ACGCGGCCATCAGATGGAGGATGACATGGCACTGTTTCCAGTGATTTCGAATTTTCAGTA
                                  M  A  L  F  P  V  I  S  N  F  Q  Y
            PstI
1861  CGACTTCGTGCTGCAGCTCGTCGCCGTCGATACGGAGAACTCGATGGACGAGGTAGCGGC
        D  F  V  L  Q  L  V  A  V  D  T  E  N  S  M  D  E  V  A  A
```

Figure 10 - *Continued*

```
1921        GGCGGCCGCGCACCATTCAGTCGGCCGTCGCGTGGCGCCCCAGCCCGGCAAGGTCGTCCG
              A  A  A  H  H  S  V  G  R  R  V  A  P  Q  P  G  K  V  V  R

1981        GGTGCGGCGTCAGGGGGGCGACCAGTTCTACCCCCGCGACGCCCGGATTGGCGACACCGA
              V  R  R  Q  G  G  D  Q  F  Y  P  R  D  A  R  I  G  D  T  D
                                  EcoRI                 RBS
2041        TATCAAGCCGATGGAGTCGCTCGAATTCATCTTTTGCGATGCATGAGGTCACCATGAATT
              I  K  P  M  E  S  L  E  F  I  F  C  D  A stop       M  N

2101        TCCAGAAAGTCTCCACGCTCGACGAGTTGTGGGAAGGCGACATGGCCGAAGTGGAGGTGG
            F  Q  K  V  S  T  L  D  E  L  W  E  G  D  M  A  E  V  E  V

2161        ACGGCCACGTCATCGTGCTCGTCCGCCCCGAAGGCGGCGCGCCACGCGCATTCCAGGGCA
            D  G  H  V  I  V  L  V  R  P  E  G  G  A  P  R  A  F  Q  G

2221        TCTGTCCGCACCAGGACATTCCGCTCGCAGAGGGAAAGTTCGACGGGCGCGTGCTGATGT
            I  C  P  H  Q  D  I  P  L  A  E  G  K  F  D  G  R  V  L  M

2281        GCCGGGCCCACCAGTGGACCTTCGATGCCAACACAGGCAAGGGCATCAACCCCGGTGGGT
            C  R  A  H  Q  W  T  F  D  A  N  T  G  K  G  I  N  P  G  G

2341        GCCGGCTTGCCGAGTATGCCGTCAAGGTGGATGGCGACGACATCCTCATCGCTGTCGAGG
            C  R  L  A  E  Y  A  V  K  V  D  G  D  D  I  L  I  A  V  E
                                                 RBS
2401        GCGTCGAACCACTGTTCGCCAACTGCTGATATTGCACAGGAATCGATCATGAGCAAAGAC
            G  V  E  P  L  F  A  N  C stop                 M  S  K  D

2461        CACAACACCGCCGAGGCCTACCGAAACAACCGCGTCGGCCCCGTACTGCGCGCGAGCAGC
            H  N  T  A  E  A  Y  R  N  N  R  V  G  P  V  L  R  A  S  S

2521        ATCACGTCCGGCGTCATCGAGGCCGCGCAGGAAGACAACCCAGGGAAGGAAATCCGCGTC
            I  T  S  G  V  I  E  A  A  Q  E  D  N  P  G  K  E  I  R  V

2581        GACGACAAGCTCGCATACGTGCGCATCGACACCGACGGCGAACTGATCCTGCGCCGGGCC
            D  D  K  L  A  Y  V  R  I  D  T  D  G  E  L  I  L  R  R  A

2641        ACGCTGGAGGATGCGCTGGGCCGCCCGTTCAGGATGTCCGAGCTGGAGGTCAACCTCAGC
            T  L  E  D  A  L  G  R  P  F  R  M  S  E  L  E  V  N  L  S

2701        TCGTTCGCGGGCCGCATCGAGACTACGGACGACTACGTCCGCTTCTATTACGAAAAGACG
            S  F  A  G  R  I  E  T  T  D  D  Y  V  R  F  Y  Y  E  K  T

                  RBS
2761        CTGTAACCGGAGACGAGCATGACCACGCAACCCGACGTCCTCAAGCCGCTGAAGACCTGG
              L stop          M  T  T  Q  P  D  V  L  K  P  L  K  T  W

2821        AGCCACCTGGCCGCGCGCCGGCGCAAGCCGAGCGAGTACGAGATCGTCTCGACGAACCTG
            S  H  L  A  A  R  R  R  K  P  S  E  Y  E  I  V  S  T  N  L

2881        CACTACACGACCGACAACCCCGACGCGCCGTTCGAGCTCGATCCGAACTTCGAGATGGCG
            H  Y  T  T  D  N  P  D  A  P  F  E  L  D  P  N  F  E  M  A

2941        CAGTGGTTCAAGCGTCACCGCAACGCCTCGCCGCTGAAACACGCCGACTGGAACGCCTTC
            Q  W  F  K  R  H  R  N  A  S  P  L  K  H  A  D  W  N  A  F
```

Figure10 - *Continued*

PstI

3001 CGCGATCCCGACGAACTCGTCTACCGCACCTACAACATGCTGCAGGACGGCCAGGAAACC
R D P D E L V Y R T Y N M L Q D G Q E T

3061 TATGTGTCCGGCCTGCTGGACCAGTTTTCTGAACGCGGCCACGACTCCATGCTGGAGCAC
Y V S G L L D Q F S E R G H D S M L E H

3121 TCCTGGGCCGGCACGCTGGCGCGGCTGTACACCCCGGCACGCTATCTGTTCCACGCACTG
S W A G T L A R L Y T P A R Y L F H A L

BamHI

3181 CAAATGGGATCCGCCTACCTGACGCAGATGGCCCCCGCATCCACGATCTCGAACTGCGCC
Q M G S A Y L T Q M A P A S T I S N C A

3241 GCCTACCAGACCGCCGACTCGCTGCGGTGGCTGACCCACACCGCATATCGCACGCGAGAG
A Y Q T A D S L R W L T H T A Y R T R E

3301 CTGTCTCAGACCTTCGGCGACGTGGGCTTTGGCACCGACGAGCGCAGGTACTGGGAGCAG
L S Q T F G D V G F G T D E R R Y W E Q

3361 GACCCGGCCTGGCAGGGCTGGCGCAAGCTGGTCGAACACGCGCTCGTGGCATGGGACTGG
D P A W Q G W R K L V E H A L V A W D W

3421 GCAGAGTGCTTCGTCGCCTTCAGCCTGGTATTGCGGCCGGCGATGGAGGAAGCCGTCCTG
A E C F V A F S L V L R P A M E E A V L

3481 CGCGGGCTTGGCGAGGCGGCGCGCCACAACGGCGACACCCTGCTCGGCCTGCTGACTGAC
R G L G E A A R H N G D T L L G L L T D

3541 GCGCAGCTTGCCGACGTCCAGCGGCACCGGCACTGGGCCGGCGCGCTCGTCCGCATGGCC
A Q L A D V Q R H R H W A G A L V R M A

3601 CTGGAGACGCCGGGCAATCGTGACGTGCTGGCCGGCTCGATTGCCCGGTGGGCGCCGCTC
L E T P G N R D V L A G S I A R W A P L

3661 GCGGACGATGCAATCAGTGCCTACTGCGCGGCGTTGCCCGACGCGCCGAACGCGAAGGCG
A D D A I S A Y C A A L P D A P N A K A

3721 CGGGCCTGCGCGGCCGTGCGCGACTTCTGGGACAGCATCGGCCTGGCAGGTCTGTAACGC
R A C A A V R D F W D S I G L A G L stop

RBS

3781 AGGACATGCCGGGCGATACGACTCAACAGCCACCATCGGAACCCTATGAAATACCAGATA
M K Y Q I

3841 TCGATCGAAGGCGGCGCGGTGTTCACCGTCGCCGCGGAGGAAGACACGCTGCTGCGCGGC
S I E G G A V F T V A A E E D T L L R G

3901 GCCCTGCGCGCCGGCATGGCCCTGCCGCACGAGTGCAGCGTGGGCGGCTGCGGCGCGTGC
A L R A G M A L P H E C S V G G C G A C

3961 CGCTTCGACCTTGTGGACGGGCTCATGGAATCCGTCTGGCCTGAGGCGCCCGGCCTGTCC
R F D L V D G L M E S V W P E A P G L S

4021 GAGCGTGACCGCAAGCGTGGCAAGTACCTTGCGTGCCAGTCGCGGCCGCTAAGCGACTGC
E R D R K R G K Y L A C Q S R P L S D C

Figure 10 - *Continued*

```
4081    ACGATACGTGTGCGCTGCGACGAATCGTATCGCCCGGCGGTCCGGGCGCATCGCCGCGCA
         T  I  R  V  R  C  D  E  S  Y  R  P  A  V  R  A  H  R  R  A
                                                  EcoRI
4141    GCGGAACTCCTGGCACGCCGCGCGCTGACCCCTGACATGAGCGAATTCACGTTCCGGGTT
         A  E  L  L  A  R  R  A  L  T  P  D  M  S  E  F  T  F  R  V

4201    CCAGGCGCGACCGAGTTCCGGCCCGGCCAGTACGCGCTGCTCTACCCGCCCCGTGCACCG
         P  G  A  T  E  F  R  P  G  Q  Y  A  L  L  Y  P  P  R  A  P

4261    GGCGCCCGCGCCTATTCGATGGCCAACCTGCCCAACGAGGAAGGCATCTGGAAGTTCGTG
         G  A  R  A  Y  S  M  A  N  L  P  N  E  E  G  I  W  K  F  V

4321    ATCCGCCGCGTGCCGGGCGGGGCTGGCAGCAACGCGCTGTTCGACCAGGTCGGAATCGGG
         I  R  R  V  P  G  G  A  G  S  N  A  L  F  D  Q  V  G  I  G

4381    GACAGCGTCGTGCTCGACGGGCCGTACGGCCACGCCTACCTTCGTGAGGACAGTGCCCGC
         D  S  V  V  L  D  G  P  Y  G  H  A  Y  L  R  E  D  S  A  R

4441    GACATTGTCTGCATCGCCGGTGGCTCGGGCCTGGCGCCAATGCTGTCGGTCGCACGCGGA
         D  I  V  C  I  A  G  G  S  G  L  A  P  M  L  S  V  A  R  G

4501    GCACTCGCCGGTAGCGGTTCGCGGCGCGTCCACTTCTTTTATGGCGCCCGGGGGCAGGCT
         A  L  A  G  S  G  S  R  R  V  H  F  F  Y  G  A  R  G  Q  A

4561    GACCTCGGTGCCCTCGACGCCCTGGAAAAACTTGCCGAAGACAAGCGGGTTACGCTGTCG
         D  L  G  A  L  D  A  L  E  K  L  A  E  D  K  R  V  T  L  S

4621    GTGGCACTGTCCGCACCGGAGAGCACCTGGAAGGGGCCAACGGGGTTCGTGCACGAGGAA
         V  A  L  S  A  P  E  S  T  W  K  G  P  T  G  F  V  H  E  E

4681    GTCGAGCGTAACCTGACAGCTTCCCTCGGCAGCTACGACTTCTATTTTGCCGGGCCGCCA
         V  E  R  N  L  T  A  S  L  G  S  Y  D  F  Y  F  A  G  P  P
                                                  KpnI
4741    CTCATGATCGAAGCCATGCAGGCGCTCCTGATGCACAAGCACCAGGTACCGTTCGGGCAG
         L  M  I  E  A  M  Q  A  L  L  M  H  K  H  Q  V  P  F  G  Q

4801    ATCCGCTTCGACCGCTTTGTCTAGGCCGGCGACATCTGCCTTGGGACGCACAGCGCACAG
         I  R  F  D  R  F  V  stop

4861    CCGCGACACCGGATAGCCTGATCGCAAATGCCGCGTGCGATTACCAATCGCCATATCTGG

4921    AAGTTGGCGATAAGCTCCTTCTACCGAGCACTACATGGCCTGCGGGGGCCGGTGGATATC

4981    GGTCCCCGGACTGGACCGCGCGAGGCGCGACACCGCGCTCGCGCGTCCGCAACCGCGCCA

                RBS
5041    GTCGCGATTGAGGAAATCATGGCGAAGAGGCATCCCGGAAAACCCAAGTCCGGCTCACCG
                              M  A  K  R  H  P  G  K  P  K  S  G  S  P

5101    GCGCAAGGCCATCCCGGCCGGAATCAGAAGCGCGAGTCCCCCGAGGCAATCCGGGTGCCG
         A  Q  G  H  P  G  R  N  Q  K  R  E  S  P  E  A  I  R  V  P

5161    GCGATCCACGACCTCGCCAAGCGCCTGCGCTTCGCGCCGCAACAGGGTCGCATCTGGTTG
         A  I  H  D  L  A  K  R  L  R  F  A  P  Q  Q  G  R  I  W  L
```

Figure 10 - *Continued*

```
5221    GACGACCAACGCATGATGCTAATGCACATCAGCTCTCTTGGCGCCTTGCGGCAAGAACTG
         D  D  Q  R  M  M  L  M  H  I  S  S  L  G  A  L  R  Q  E  L

5281    ATCGAAAGCCTTGGCAAGGAAACAGCGCGCGGACTGATCACCCGTATCGGCTACCAGGCC
         I  E  S  L  G  K  E  T  A  R  G  L  I  T  R  I  G  Y  Q  A

5341    GGCACGCGGGACGCAGCGATGGCGCGCAAGGTCCGCGCCGGCCTGAACACCTATGACGAC
         G  T  R  D  A  A  M  A  R  K  V  R  A  G  L  N  T  Y  D  D

5401    TTCCTGGCCGGTCCACAACTGGTCTCGCTGGAGGGTATGGTGCATTGCGAACCGGTGGCG
         F  L  A  G  P  Q  L  V  S  L  E  G  M  V  H  C  E  P  V  A

5461    CTGGACATCGATGTCCAGCGTGGCCACTACTTCGGCGATTTTTATCTGGTGGACAGCTCC
         L  D  I  D  V  Q  R  G  H  Y  F  G  D  F  Y  L  V  D  S  S

5521    GAGGCGGAAGCCCACATCGCCGGCTATGGTATCGGCAATGAATCCGTGTGCTGGATGCTG
         E  A  E  A  H  I  A  G  Y  G  I  G  N  E  S  V  C  W  M  L

5581    ATCGGTTATGCATGCGGCTATACCAGTGCCTTCATGGGCCGTCCCATCCTGTGGAGGGAA
         I  G  Y  A  C  G  Y  T  S  A  F  M  G  R  P  I  L  W  R  E

5641    ACCGAATGCCGGGGGATGGGGCATGTGAAATGCCGCGTGGTAGGCAAGCCGGTGGAGGAA
         T  E  C  R  G  M  G  H  V  K  C  R  V  V  G  K  P  V  E  E

5701    TGGGAAGACGCCCAGGACGACCTGCGCTTCCTGAGGATCGGCGATTTCGTCAAATGGGCA
         W  E  D  A  Q  D  D  L  R  F  L  R  I  G  D  F  V  K  W  A

5761    CCGGTGGACGAGGCGGCCCTGCCCGCCACGAGCCGCATCGCGGCGCGGCTGTCCAGCGCC
         P  V  D  E  A  A  L  P  A  T  S  R  I  A  A  R  L  S  S  A

5821    CCGGAGAACAGCTTCGGCGTGGTCGGCATCTCCGCCGGCTTCAACACCGTCTGCCACATG
         P  E  N  S  F  G  V  V  G  I  S  A  G  F  N  T  V  C  H  M

5881    GTCAACAAGGTGGCGCCCACCGACGCCACCGTGCTGTTCCTGGGGGAAAGCGGTGTTGGC
         V  N  K  V  A  P  T  D  A  T  V  L  F  L  G  E  S  G  V  G

5941    AAGGAAGTCTTTGCGAACAACCTGCATCGCCTGAGCAAGCGCGCCGACGGCCCTTACGTC
         K  E  V  F  A  N  N  L  H  R  L  S  K  R  A  D  G  P  Y  V

6001    GCGGTGAACTGTGCGTCCATTCCGGAACACCTGATGGAATCCGAGTTATTCGGCGTCGAG
         A  V  N  C  A  S  I  P  E  H  L  M  E  S  E  L  F  G  V  E

6061    CGCGGCGGCTTTACGGGCGCCACCACATCCCGCGCCGGCCGCTTCGAGCGGGCCGATGGT
         R  G  G  F  T  G  A  T  T  S  R  A  G  R  F  E  R  A  D  G

6121    GGCACGCTGTTTCTCGACGAGGTCGGCACACTGAGCTTCACGGCACAGGGAAAGCTGCTG
         G  T  L  F  L  D  E  V  G  T  L  S  F  T  A  Q  G  K  L  L

6181    CGCGCGCTACAGCAGGGTGAGATCGAGCGTGTGGGCGATACACGCACCCGGAAAGTCAAC
         R  A  L  Q  Q  G  E  I  E  R  V  G  D  T  R  T  R  K  V  N

6241    GTCAGGGTGGTTGCCGCCACGAACGTGAACCTGCGTGAAGCTGTCAAGGCTGGCCACTTC
         V  R  V  V  A  A  T  N  V  N  L  R  E  A  V  K  A  G  H  F

6301    CGCGAGGATCTGTTCTTCCGGCTGAACGTCTTTCCGATCCAGGTGCCGCCGCTGCGAGAG
         R  E  D  L  F  F  R  L  N  V  F  P  I  Q  V  P  P  L  R  E
```

Figure 10 - *Continued*

```
6361    CGCCGCGACGACATCCCGCTGATGATGAACTGGTTCCTCCAGCGCATGGCACGCAAGCAT
         R  R  D  D  I  P  L  M  M  N  W  F  L  Q  R  M  A  R  K  H

6421    GACAAGCACATCACCGGCTTCCGCGAACGCGCCGTGGACGCGATGTTCGCCTATGACTGG
         D  K  H  I  T  G  F  R  E  R  A  V  D  A  M  F  A  Y  D  W

6481    CCCGGCAACGTCCGAGAGCTGGAGAACATGATCGAGCGCGCGGTCATTCTGGCCGAGGAC
         P  G  N  V  R  E  L  E  N  M  I  E  R  A  V  I  L  A  E  D

6541    GGTGGCGCGCTCGACCTGTGCCACCTGTTCACCAGCGGCGAGGAAGTTGATACCACCGCT
         G  G  A  L  D  L  C  H  L  F  T  S  G  E  E  V  D  T  T  A

6601    TTCATGCTGAAGCGCAGCGGCAGCATCGGACGCGTCAGCGAAGCCAGCGAAGCGGAATCG
         F  M  L  K  R  S  G  S  I  G  R  V  S  E  A  S  E  A  E  S

6661    CCGCCGAGCGCTGCCGAAGGGCGACCTGGTCTGGCCGAAACGGAGGTGGCCATGCTGCGT
         P  P  S  A  A  E  G  R  P  G  L  A  E  T  E  V  A  M  L  R

6721    GCAGCCGTTGCCGAAGCCAACGGCAATCTGTCGCGCGCAGCCCGGGTGTTGGGAATCAGC
         A  A  V  A  E  A  N  G  N  L  S  R  A  A  R  V  L  G  I  S
                                 PstI
6781    CGTCCGACGCTGGCGTACAGGCTGCAGAAATACGGCATTACGCCTGAAGCGCAATGACGA
         R  P  T  L  A  Y  R  L  Q  K  Y  G  I  T  P  E  A  Q stop
                                                          (stop) F  R  K
6841    AATGCCCCCCGGCGCGGCCGCATAGCGCTGCGCCAGGGGGCTCGCTGCGCTAGAAGCGCT

         R  Y  A  L  V  A  N  L  Q  S  H  R  V  T  L  P  V  A  T  N
6901    TGCGGTATGCCAGAACCGCGTTGAGCTGCGAATGCCGCACGGTGAGCGGTACCGCAGTAT
                                                          KpnI
         P  Q  S  A  N  G  V  T  K  P  L  V  V  S  L  A  F  D  I  A
6961    TCGGCTGGCTGGCGTTCCCCACGGTCTTTGGTAACACCACCGACAAGGCAAAATCGATCG

         D  D  K  G  F  A  Y  T  A  G  G  S  L  T  T  T  P  I  A  P
7021    CGTCGTCCTTGCCGAATGCGTAAGTCGCGCCGCCACTCAGGGTGGTCGTGGGAATGGCCG

         V  V  A  L  L  M  G  N  P  I  A  E  Q  A  Y  H  F  G  G  R
7081    GCACAACGGCTAGCAGCATGCCGTTCGGTATGGCTTCTTGCGCATAGTGGAACCCGCCGC

         V  T  W  A  S  D  F  R  Y  A  V  G  L  G  F  V  N  T  D  R
7141    GCACCGTCCAGGCCGAATCGAAACGGTACGCCACGCCAAGGCCGAACACGTTGGTATCGC

         Y  N  Q  P  L  S  L  D  L  N  A  G  G  R  T  F  T  V  N  I
7201    GGTAGTTCTGCGGTAGCGACAGGTCGAGGTTCGCGCCCCCACGCGTGAAGGTGACGTTGA

         D  R  M  V  S  S  W  F  V  R  Q  Y  D  A  S  A  S  L  R  E
7261    TGTCACGCATCACGCTCGACCAGAACACTCGCTGGTAGTCCGCCGAAGCCGACAGTCGCT

         N  F  Q  H  S  I  G  V  T  F  Q  A  P  M  Q  F  D  R  V  R
7321    CGTTGAACTGGTGGCTGATGCCCACCGTGAACTGCGCCGGCATCTGGAAGTCCCGCACCC

         V  E  G  S  L  P  I  N  G  A  V  T  S  V  A  A  L  T  A  Q
7381    TGACTTCGCCGCTCAGCGGAATGTTGCCCGCGACGGTGCTGACAGCCGCAAGCGTGGCCT

         G  R  L  D  G  V  R  T  K  A  N  Y  A  L  G  V  R  T  D  P
7441    GCCCGCGAAGATCGCCCACCCGCGTTTTCGCGTTGTAGGCCAGTCCTACGCGGGTATCGG
```

Figure 10 - *Continued*

```
          T  I  D  Y  T  L  G  L  K  G  G  I  G  W  A  D  A  G  G  G
7501      GCGTGATGTCGTAGGTCAGCCCCAGTTTTCCGCCGATGCCCCAGGCATCGGCCCCGCCAC

          V  P  A  S  N  S  F  G  L  Y  G  G  S  L  G  P  V  S  L  L
7561      CGACGGGCGCGCTGTTCGAGAAGCCCAGGTACCCCCCGGAAAGGCCGGGCACGGAAAGCA
                                        KpnI
          T  P  V  L  S  G  S  V  R  R  Q  S  A  L  T  G  I  Q  T  V
7621      GCGTGGGCACCAGCGAACCAGACACCCGCCGCTGGCTGGCAAGCGTGCCGATCTGCGTGA

          D  L  L  T  G  L  N  L  S  T  W  V  A  D  L  S  A  G  L  T
7681      CGTCGAGCAGCGTGCCGAGATTGAGCGACGTCCAGACCGCATCCAGCGAGGCGCCGAGCG

          L  K  D  T  P  R  Y  A  V  A  F  P  I  R  L  V  L  L  R  S
7741      TCAGCTTGTCCGTCGGCCGATAGGCCACCGCAAACGGAATGCGCAGCACCAGCAACCGGG

          F  Q  D  L  G  T  Q  V  G  N  S  T  R  S  L  F  S  S  G  G
7801      AGAACTGGTCCAGGCCCGTCTGCACGCCATTGGACGTGCGCGACAGGAAACTGCTGCCCC

          Y  Q  T  G  L  G  A  E  A  F  I  G  A  G  L  A  I  N  D  H
7861      CGTATTGCGTACCGAGGCCCGCCTCCGCAAAGATTCCGGCGCCTAGCGCGATGTTGTCAT

          R  Y  V  F  A  A  E  P  A  F  Y  P  G  N  N  N  G  H  N  G
7921      GACGGTAGACGAACGCGGCCTCGGGCGCAAAGTAAGGCCCGTTGTTGTTGCCGTGGTTGC

          S  R  A  T  E  G  T  A  T  N  T  A  K  I  D  T  T  V  M  D
7981      CGGACCGGGCCGTCTCGCCCGTTGCCGTATTGGTGGCCTTGATGTCGGTGGTCACCATGT

          L  G  L  H  L  H  N  G  E  A  M  L  G  L  T  A  P  N  A  M
8041      CGAGCCCAAGATGCAGGTGATTCCCCTCGGCCATCAGGCCAAGTGTTGCCGGATTCGCCA

          M  A  A  P  G  I  D  F  A  A  G  T  G  G  M  A  R  S  V  P
8101      TCATCGCCGCTGGCCCGATGTCGAAGGCCGCTCCGGTCCCGCCCATAGCGCGGGAAACTG

          G  F  G  E  L  N  F  V  D  T  A  G  A  P  T  G  C  A  A  A
8161      GACCAAAGCCCTCCAGGTTGAACACGTCCGTTGCTCCCGCTGGTGTTCCGCACGCCGCAG

          C  L  A  V  A  V  R  V  Y  N  G  R  V  L  T  E  K  D  N  E
8221      CGCATAGCGCCACGGCCACGCGAACGTAGTTGCCTCTCACGAGTGTCTCCTTGTCATTTT

          P  S  L  S  A  R  P  M (RBS)
8281      CGGGGGATAGCGAAGCGCGCGGCATCGCCGGGGAAACGGACGAGCCTGCGCATTCGCAGA

8341      GTGATGCCTGCGGCCGGCCTGGCGTTGCAGCGCGGTCGCGTCAGTCGTATTGCAGAAGCC

8401      GTACCAGCTCGGCAGGCCACTCCGCTAAATCTCGATATTTACAGGGAAAACCATGAGGGT

8461      TTTCCGTCTCGACATGACCCTCCGCATGGACCTCCAGCTCCGTGCGACGCCTCTTGTCTC

8521      AATTTGACGATATGATCTACGCATCAGAATGTCCCGGTTTCATCAAATGATCGAATCCGG

8581      TGTGCGCGTGGGACGGTCCTTGCATCGCCCGGTAGGATCC
                                          BamHI
```

Figure10 - *Continued*

P1 from *Burkholderia pickettii* PKO1 (8), Pu from *P. putida* mt-2 pWWO (1) and Po from *Pseudomonas* sp. CF600 pVI150 (101) indicated that the *phl* promoter has a high degree of nucleotide sequence homology to these σ^{54}-dependent promoters (Figure 11).

Inducible expression of all known σ^{54}-dependent genes depends on and is positively regulated by enhancer-binding transcriptional activator proteins which typically bind to specific sequences located 100 to 200 bp upstream from the promoters they regulate (98). Consistent with this, a 63 bp enhancer-like palindromic region located 176 bp upstream of the putative *phlKLMNOPR* promoter was identified (Figure 10, nucleotides 18 to 62). This putative operator region contains a 13 bp imperfect inverted repeat and shares a high degree of identity with transcriptional activator binding sites of the *tbu*, *xyl* and *dmp* operons (Figure 12) (9, 15, 99). Overlapping this region is a 13 bp region homologous to the core integration host factor (IHF) consensus-binding site of WATCAANNNNTTR (W = A/T, R = A/G) (13) (Figure 10, nucleotides 57 to 69). IHF, a DNA bending protein, has been shown to facilitate loop formation and is associated with several σ^{54}-dependent transcriptional activators (83). Core IHF-binding sequences have also been found near the transcriptional activator binding sites of the *tbu*, *xyl* and *dmp* operons (Figure l2) (9, 15, 99).

An eighth ORF, termed *phlX*, was found downstream and encoded divergently of the *phlKLMNOPR* gene cluster. Examination of the region upstream of *phlX* revealed no obvious promoter or operator sequences. Considering its proximity to the vector promoter, it is likely that *phlX* is transcribed constitutively from the vector-encoded promoter.

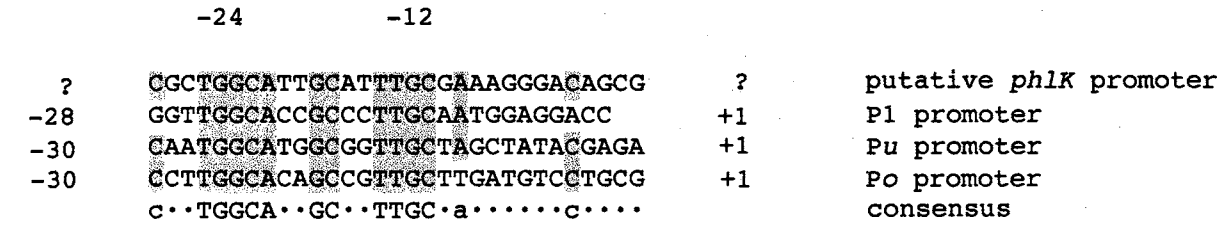

Figure 11. DNA sequence alignment of the *phl* promoter region and the promoter region of related σ^{54}-dependent promoter of P1 from *B. pickettii* PKO1, Pu from *P. putida* mt-2 pWWO, and Po from *Pseudomonas* sp. CF600 pVI150. Where determined, the transcription start site is indicated with a +1 designation. The -12 and -24 consensus sequences are indicated above the sequences as such. A consensus sequence of these promoter regions is given below the sequence. Uppercase letters in the consensus sequence indicate 100% identity while lowercase letters indicate 75% identity.

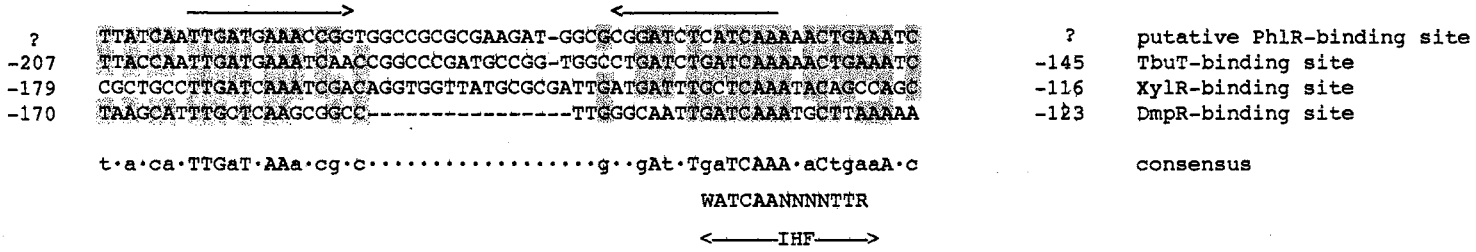

Figure 12. DNA sequence alignment of the putative PhlR transcription activator binding site with palindromic regions containing the TbuT, XylR and DmpR σ54-dependent transcriptional activator binding sites upstream of P1, Pu and Po promoter regions, respectively. The 13 bp imperfect inverted repeat is indicated by arrows above the respective sequence. The location of a common putative IHF-binding site is shown below the sequences. Where determined, the position relative to the transcription start site is indicated adjacent to the respective sequence. A consensus sequence derived from the comparison is displayed below the sequence alignment. Uppercase letters in the consensus sequence indicate 100% identity while lowercase letters indicate 75% identity. To maximize alignments, gaps were introduced and are indicated by dashes.

Comparison and analysis of the deduced amino acid sequences.

The deduced amino acid sequence of all eight ORF's identified is shown in Figure 10. Results from database searches of the deduced amino acid sequences (summarized in Table 9) revealed significant identity and homology between the putative polypeptide products of the *phlKLMNOP* genes and several multicomponent enzymes involved in the hydroxylation of phenol. The putative *phlR* gene product shares significant homology to TbuT, DmpR and XylR σ^{54}-dependent transcriptional activators. The eighth ORF, *phlX*, encodes a putative polypeptide with considerable homology to several putative aromatic transport facilitator proteins.

(1) PhlK, PhlO and PhlL. The first ORF, termed *phlK* encodes a putative polypeptide 502 amino acids in length with a deduced molecular mass of 57.6 kDal and represents the largest product of the putative catabolic enzyme. It was found that PhlK shares homology with oxygenase components of several toluene monooxygenase and phenol hydroxylase systems, including TbuA1 from toluene-3-monooxygenase of *Burkholderia pickettii* PKO1(8), BmoA component from benzene monooxygenase of *Pseudomonas aeruginosa* JI104 (50), TmoA component from toluene-4-monooxygenase of *P. mendocina* KR1 119), DmpN component from phenol hydroxylase of *Pseudomonas* sp. CF600 (77) and MopN component from phenol hydroxylase of *Acinetobacter calcoaceticus* (20). Amino acid sequence alignment of the above proteins is shown in Figure 13. Two copies of the amino acid sequence motif (D/E)X(~30)DEXRH have been identified in each peptide aligned (Figure 13). This motif contains potential iron ligating residues which are indicated and are associated with four non-contiguous α-helices (not shown) resembling the structure of class II diiron proteins as in the R2 component of *E. coli* ribonucleotide reductase (27). Consistent with the

Table 9. Organization of the *phl* open reading frames and comparison of deduced products with homologous genes

phl ORF	Coordinates (nt)[a]	Number of aa residues (deduced)	kDal (deduced)	Similar gene[b]	% aa identity[c]	% aa similarity[c]	Function
phlK	296-1801	502	57.6	*tbuA1*	93	97	oxygenase component
				bmoA	72	84	oxygenase component
				tmoA	67	82	Tmo component
				dmpN	24	49	oxygenase component
				mopN	27	51	hydroxylase component
				ph1D	24	49	hydroxylase component
				phhN	24	49	hydroxylase component
phlL	*1826-2086*	*87*	*9.6*	*tbuU*	*91*	*98*	*Tbu component*
				bmoB	67	88	Bmo component
				tmoB	44	70	Tmo component
phlM	2094-2429	112	12.1	*tbuB*	91	95	ferredoxin protein
				bmoC	62	83	ferredoxin component
				tmoC	47	71	Tmo component
phlN	2449-2763	106	11.9	*tbuV*	9594	97	Tbu component
				bmoD1	64	81	Bmo component
				tmoD	55	73	Tmo component
				tbmC	36	54	Tbm component
				mopM	27	55	hydroxylase component
				dmpM	27	51	hydroxylase component
				phhM	27	51	hydroxylase component
				ph1C	25	51	hydroxylase component
phlO	2779-3777	333	37.5	*tbuA2*	88	95	oxygenase component
				tmoE	55	70	oxygenase component
				bmoL	25	48	hydroxylase component
				phhL	25	48	hydroxylase component
				ph1B	25	48	hydroxylase component
				tbmB	24	48	hydroxylase component
				mopL	25	48	hydroxylase component

[a] Coordinated of open reading frames as in Figure 10.

[b] Genes noted in the text are as follows: *tbu*,toluene-3-monooxygenase; *bmo*, benzene monooxygenase; *tmo*, toluene-4-monooxygenase; *dmp*, phenol hydroxylase; *tbm*, toluene/benzene-2-monooxygenase; *mop*, phenol hydroxylase; *phh*, phenol hydroxylase; *ph1*, phenol hydroxylase; *xyl*, xylene monooxygenase; *cum*H, cumene outer membrane protein; *xyl*N, toluene-specific porin; *tod*X, toluene transport facilitator.

[c] Sequences were obtained from the GenBank and SwissProt databases using the BLASTP program and comparisons were performed using the GCG software package from the University of Wisconsin.

Table 9. *Continued*

phl ORF	Coordinates (nt)[a]	Number of aa residues	kDal (deduced)	Similar gene[b]	% aa identity[c]	% aa similarity[c]	Function
phlP	3826-4824	333	36.1	*tbuC*	77	86	oxidoreductase
				tmoF	37	60	electron transfer component
				mopP	31	55	hydroxylase component
				ph1F	32	54	hydroxylase component
phlR	5059-6837	593	65.1	*tbuT*	88	93	transcriptional activator
				dmpR	46	67	transcriptional activator
				mopR	44	64	transcriptional activator
				tbmR	45	67	transcriptional activator
				xylR	45	66	transcriptional activator
				phhR	30	53	transcriptional activator
				ph1R	47	68	transcriptional activator
phlX	8305-6890	471	49.3	*cumH*	47	67	outer membrane protein
				xylN	41	64	toluene-specific porin
				todX	45	69	toluene transport facilitator

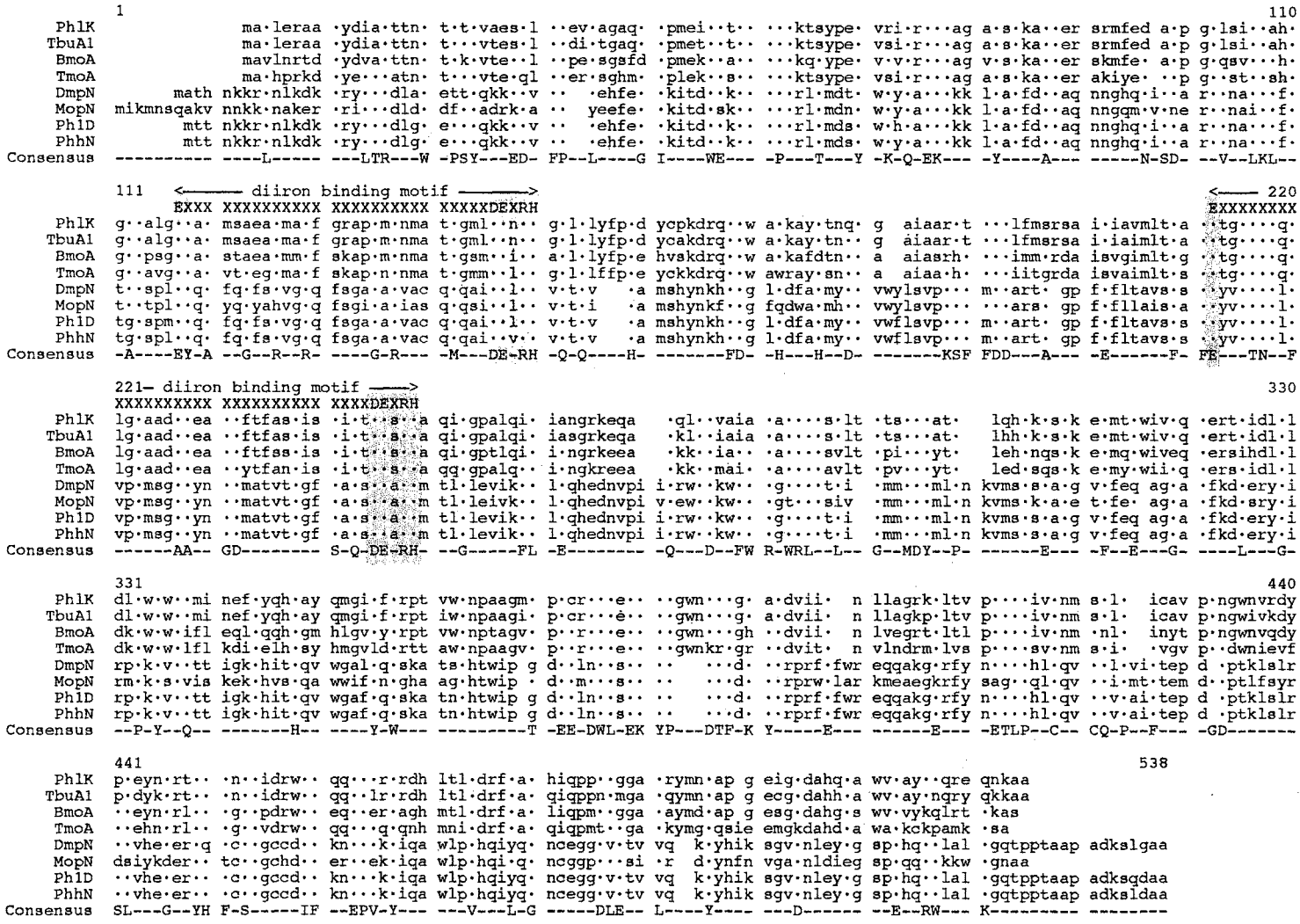

Figure 13. The amino acid sequence alignment of PhlK and several related toluene and phenol oxygenase components. Sequences were obtained from the GenBank or SwissProt databases using the BLASTP program while comparisons and consensus were performed using the Pileup program of the University of Wisconsin GCG software package. Conserved amino acids are indicated as dots. Gaps are represented by spaces. Alignment with the diiron amino acid sequence motif is given and the four shaded regions represent conserved amino acid residues believed to serve as potential iron ligand domains of class II diiron binding proteins.

identification of this motif, *in vitro* analysis of TmoA and DmpN has indicated that these two proteins contain a binuclear iron center (86, 88).

The deduced amino acid sequence of *phlO* (333 amino acids and 37.5 kDal) showed significant identity and homology to TbuA1 and TmoE components of toluene oxygenase as well as to DmpL and several other components of various phenol hydroxylases. TbuA1, TmoE and DmpL peptides are additional hydroxylase components of their respective systems. The smallest ORF identified, termed *phlL*, encodes a putative polypeptide 87 amino acids in length with a deduced molecular mass of 9.6 kDal which shares extensive homology with TbuU and TmoB toluene monooxygenase components and BmoB benzene monooxygenase component. Biochemical and genetic analysis have suggested that the proteins similar to PhlO, PhlL and PhlK comprise the oxygenase components for their respective systems. The oxygenase component of Tmo (toluene-4-monooxygenase) is a dimeric protein composed of three subunits (TmoA, TmoB and TmoE) that contains the catalytically competent diiron centers and putative substrate binding site(s) (86). Based on the similarities of size, amino acid sequence homology and the conserved iron binding domains, it is likely that PhlO, PhlL and PhlK are subunits of the hydroxylase component of Phl.

(2) PhlM and PhlP. The *phlM* ORF encodes a putative polypeptide 112 amino acids in length with a deduced molecular mass of 12.1 kDal. Database searching and amino acid sequence alignments of PhlM show significant homology to the Rieske-type ferredoxin components TbuB, BmoC and TmoC of toluene-3-monooxygenase (8), benzene monooxygenase (50) and toluene-4-monooxygenase (86), respectively. Rieske-type [Fe_2-S_2] centers are similar in function to other ferredoxin [Fe_2-S_2] centers but differ with mixed cysteine and histidine ligation. Amino acid sequence alignment of these four proteins revealed two regions 16 amino acids apart containing conserved cysteine and histidine

residues separated by one or two residues (Figure 14). This arrangement suggests these residues are involved in the coordination of a Rieske-type iron-sulfur cluster (93).

The *phlP* gene encodes a putative protein of 333 amino acids and a deduced molecular mass of 36.1 kDal with significant homology to several NAD(P)-dependent oxidoreductase proteins including TbuC (8) and TmoF (118) components of toluene monooxygenases and MopP (20) and Ph1F (40) components of phenol hydroxylases. Based on biochemical, genetic and DNA sequence analysis of purified protein, TmoF, an NADH-dependent oxidoreductase protein, contains features consistent with flavin and [Fe_2-S_2] domains (86). Amino acid sequence alignment of PhlP with related oxidoreductatase peptides shows putative FAD-isoalloxazine ring binding and NAD(P)-ribose-binding domains conserved in each of these proteins (Figure 15). In addition, a ferredoxin [Fe_2-S_2] binding motif which contains four conserved cysteine residues believed to serves as iron-sulfur ligands has been identified. Identification of such functional motifs is consistent with observations in other oxygenases where an FAD-dependent ferredoxin containing flavoprotein reductase mediates the transfer of electrons from NAD(P)H to the terminal oxygenase component (63).

The deduced composition of Tmo indicates that toluene-4-monooxygenase is composed of four components. Based on biochemical analysis, TmoF and TmoC are closely associated components but represent individual components of the catabolic enzyme (86). Based on the similarities in amino acid composition and the identification of similar functional motifs, PhlM and PhlP are likely oxidoreductase subunits of phenol hydroxylase involved in NAD(P)H-FAD-dependent electron transfer which, in a composition resembling that of Tmo, may comprise individual components of the catabolic enzyme. However, it is also

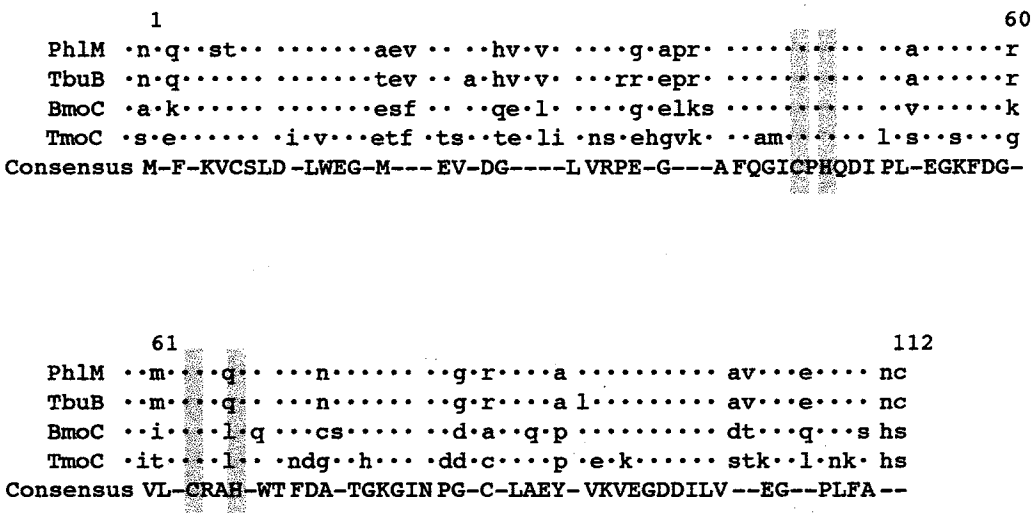

Figure 14. The amino acid sequence alignment of PhlM and related ferredoxin peptides. Sequences were obtained from the GenBank or SwissProt databases using the BLASTP program while comparisons and consensus were performed using the PILEUP program of the University of Wisconsin GCG software package. Conserved amino acids are indicated as dots. Gaps are represented by spaces. The shaded regions represent conserved cysteine (C) and histidine (H) residues present in Rieske-type ferredoxins.

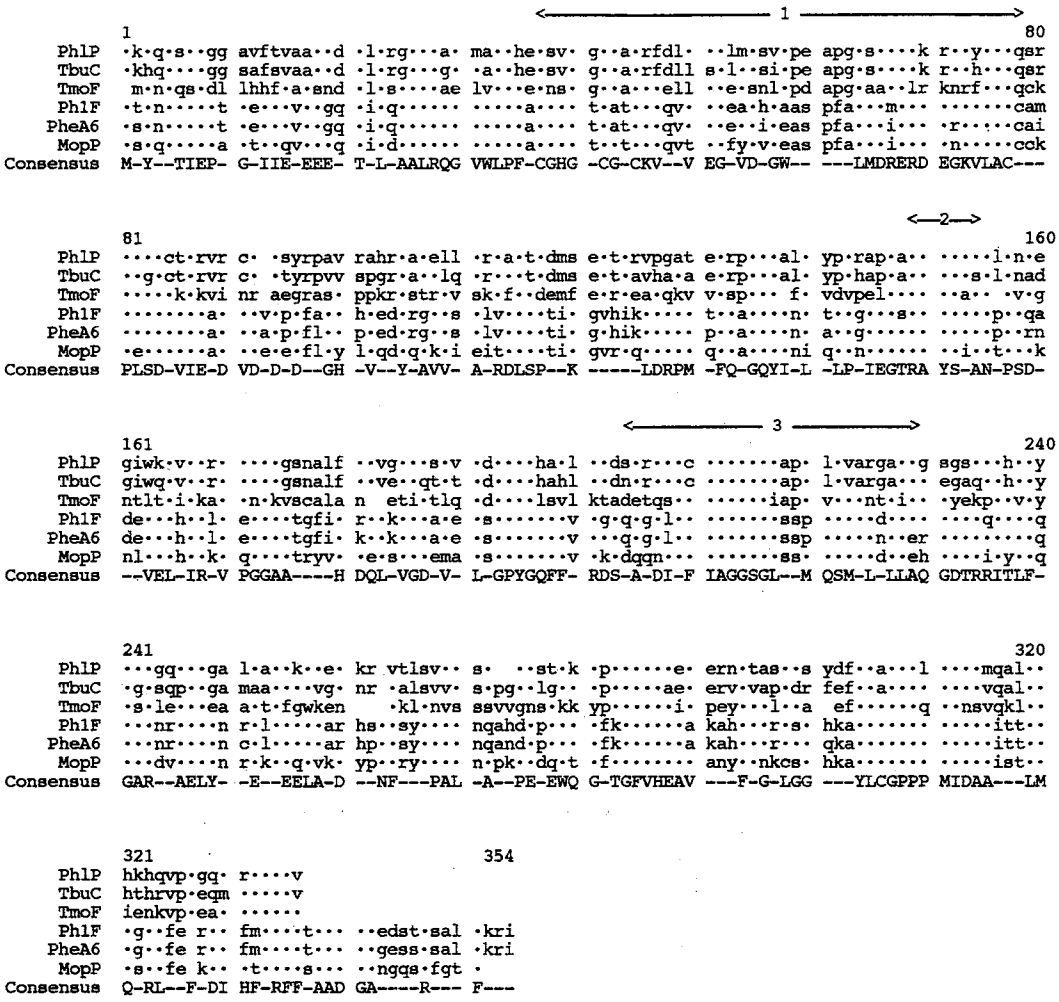

Figure 15. The amino acid sequence alignment of PhlP with related oxidoreductase peptides. Sequences were obtained from the GenBank or SwissProt databases using the BLASTP program while comparisons and consensus were performed using the PILEUP program of the University of Wisconsin GCG software package. Conserved amino acids are indicated as dots. Gaps are represented by spaces. The boundaries of four functional domains which include (1) a putative ferredoxin 2FE-2S iron sulfur cluster binding domain containing conserved cysteine (C) residues, (2) a possible FAD-binding domain and (3) a possible NAD(P)-binding domain are indicated with solid lines above the respective regions (motifs were identified using the Motif Finder program at University of Kyoto, Japan and Pfam program at the Sanger Centre, UK).

possible that PhlM and PhlP are more intimately associated than in Tmo and could exist together as subunits of the redox component in a composite structure resembling the three component phenol hydroxylase Dmp (87).

(3) PhlN. The deduced amino acid sequence of the *phlN* ORF (106 amino acids and 11.9 kDal) shares homology to TbuV and TmoD toluene monooxygenase components; BmoD1 and TbmC benzene and toluene/benzene monooxygenase components, respectively; and MopM, DmpM, PhhM, and Ph1C phenol hydroxylase components. While these homologous polypeptides are not associated with any known cofactors or redox-active metal ions, biochemical and genetic studies suggest TmoD and DmpM are essential components of their respective enzymes and act as dissociable, monomeric effector or activator proteins which bind to the oxygenase component, enabling interaction with the respective oxidoreductase component and subsequent catalytic activity (86, 87). The similarities in size and composition with TmoD and DmpM suggest PhlN may play a similar role in Phl catalytic activity.

These data provide strong indications toward understanding the composition and polypeptide requirements for Phl enzymatic activity of this multicomponent phenol hydroxylase. Comparisons of amino acid sequence homolgy and deduced peptide size with the deduced composition of characterized related mono- and di-oxygenases indicates that Phl most resemble the four component toluene-4-monooxygenase (Tmo) (86, 118, 119). Biochemical analysis of Phl would assist in further determining the composition of this aromatic oxygenase. A schematic representation of the deduced compositions of Tmo, Dmp and a hypothetical composition of Phl is provided in Figure 16. The oxygenase component of Phl is likely composed of three subunits, PhlK, PhlL and PhlO, which contain a diiron binding motif and a putative catalytic site. The proposed presence of an NAD(P)H domain, an FAD domain, and a

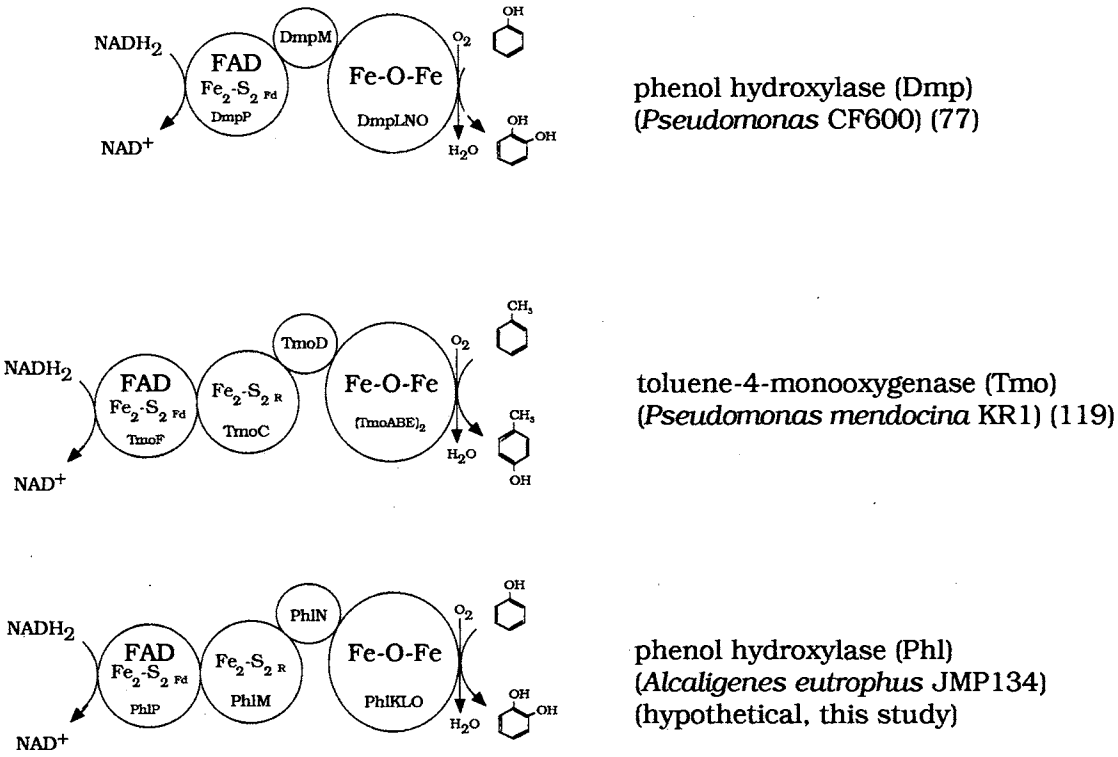

Figure 16. Comparison between the deduced composition of Dmp and Tmo and the hypothetical composition of phenol hydroxylase (Phl) of *Alcaligenes eutropus* JMP134. (Fd) denotes ferredoxin-type [Fe_2-S_2] center. (R) denotes Rieske-type [Fe_2-S_2] center.

ferredoxin center suggest a role for PhlP as an oxidoreductase component most likely associated with the small ferredoxin component, PhlM. Similar to the deduced role of TmoC, PhlM is most likely an intermediate electron carrier that functions to assist the transfer of electrons from the oxidoreductase component to the oxygenase component in this multicomponent phenol hydroxylase. Perhaps closely associated with the oxygenase component is PhlN which serves as an effector protein able to assist in complex formation and/or increase complex stability.

(4) PhlR. The deduced amino acid sequence of the seventh ORF (*phlR*) (593 amino acids and 65.1 kDal) was compared with those in the Genbank and SwissProt databases, and homology was found with TbuT (82), DmpR (99) and several other σ^{54}-dependent transcriptional activator proteins, all members of the NtrC family of regulatory proteins (19, 98), which activate a variety of genes all involved in the degradation of aromatic compounds (Table 9). This finding is consistent with the identification of σ^{54}-dependent transcriptional activator binding site and a σ^{54}-dependent promoter upstream of the catabolic genes (Figure 10). Analysis of the sequences upstream from the putative ribosome binding site for the *phlR* gene revealed no obvious promoter sequences, suggesting *phlR* is part of the *phlKLNMOP* operon.

Although unusual, this configuration in which the transcriptional activator is located downstream of the catabolic genes and within the same operon that it controls has been observed in the homologous Tbu system of toluene-3-monooxygenase from *Burkholderia pickettii* (9). Using *lacZ*-gene fusions, Byrne and Olsen (9) demonstrated that the *tbuT* gene is constitutively expressed at a low level in the absence of inducing substrate. Activation of TbuT resulted in transcription of the catabolic genes, (*tbuA1UBVA2C*) and read-through transcription of *tbuT* and increased synthesis of catabolic enzyme and TbuT (9).

This arrangement differs significantly from homologous transcriptional regulators reported from other phenol hydroxylase systems (42, 75, 95, 99) where the regulator genes are typically self-regulated but are transcribed divergently from the catabolic genes (68, 75, 95, 101, 109).

Members of the NtrC family of regulatory proteins activate σ^{54}-dependent promoters and contain three highly conserved domains located in the central and carboxy regions of the proteins and a fourth less conserved domain located in the amino region. These domains include: (1) a carboxy-terminal domain containing a conserved helix-turn-helix DNA binding motif (Domain D), (2) a central ATP-dependent σ^{54}-interaction domain (Domain C) and (3) a less conserved amino-terminal signal reception domain (Domain A). A small, flexible, domain (Domain B) exists between the signal reception and activation domains. Amino acid sequence alignment of PhlR and several related σ^{54}-dependent transcriptional activators shows extensive homology which can be localized according to these functional domains (Figure 17).

Aromatic effector compounds interact directly with the N-terminal Domain A of TbuT, DmpR, XlyR and MopR and are believed to stimulate ATPase activity in Domain C and subsequent activation of transcription (9, 95, 102). Transcriptional activation responses of TbuT, DmpR, XylR, and PhhR have generated an effector specificity profile for each. Each is activated by their respective aromatic substrate, catabolic intermediates and several structural analogues (such as methyl- and chloro-substitutes) (9, 75, 95, 101). Trichloroethylene (TCE) is also able to act as an efficient effector molecule in the activation of TbuT and toluene-3-monooxygenase (9). Further, TCE is able to induce toluene- and TCE-oxidizing activities in *B. pickettii* PKO1 whole cells (55), which correlates well with previous observations of TCE-mediated induction of phenol hydroxylase in AEK301/pYK3021 (Figure 5). Point mutations and allelic

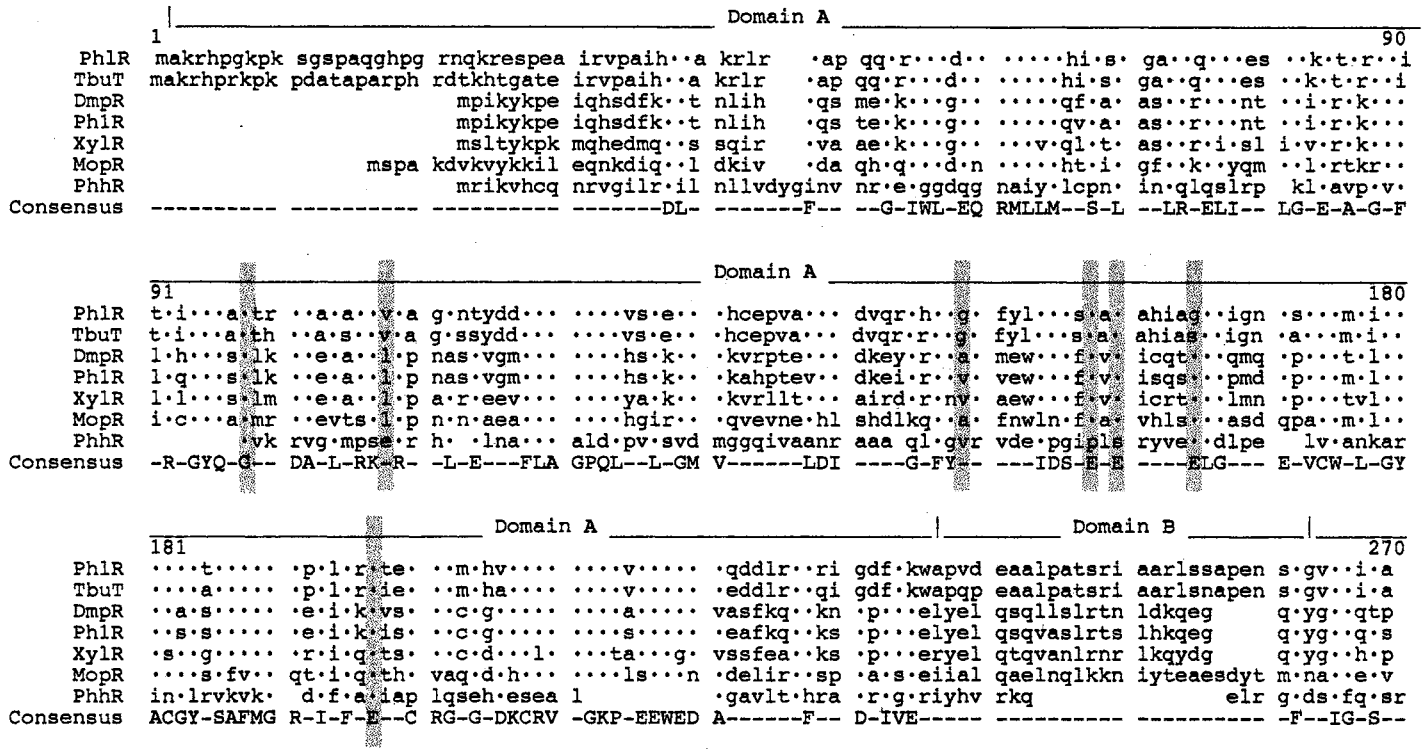

Figure 17. Amino acid sequence alignment of PhlR and several related σ54-dependent transcriptional activators. Sequences were obtained from the GenBank and SwissProt databases using the BLASTP program while comparisons and consensus were performed using the PILEUP program of the University of Wisconsin GCG software package. Motifs were identified using the Motif Finder program at University of Kyoto, Japan and Pfam program at the Sanger Centre, UK. Conserved amino acids are indicated as dots. Gaps are represented by spaces. The boundaries of the four functional domains which include Domain A (signal reception), Domain B (linker), Domain C (ATP-dependent, σ^{54}-RNA polymerase activation), and Domain D (DNA binding) are indicated with solid lines above the respective regions. The locations of a putative ATP-binding site, ATP-hydrolysis site and helix-turn-helix DNA binding motif are also indicated. The shaded regions represent alignment of residues known to be involved in effector binding and subsequent activation in DmpR or XylR.

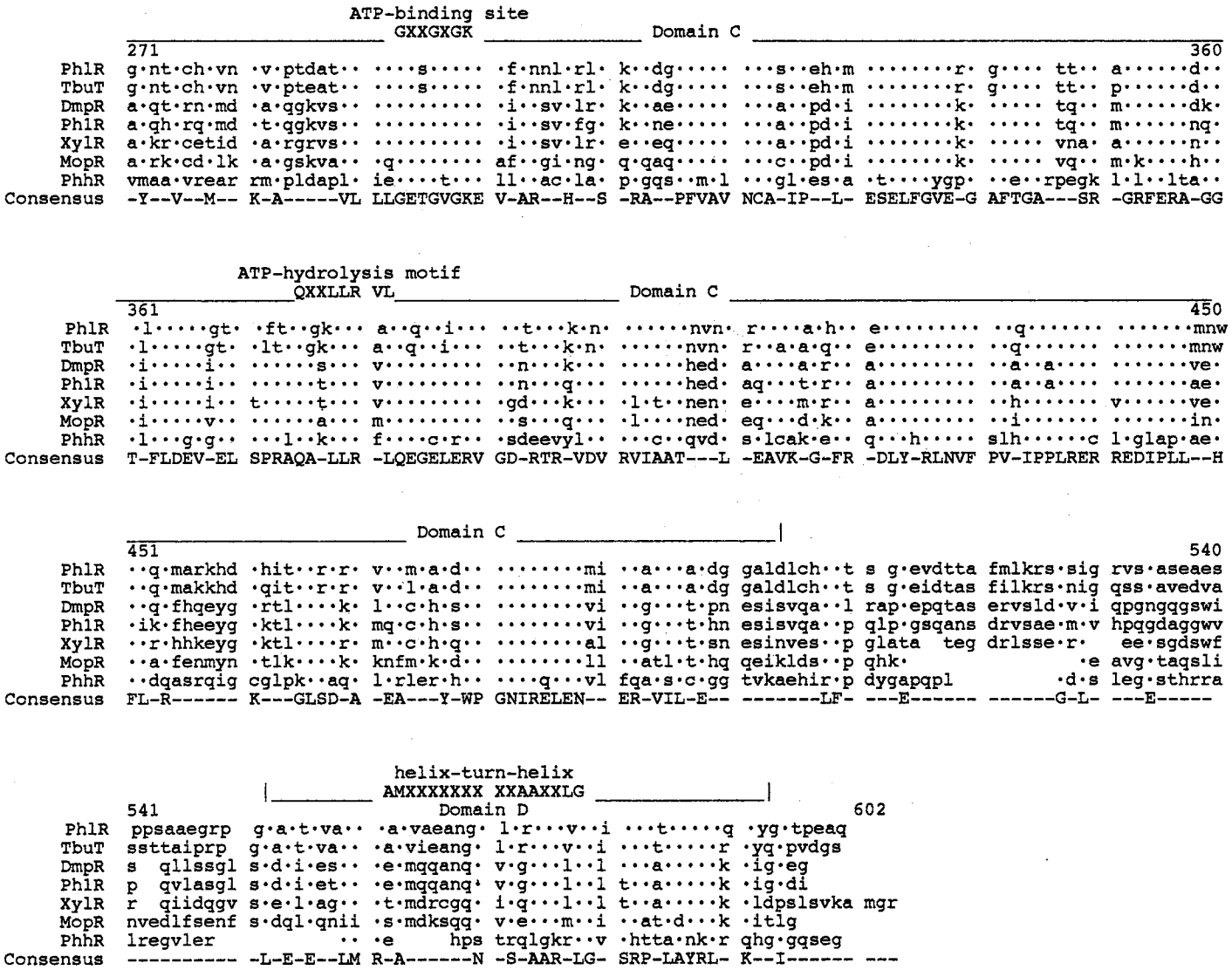

Figure 17 - *Continued*

exchange of *dmpR* or *xylR* which altered amino acid composition of the Domain A region of their respective proteins, resulted in alterations of the effector profiles and have implicated several residues believed to interact directly with effector molecules (Figure 17) (16, 98, 101, 102). These observations suggest that minor changes in the amino acid sequence of this domain can result in alterations of the growth substrate range of the organism.

(5) PhlX. The deduced amino acid sequence of *phlX* (471 amino acids and 49.3 kDal) showed significant homology to CumH, putative outer membrane protein closely linked to isopropylbenzene (cumene) dioxygenase of *P. fluorescens* IP01 (32); XylN, putative toluene specific porin of *P. putida* TOL plasmid pWWO (115); TodX, putative toluene transport facilitator of *P. putida* F1 (115); and lesser homology to numerous other outer membrane proteins. Amino acid sequence alignment of PhlX and other related proteins is given in Figure 18. Analysis of the deduced amino acid sequence of PhlX revealed five putative transmembrane helices (determined by TMpred) each ranging from 17 to 26 amino acid residues in length which are indicated on Kyte-Doolittle hydrophobicity plots (Figure 19). In addition, hydrophobicity plots of CumH, XylN and TodX are also provided with the location of predicted transmembrane helices indicated. Considering the apparent lack of promoter sequences upstream of *phlX* and its proximity to the vector promoter, it is likely that *phlX* is transcribed constitutively in AEK301 from the vector-encoded promoter.

A putative outer membrane protein encoded divergently downstream from the *tbuA1UBVA2CT* operon, termed TbuX (not shown), and showing homology to TodX has also been reported (11). Analysis of the sequences upstream of *tbuX* revealed a weak σ^{54}-dependent promoter, a putative activator binding site 300 to 400 bp upstream of the start codon and possible activation by the toluene-inducible TbuT σ^{54}-dependent transcriptional activator (10, personal

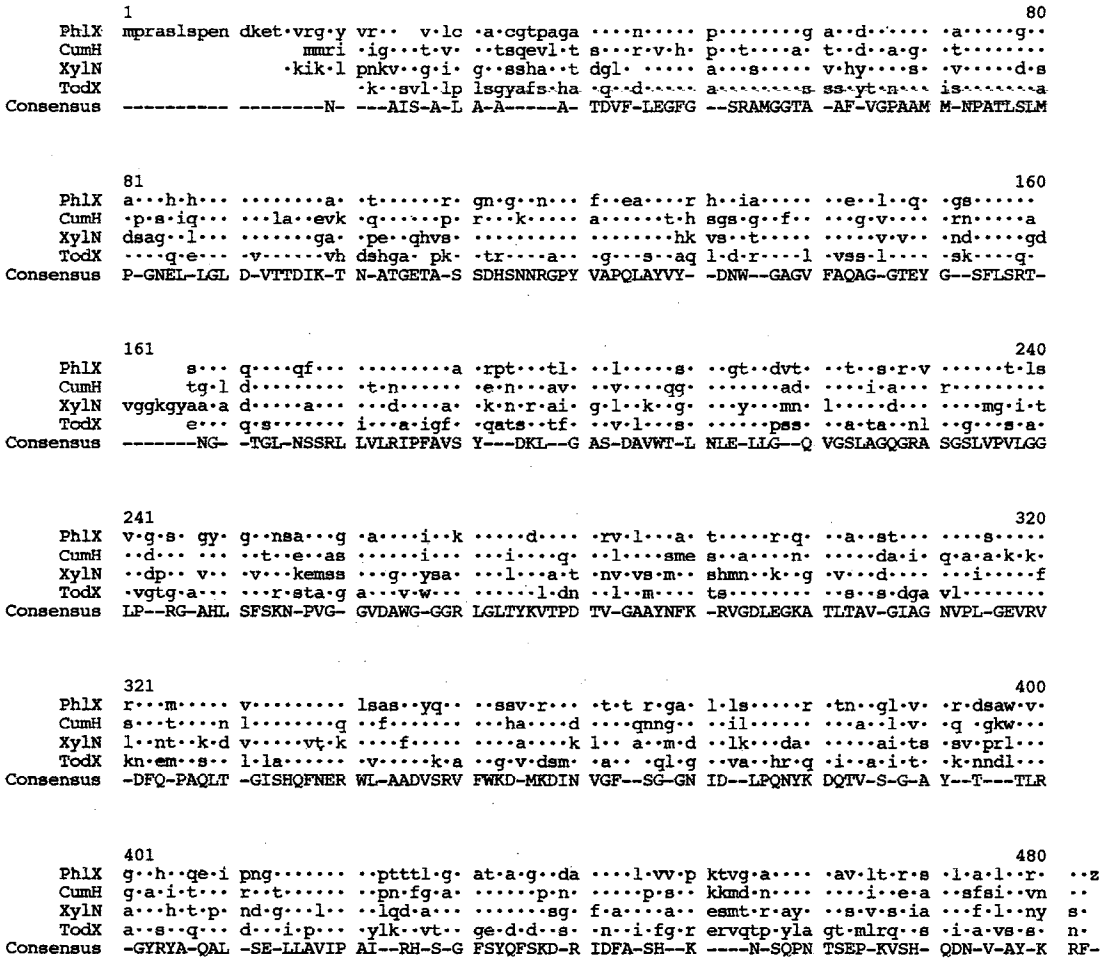

Figure 18. Amino acid sequence alignment of PhlX with similar putative aromatic transport facilitators. Scquenccs wcrc obtainccl from thc GcnBank databasc using thc BLASTP program whilc comparisons and consensus were performed using the University of Wisconsin GCG software package. Conserved amino acids are indicated as dots. Gaps are represented by spaces.

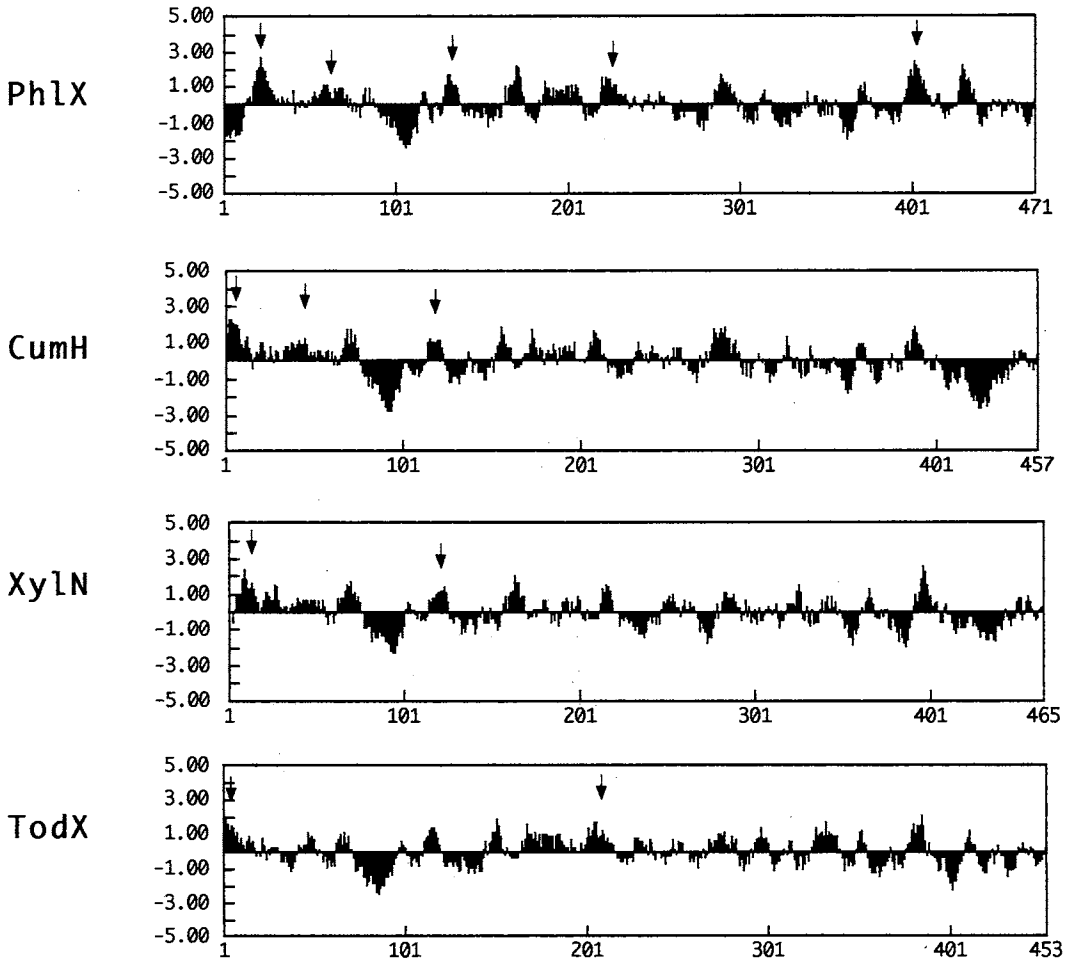

Figure 19. Kyte-Doolittle hydrophobicity plots (by MacDNASIS Pro) of PhlX, CumH, XylN and TodX. Regions with values greater than +0.5 are predicted to be membrane embedded. The arrows indicate the location of predicted transmembrane helices (by TMpred).

communication). These data suggest a role for this putative outer membrane protein in toluene metabolism and possibly involvement in facilitating the transport of toluene into the cell where this aromatic compound is able to activate transcription of *tbuX* and the *tbuA1UBVA2CT* operon through acitvation of TbuT (11, 10). Considering the overall similarities in gene organization, size and homology of corresponding genes of these two highly homologous gene clusters, it is likely that PhlX plays a role similar to that of TbuX in the metabolism of phenol in *Alcaligenes eutrophus* JMP134. While facilitation in transport of aromatic substrate is likely, involvement of PhlX and other homologous proteins in signal transduction or some other similar process cannot be overlooked. It is interesting to note that constitutive over-expression of trichloroethylene co-metabolizing phenol hydroxylase catabolic genes in *P. putida* KN1 resulted in relatively poor trichloroethylene degradation rates compared to phenol-induced wild-type. These observations indicate that transport of TCE into the cell rather than expression of the catabolic enzyme can be a rate-limiting step in TCE degradation (69). Interestingly, while AEK301/pYK3021 most likely expresses PhlX constitutively and is able to degrade TCE in the absence of phenol induction, phenol hydroxylase activity in crude extracts (determined by TCE degradation) was only observed following incubation of whole cells with TCE (data not shown) implying the need for a TCE-mediated induction of the catabolic genes in this construct. This observation suggests that constitutive expression of PhlX by this construct facilitates a rate-limiting step in TCE degradation. This rate-limiting step is most likely TCE transport into the cell or a TCE-mediated signal transduction, followed by a TCE-mediated transcriptional activation of the catabolic genes and subsequent degradation of TCE.

Conclusions

The complete nucleotide sequence and analysis of the genes involved in phenol hydroxylase activity and TCE oxidation in the absence of phenol induction by a JMP134 derivative has been presented. Analysis of the region encoding the catabolic enzyme has revealed that it is a multicomponent hydroxylase encoded by six tightly clustered ORF's which have been designated *phlKLMNOP*. The region encoding the PhlR transcriptional activator is located immediately downstream from the catabolic genes. The *phlKLMNOPR* gene cluster appears to comprise an operon and is proceeded by two regions which show significant homology to σ^{54}-dependent promoters. Analysis of sequences upstream from the σ^{54}-dependent consensus promoter sequence revealed the presence of 13 bp imperfect inverted repeats which share significant homology to related σ^{54}-dependent transcriptional activator binding sites. A sequence with significant homology to the core integration host factor (IHF)-binding sequence was also revealed within this putative operator region.

Based on deduced amino acid sequence comparisons with the GenBank and SwissProt databases, the first six genes of the *phlKLMNOPR* operon appear to encode for a multicomponent protein involved in the hydroxylation of phenol. This conclusion is further supported by the identification of a putative ferredoxin [Fe_2-S_2] iron-sulfur cluster binding domain and a putative FAD/NAD-binding oxidoreductase domain located within PhlP, a Rieske-type iron-sulfur cluster binding domain located within PhlM and a diiron binding motif located within PhlK. The seventh gene, *phlR*, appears to encode a transcriptional activator of the NtrC family. The locations of the functional domains of PhlR as a member of the σ^{54}-dependent regulator family have been indicated. This conclusion is further supported by the identification of a putative σ^{54} interaction domain, ATP-binding site and ATP-hydrolysis domain within the indicated RhoN-RNA

polymerase-activation Domain C and a putative helix-turn-helix motif within the indicated DNA binding Domain D. An eighth gene, *phlX*, appears to encode for an outer membrane protein with five hydrophobic regions (ranging from 17 to 26 residues) having a strong tendency to form transmembrane helices. Considering the lack of promoter sequences upstream of *phlX* and its proximity to the vector promoter, it is likely that *phlX* is transcribed constitutively from the vector-encoded promoter. Interestingly, DNA sequences further upstream of *phlX* previously reported to contain a regulatory element (48, 49) were deleted by subcloning in the construction of pYK3021 from the cosmid pYK301 (Figure 9). Deletion of this upstream DNA fragment resulted in TCE degradation in the absence of phenol induction by the AEK301/pYK3021 construct. Examination of this DNA region would be of interest to further characterize the overall regulation scheme of this interesting cluster of genes.

It is interesting that while Tbu and Phl share extensive homology, growth substrate ranges of *B. pickettii* PKO1 and *A. eutrophus* JMP134 are different. While *B. pickettii* PKO1 is able to grow on phenol or toluene as a sole source of carbon and energy, *A. eutrophus* JMP134 cannot grow on toluene as a sole source of carbon and energy. In fact, toluene degradation assays with AEK301/pYK3021 whole cells revealed only slight toluene degradation activity (not shown). Further, while TCE is able to induce toluene degradation activity in *B. pickettii* PKO1 whole cells, TCE is unable to induce its own degradation in *A. eutrophus* JMP134 wild type whole cells. These observations indicate important differences between these two species beyond the identities of the homologous catabolic proteins. The observed differences in growth substrate ranges of *B. pickettii* PKO1 and *A. eutrophus* JMP134 could be due to the effector activation specificities of the regulators of these systems. However, this explanation is not sufficient to explain the observed differences in TCE-mediated induction of

enzyme activity in *B. pickettii* PKO1 and *A. eutrophus* JMP134. The differences in growth substrate ranges and TCE-mediated induction of the catabolic proteins of *B. pickettii* PKO1 and *A. eutrophus* JMP134 are likely due to the induction and/or specificity of the putative outer membrane proteins rather than the substrate specificities of the catabolic enzymes.

CHAPTER V

DEVELOPMENT OF A PLASMID-FREE, GENETICALLY ENGINEERED MICROORGANISM FOR THE DEGRADATION OF TRICHLOROETHYLENE

Introduction

Trichloroethylene (TCE) is one of the most common ground water contaminants in the United States. TCE has long been widely used in numerous industries as a solvent for degreasing and washing. Although no microorganism has been identified that can use TCE as a sole carbon and energy source, TCE has been found to be co-metabolized by organisms growing on a variety of substrates including methane (58, 79), propene (92), toluene (71, 120) and phenol (48, 69, 110). We have recently reported on the development of a genetically engineered *Alcaligenes eutrophus* JMP134 derivative which is able to degrade TCE in the absence of aromatic induction (48). The genes responsible for phenol metabolism and TCE co-metabolism in JMP134 were cloned, uncoupled from a regulatory gene and subcloned using the pMMB67EH vector to generate the recombinant plasmid termed pYK3021 and introduced back into a JMP134 derivative deficient in phenol metabolism (48). Studies using this construct have shown a high capacity for TCE removal with limited sensitivity to TCE-mediated toxicity.

Although recombinant plasmids such as pYK3021 are readily maintained in bacterial monocultures under the carefully controlled conditions of the laboratory, they are frequently unstable in the absence of selective pressure or

when the host organism is subjected to less than ideal conditions such as those encountered outside of the laboratory. As an alternative to using a plasmid vector, a transposon-delivery system was examined as a method to insert the genes responsible for TCE degradation into the chromosome of AEK301 to construct a strain with improved stability and overall usefulness.

Materials and Methods

Bacterial strains and plasmids. The bacterial strains and plasmids relevant to this study are listed in Table 10. Strains of *Escherichia coli* were grown with aeration at 37°C in Luria-Bertani (LB) medium (61). Cultures of *Alcaligenes eutrophus* were grown in tryptone-yeast extract-glucose agar (TNB) (81) or in minimal salts medium (MMO) (107) supplemented with 10 mM sodium citrate and 2.5 mM phenol where indicated. Antibiotics were used at the following concentrations: ampicillin, 100 μg/ml (*E. coli*); carbenicillin, 50 μg/ml (*A. eutrophus*); kanamycin, 100 μg/ml, (*E. coli* or *A. eutrophus*); and spectinomycin, 50 μg/ml (*E. coli* or *A. eutrophus*). Yeast extract, tryptone and agar were purchased from Difco. Other media additives, bovine serum albumin, NADH and chromatography quality *n*-pentane were all purchased from Sigma. Chromatography quality trichloroethylene (TCE) and 1,2-dibromoethane (EDB) were purchased from Aldrich. Teflon/butyl septa and reactor vials were purchased from Fisher Scientific.

General DNA protocols. Preparation of competent *E. coli* cells and plasmid transformation were performed as described by Inoue, *et al.* (41). Plasmid DNA was isolated by rapid alkaline-sodium dodecyl sulfate extraction (5). For highly purified plasmid DNA, extraction was followed by sedimentation on cesium chloride-ethidium bromide density gradients. Restriction enzyme mapping, agarose gel electrophoresis and electroelution of DNA fragments from

Table 10. Bacterial strains and plasmids relevant to this study.

Strain or plasmid	Relevant characteristics[a]	Reference or source
Strains		
A. eutrophus JMP134	Prototroph, Phl^+, Tfd^+, Hg^r	17
A. eutrophus AEO106	Prototroph, Phl^+, Tfd^-, Hg^- derivative of JMP134	36
A. eutrophus AEK301	Rif^r, Phl^-, $C23O^-$, Km^r derivative of AEK106	48, 49
A. eutrophus AEP6	Rif^r, Phl^+, $C23O^-$, Km^r Sp^r derivative of AEK301	This study
E. coli S17(λ*pir*)	*recA, thi, pro, hsdR⁻M⁺* RP4:2-Tc:Mu:Km Tn*7*, λ*pir*	104
Plasmids		
pUT mini-Tn*5* (Sm/Sp)	Amp^r Sm^r Sp^r, mini-Tn*5* encoding Sm^r/Sp^r with a unique *Not*I site for insertion of cloned fragments on broad-host-range suicide plasmid	14
pVK102	IncP, cos^+, Km^r, Tc^r	51
pMMB67EH	Amp^r, Tac expression cloning vector	29
pYK301	Tc^r, 16.8 kb *Hind*III fragment of AEO106 DNA in pVK102	48, 49
pYK3021	Amp^r, 8.6 kb *Xho*I/*Bam*HI fragment from pYK301 containing the *phl*KLMNOPRX genes cloned into pMMB67EH	48, 49

[a]Abbreviations: Amp, ampicillin; Hg, mercury; Km, kanamycin; Rif, rifampin; Sm, streptomycin; Sp, spectinomycin; Tc, tetracycline; Phl, phenol hydroxylase; C23O, catechol 2,3-dioxygenase.

agarose gels were performed using standard procedures (4, 61). Restriction endonucleases, Klenow fragment, dNTP's (all four) and T4 DNA ligase were purchased from Bethesda Research Laboratories (BRL) while shrimp alkaline phosphatase was purchased from United States Biochemical Company (USBC) and each were used according to the directions of the suppliers. RnaseA was purchased from Sigma. DNA-DNA hybridization was performed using the DIG High Prime Labeling and Detection kit (Boehringer-Mannheim) for random primed DIG-labeled DNA (with digoxigenin-dUTP) and color detection of hybrids with an anti-DIG-alkaline phosphatase conjugate and the colorometric substrates NBT/BCIP.

Construction of a mini-Tn*5* delivery system for the chromosomal insertion of the phenol hydroxylase gene cluster. A mini-Tn*5* transposon delivery vector, pUT/mini-T*n5* Sm/Sp (14), developed for generating genomic promoter fusions and chromosomal insertion of cloned DNA was selected as a vehicle to mobilize the phenol hydroxylase gene cluster from pYK3021 into the chromosome of AEK301. The pUT plasmid has a host-limiting, π-protein dependent R6K origin of replication, carries an *oriT* for conjugal transfer, encodes for the transposase needed for transposition of the mini-Tn*5* element and can be maintained in λ*pir* lysogens of *E. coli* K-12 such as S17(λ*pir*) or SM10((λ*pir*) (39). In pUT/mini-T*n5* Sm/Sp, a unique *Not*I restriction site is located within the 19 bp-Tn5 ends adjacent to a streptomycin-spectinomycin resistance cassette and is suitable for the insertion of foreign DNA fragments and subsequent mobilization of the inserted DNA and Sm/Sp antibiotic resistance.

The plasmid pYK3021 was first digested with *Pvu*II and *Hind*III, and a 10.1 kb DNA fragment containing the phenol hydroxylase gene cluster and the vector encoded *Tac* promoter was isolated, blunt-ended and ligated to *Not*I digested, blunt-ended, dephosphorylated pUT/mini Tn*5* (Sm/Sp) (Figure 20).

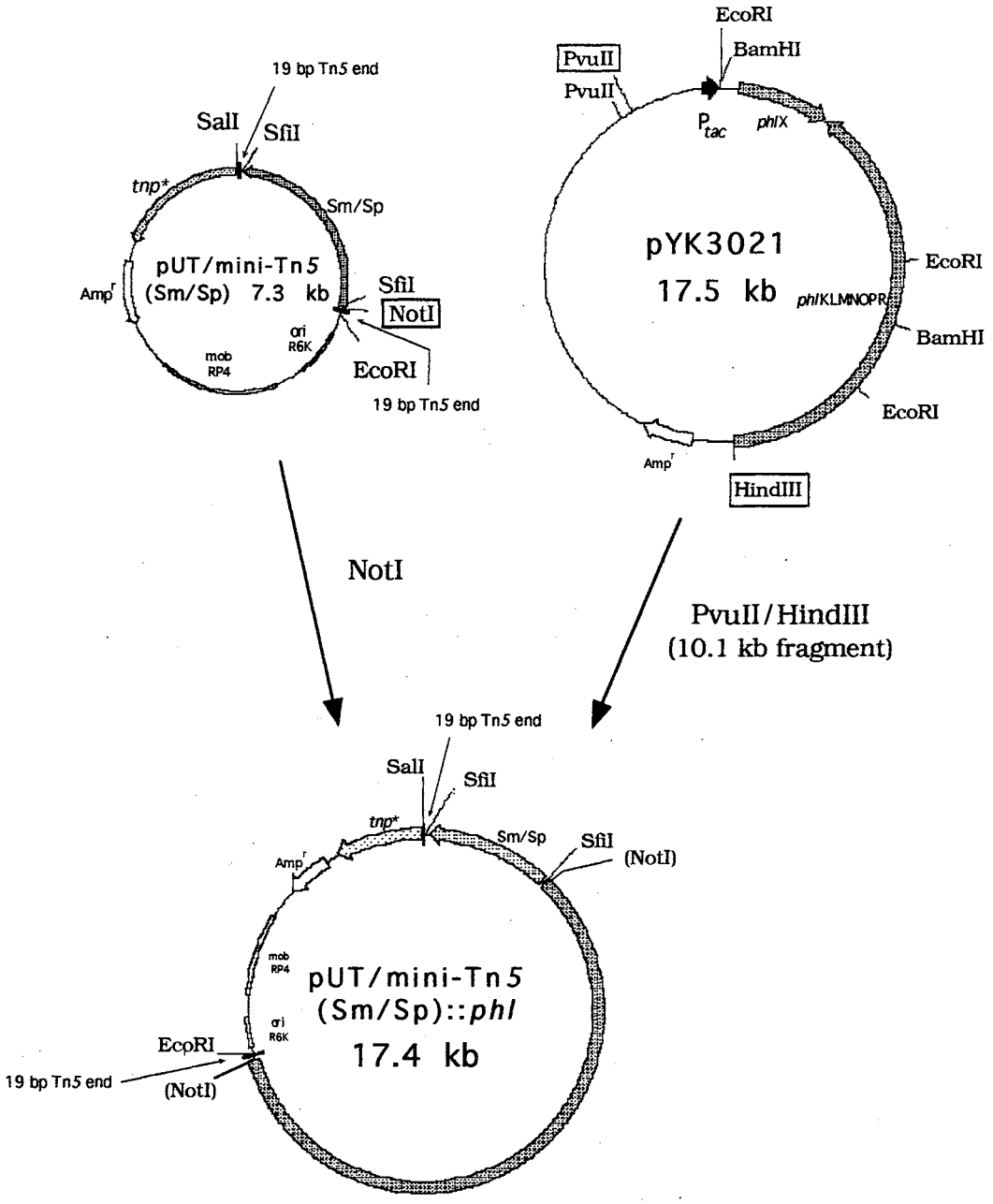

Figure 20. Construction of a mini-Tn5 delivery system for the insertion of the genes required for phenol hydroxylase activity into the AEK301 chromosome. A 10.1 kb blunt-ended *Pvu*II/*Hind*III fragment from pYK3021 was ligated to the *Not*I (blunt-ended) site of the pUT/mini-Tn5 (Sm/Sp) suicide transposon-delivery plasmid.

This ligation mixture was transformed into *E. coli* S17(λ*pir*). As previously observed (de Lorenzo, 1990 #203]), several unsuccessful attempts were made to recover pUT/mini Tn*5* (Sm/Sp) or a stable recombinant plasmid in *E. coli* S17(λ*pir*). Thus, transformation of *E. coli* S17(λ*pir*) with ligation mixture was immediately followed with conjugation to the final recipient (AEK301) such that transformants of *E. coli* S17(λ*pir*) with recombinant plasmid would serve as donors in conjugation with AEK301.

Bacterial conjugation. Following overnight incubation, recipient cells (AEK301) were harvested from selective medium, washed twice in fresh TNB to remove traces of antibiotics and resuspended in an equal volume of recovery medium (34). Following transformation of *E. coli* S17(λ*pir*) by heat shock with pUT/mini Tn*5* (Sm/Sp) or recombinant plasmid ligations, the cell suspensions in SOC (1 ml) were mixed with three volumes of washed AEK301. After brief mixing, cells were pelleted at 3000 x g for 10 minutes, resuspended in 100 μL of SOC and spotted onto antibiotic-free LB plates. The plates were incubated cell-side-up at 30°C for 6 to 8 hours. Following incubation, the cells were harvested in 1 to 3 ml of fresh LB broth and plated on enriched medium containing kanamycin and spectinomycin to select for resulting transconjugants. Transconjugants were scored for phenol hydroxylase activity, prototrophism and unselected antibiotic markers (carbenicillin) by replica plating onto appropriate medium. Preliminary phenol hydroxylase activity was determined in a plate assay using MMO medium containing sodium citrate as a carbon source and phenol. This assay relied on a color change that occurs following phenol oxidation by JMP134-derivatives. Phenol utilizing colonies turn the surrounding medium dark brown on solid medium containing phenol due to the formation and autooxidation of accumulated catechol. Prototrophism was determined on MMO

containing 10 mM sodium citrate as a sole carbon and energy source and no additional additives.

Standard TCE degradation kinetics assay. AEK301/pYK3021 or AEP6 were grown in MMO containing 10 mM sodium citrate and the appropriate antibiotics at 30°C shaking at 180 RPM to mid-log phase at an optical density of 0.6 to 0.8 at 425 nm. Cells were harvested by centrifugation at 8000 x g for 10 minutes. Cell pellets were then suspended in fresh MMO containing 10 mM sodium citrate to an optical density of 1.0 at 425 nm. The cultures were then returned to 30°C shaking at 180 RPM. After one hour, 2 ml samples were dispensed into 20 ml glass vials and crimp-sealed with Teflon/butyl septa. The appropriate volume of an 8 mM TCE stock was added by injection through the septum with a gas-tight syringe (Hamilton, Reno, Nev.). The vials were inverted and returned to 30°C shaking at 180 RPM. At the appropriate time, the reactions were stopped by the addition of 2 ml of *n*-pentane containing 1 ppm EDB. EDB was added as an internal standard to correct for GC sampling imprecision. The vials were placed at room temperature on a shaker platform for 15 minutes and then centrifuged at 4000 x g for 10 minutes to aid in the separation of the organic phase. Following centrifugation, approximately 0.5 ml was transferred with a gas-tight syringe to a Teflon/butyl septum-sealed vial. A 1 µL sample was then removed and analyzed on the GC for TCE concentrations. Control samples of sterile medium gave TCE recoveries of 95-97% under these conditions. The data represent an average of two or more samples. TCE stocks of 8 mM were prepared by completely filling a 20 ml glass vial containing eight 3-mm diameter glass beads (to facilitate mixing) with sterile water. Once crimp-sealed with a Teflon/butyl septum with no trapped air, the appropriate volume of pure TCE was added by injection through the septum which was then allowed to dissolve completely overnight at room temperature with constant mixing.

Analytical methods. TCE was measured by gas chromatography analysis with a Hewlett-Packard 5890 gas chromatograph equipped with a 25 m cross-linked methyl silicone gum capillary column (Hewlett-Packard) and electron capture detection system. Peak integrations were obtained with a Hewlett-Packard 3390A integrator. The following operating conditions were used: injector temperature, 150°C; detector temperature, 250°C; column temperature 40°C to 100°C at 20°C/min; helium carrier gas flow 6 ml/min. Under these conditions TCE and EDB (internal standard) in pentane extracts had retention times of 2.2 and 2.9 minutes, respectively.

Protein determinations. Cell suspensions were solubilized by the addition of 0.2 volumes of 5 M NaOH and heating at 85°C for 10 minutes. Following the addition of 0.2 volumes of 4 M HCl, the total protein concentrations were determined by the Lowry assay (59). Bovine serum albumin which had been treated with NaOH, heat and HCl in parallel was used as a standard in these assays.

Preparation of cell-free crude extract. Cultures were grown in MMO containing 10 mM sodium citrate and appropriate antibiotic selection at 30°C shaking at 180 RPM to mid-log phase at an optical density of 0.6 to 0.8 at 425 nm. Where indicated, cultures were induced in gas tight reactors with the addition of 100 μM TCE for two hours prior to cell harvest. Cells were harvested by centrifugation at 8000 x g for 10 minutes and resuspended (1 ml per 1 gram wet weight) in HMCS buffer (50 mM HEPES-NaOH, pH 7.0; 5 mM $MgCl_2$; 5 mM $CaCl_2$ and 1 M sucrose) (7) containing 5 μM ferrous ammonium sulfate. Cells were disrupted by constant agitation for three minutes with two volumes of 0.1 mm glass beads using a Braun homogenizer. Cell disruption was confirmed by microscopic examination. Cell debris and glass beads were removed from cell extracts by centrifugation at 10K RPM, and the resulting cell-free homogenate

was diluted with 10 volumes of HMCS containing 5 μM ferrous ammonium sulfate.

Phenol hydroxylase activity from crude extracts. Crude extract was transferred to reactor vials, NADH was added to a final concentration of 1 mM and this mixture was sealed and used immediately for TCE degradation assays. Reactions were initiated upon addition of the appropriate volume of TCE by injection through the septum with a gas-tight syringe. The reactor vials were incubated with agitation at room temperature for two hours and the reactions were terminated by the addition of an equal volume of n-pentane containing 1 ppm EDB and assayed for remaining TCE by GC analysis of the organic phase.

Results and Discussion

Isolation of a plasmid-free TCE-degrading derivative of AEK301/pYK3021. A mini-Tn5 transposon delivery vector was selected as a vehicle to mobilize the phenol hydroxylase gene cluster from pYK3021 into the chromosome of AEK301. The phenol hydroxylase gene cluster from pYK3021 and the vector encoded *Tac* promoter where ligated to pUT/mini-Tn5 Sm/Sp as described. The vector encoded promoter was included in this construct to allow *Tac*-mediated constitutive expression of the *phlX* open reading frame. Following the construction of this mini-Tn5 delivery vector and subsequent conjugation into AEK301 as described above, 174 Km^r Sp^r transconjugants were isolated. All transconjugants were able to grow on MMO containing sodium citrate as a sole source of carbon and energy with no additional media additives indicating that none were auxotrophic mutants. Based on the preliminary plate assay for phenol hydroxylase activity as described above, 171 of these Km^r Sp^r transconjugants demonstrated phenol hydroxylase activity. Although phenol hydroxylase activity was observed in most transconjugants, no transconjugant was able to grow on

phenol as a sole source of carbon and energy consistent with previous observations of AEK301/pYK3021 (48, 49). Interestingly, 88% of the transconjugants (153 isolates out of 174) were carbenicillin resistant. This observation suggests a relatively high degree of integration of the entire pUT/mini-Tn*5*(Sm/Sp)::*phl* product into the recipient AEK301 genome in the absence of a transpositional event.

The remaining 21 isolates (termed AEP1 through AEP21) which were Km^r Sp^r Cb^s and Phl^+ were selected for specific phenol hydroxylase activity assays and the ability to degrade TCE in the absence of aromatic induction using a standard TCE degradation assay with an initial TCE concentration of 80 μM. Following incubation with TCE at 30°C for two hours, these isolates exhibited a range of TCE degradation activity but none were able to remove TCE to the same degree as AEK301/pYK3021 (not shown). One isolate (AEP6), exhibiting the highest degree of TCE removal in two hours, was selected for further analysis

Physical analysis of AEP6 by DNA-DNA hybridization. For physical characterization of AEP6, total genomic DNA was isolated from AEP6, AEK301 and AEO106 and digested with *Kpn*I or *Sst*II and used in Southern hybridization analysis using a 5.5 kb *Bam*HI restriction fragment from the phenol hydroxylase (*phl*) gene cluster in pYK3021 or pUT (without the Tn*5*/Sm/Sp sequences) as probes. All three strains examined are expected to contain a similar wild type genomic copy of the *phl* genes with restriction fragments of similar size reacting with the 5.5 kb *Bam*HI probe. AEP6 is expected to contain an additional copy of the *phl* genes resulting in the appearance of additional restriction fragments reacting with the 5.5 kb *Bam*HI probe. Schematic representation of the generated restriction fragments expected to react with the phenol hydroxylase probe is provided in Figure 21.

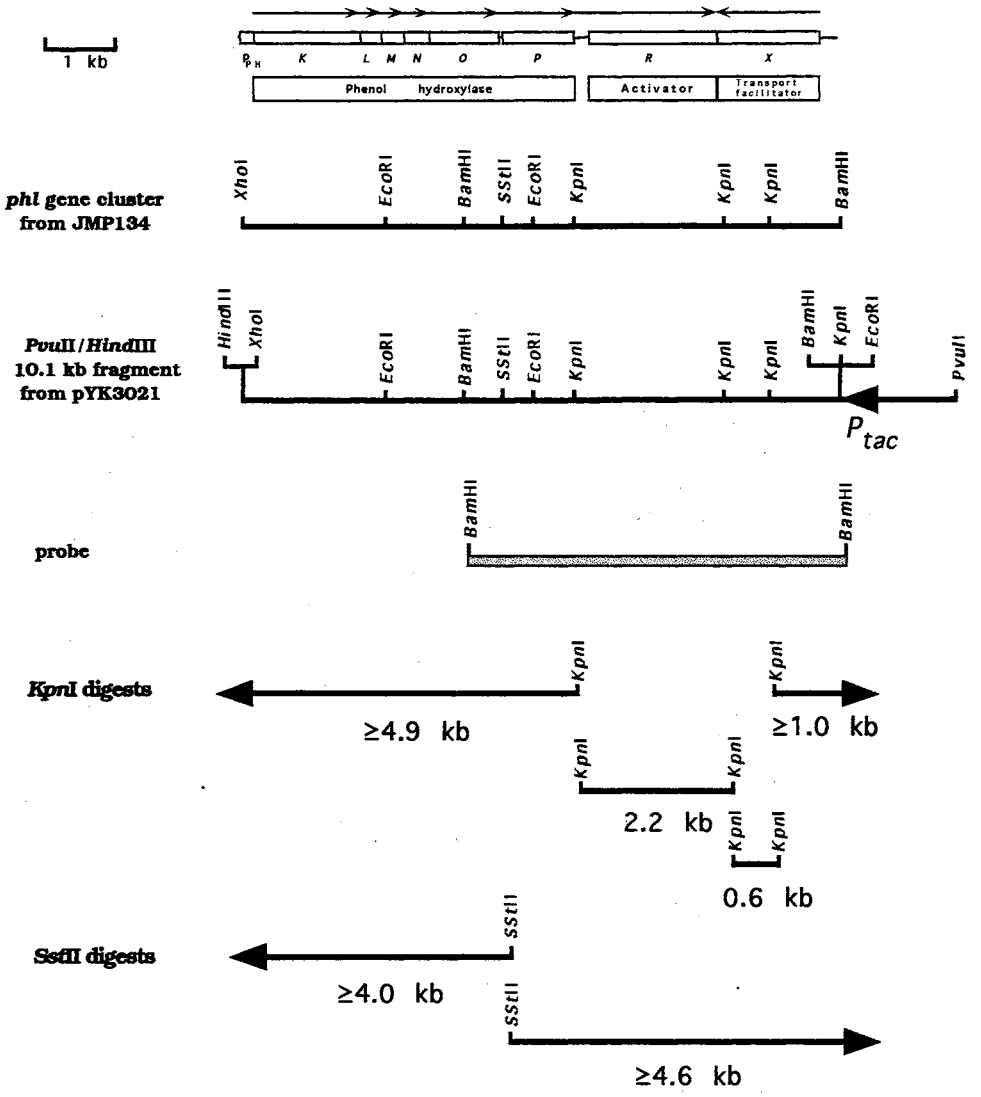

Figure 21. Schematic representation of the predicted restriction fragments generated from *Kpn*I or *Sst*II digests of chromosomal DNA and the probe used for DNA-DNA hybridization.

As expected, no reaction with the pUT probe was detected in any of the strains tested indicating the absence of these sequences in AEP6 (data not shown). As expected, four different *Kpn*I restriction fragments common to each strain reacted with the 5.5 kb *Bam*HI probe (Figure 22). Two internal *Kpn*I fragments of 2.2 kb and 0.6 kb are visible in all three isolates and are expected to remain unchanged between the wild type or Tn*5*-induced insertion of the *phl* genes. This probe also reacted with two other *Kpn*I fragments of 9.4 kb and 4.3 kb which most likely represent the *phlK* and *phlX* ends of the phenol hydroxylase gene cluster respectively (refer to Figures 21 and 22) and are present in each strain. Interestingly, the only additional *Kpn*I fragment detected in AEP6 by hybridization with the 5.5 kb *Bam*HI *phl* probe was a 1.0 kb *Kpn*I fragment which represents DNA from the *phlX* end of the Tn*5*-induced insertion of the phenol hydroxylase genes which, as predicted, resulted in the introduction of an additional *Kpn*I site between the *phlX* gene and the *Tac* promoter.

Examination of *Sst*II digests following hybridization with the 5.5 kb *Bam*HI *phl* probe revealed two detectable fragments of 9.0 kb and 4.1 kb common to all three strains (Figure 22). Based on the fragment size and intensity of the band, the larger 9.0 kb fragment most likely represents the *phlX* end of the phenol hydroxylase gene cluster. The *phlK* end of this gene cluster is expected to react weakly with the 5.5 kb *Bam*HI *phl* probe due to limited overlapping sequences and is most likely represented by the 4.1 kb *Sst*II fragment (Figures 21 and 22). A third *Sst*II fragment of 6.7 kb reacting with the probe is also detectable in AEP6. Based on the intensity of the reacting band, this fragment most likely represents a second copy of the *phlX* end of the phenol hydroxylase gene cluster. As in the *Kpn*I digests, a second copy of the *phlK* end of this gene cluster is not detectable under the conditions tested.

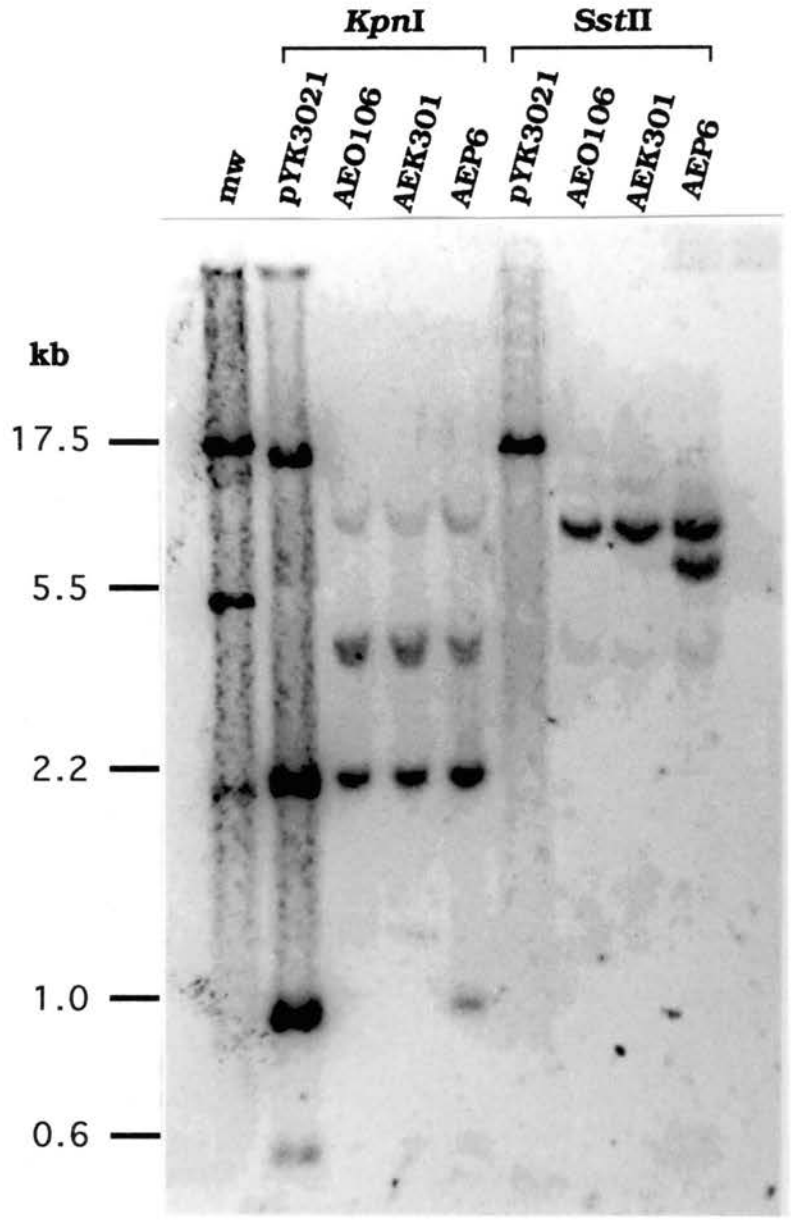

Figure 22. Southern blot of purified pYK3021 DNA and total genomic DNA from AEO106, AEK301 and AEP6 digested with *Kpn*I or *Sst*II. The hybridization probe was the 5.5 kb *Bam*HI fragment of pYK3021 labeled with digoxigenin-dUTP.

These hybridization data indicate that AEP6 contains a wild type copy and an additional, partial copy of the phenol hydroxylase gene cluster. The second, partial copy of these genes in AEP6 contains the *phlX* open reading frame and the *Tac* promoter originally encoded from the pMMB67EH vector. Other open reading frames from the end of the *phlKLMNOPR* operon such as *phlP* and *phlR* may also be duplicated in this strain. In addition, sequences homologous to the pUT vector were not detected in this strain, indicating a genomic insertion of the second partial copy of the phenol hydroxylase gene cluster. This configuration is adequate to provide the sequences necessary for TCE degradation by AEP6 in the absence of phenol induction. Perhaps TCE degradation by AEP6 is aided by constitutive expression of the *phl*X gene from the *Tac* promoter sequences and a random promoter fusion of partial *phlKLMNOPR* sequences introduced during the Tn5-induced insertion of these genes into the chromosome of AEK301 resulting in phenol/TCE independent transcription of a second *phlR* transcriptional activator gene and subsequent TCE-mediated activation of the wild type *phlKLMNOPR* operon. Such random promoter fusions of *phlR* with AEK301 genomic promoters in the generation of AEP1 through AEP21 strains could account for the differences observed in TCE degradation capacity observed for each isolate. A more detailed DNA-DNA hybridization analysis of this region is required to further understand the extent of this Tn5-induced insertion of the phenol hydroxylase gene cluster in AEP6.

Time course of TCE degradation by AEP6. To more closely examine the degradation of TCE by AEP6, a study of TCE degradation progression with samples collected every 15 minutes over a 3 hour period was conducted with an initial concentration of 80 μM TCE. These data were then plotted with data from a similar assay generated from AEK301/pYK3021 for comparison of these two strains (Figure 23).

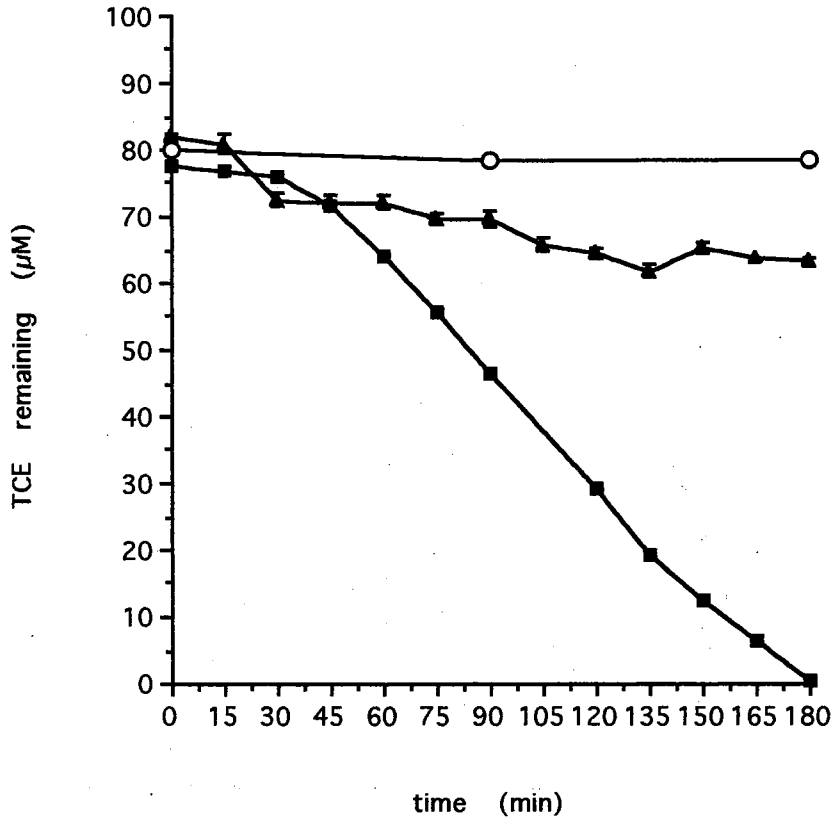

Figure 23. Progression of TCE degadation by (▲)AEP6, (■) AEK301/pYK3021, and (O) AEK301 (negative control). TCE was added to each at an initial concentration of 80 μM. Cultures were grown in MMO supplemented with 10 mM sodium citrate to mid-log phase, harvested by centrifugation and suspended in fresh medium to an optical density of 1.0 at 425 nm. After one hour at 30°C, 2 ml samples of each strain were then distributed into vials and sealed. Reactions were initiated by the injection of TCE through the septum. Samples were collected in duplicate every 15 minutes for a total of three hours. Each data point represents the average of two or more samples and error bars are provided where visible.

Comparison of these two strains (AEK301/pYK3021 and AEP6) indicates that while AEP6 is able to degrade TCE in the absence of phenol induction, a significant difference in the kinetics of TCE degradation is apparent. The rate of TCE removal by AEP6 is significantly less than that observed by AEK301/pYK3021. These observed differences could be attributed to differences in a rate limiting step such as transport of substrate into the cell and/or differences in the copy number of the catabolic genes present in the multi-copy plasmid-bearing strain and the AEP6 isolate. To assist in determining the basis of these observed differences, crude extract was prepared from each isolate, and the specific phenol hydroxylase activity was examined.

Specific enzyme activity from crude extracts. Using a TCE degradation assay, phenol hydroxylase activity was measured in crude extracts prepared from AEK301/pYK3021, AEP6 or AEK301. Each strain was incubated to mid-log phase in MMO containing sodium citrate as a carbon source and crude extracts were prepared as described above. Initially, no detectable phenol hydroxylase activity was observed in crude extracts prepared in this manner (not shown). However, induction with 100 μM TCE for 2 hours prior to cell disruption resulted in detectable amounts of enzyme activity in crude extract prepared from AEK301/pYK3021 and AEP6 but not AEK301 supporting earlier conclusions of TCE-mediated induction of the catabolic genes for phenol hydroxylase in AEK301/pYK3021.

Specific phenol hydroxylase activity from crude extracts was determined from TCE induced AEK301/pYK3021, AEP6 or AEK301 at three different initial concentrations of TCE (40, 80 and 220 μM). The amount of TCE removed from reactor vials was determined (nmoles/mg total protein) and these values were plotted as a function of the initial TCE concentration (Figure 24). Both AEK301/pYK3021 and AEP6 crude extracts contained measurable phenol

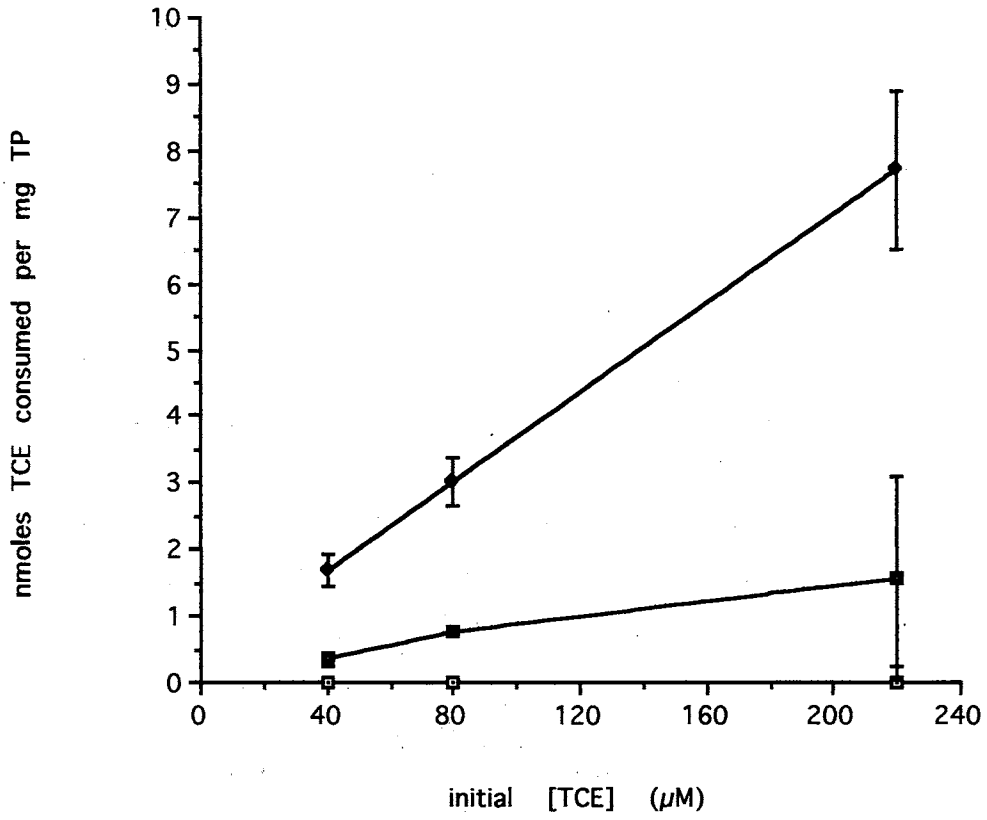

Figure 24. Specific phenol hydroxylase activity from crude protein extracts prepared from (■) AEP6, (◆) AEK301/pYK3021 and (▣) AEK301 (negative control). Crude extracts were prepared as described. The removal of TCE was measured in duplicate samples following two hours of incubation at room temperature. Each data point represents the average of two samples and error bars are provided where visible.

hydroxylase activity at all three initial concentrations of TCE. While the amount of TCE consumed (nmoles/mg total protein) increased with increasing amounts of substrate, significant differences between AEK301/pYK3021 and AEP6 were observed. At each initial concentration of substrate, crude extract prepared from AEK301/pYK3021 cells removed about 4 to 5 times more TCE than crude extract prepared from AEP6 cells, indicating a higher level of phenol hydroxylase expression in AEK301/pYK3021. This difference is probably due to a higher number of the phenol hydroxylase genes present in AEK301/pYK3021 on the multi-copy pMMB67EH vector resulting in greater capacity to degrade TCE compared to AEP6.

Stability of TCE degradation capacity. Previous observations have indicated a decrease in phenol hydroxylase activity with the prolonged culture of AEK301/pYK3021 in medium containing TCE (49) or phenol (not shown). To determine the basis for this observed loss of phenol hydroxylase activity, AEK301/pYK3021 was incubated for 48 hours in MMO broth containing the appropriate antibiotics, sodium citrate and phenol. Limited growth was observed after 24 hours of incubation (with an optical density at 425 nm of 0.235), and the culture was incubated another 48 hours. Isolates from this broth culture were tested for phenol hydroxylase activity and antibiotic resistance based on replica plating assays. Such isolates retained carbenicillin resistance but lost phenol hydroxylase activity, suggesting the loss of sequences required for catabolism of phenol. This loss could be the result of recombination between the plasmid-borne phenol hydroxylase genes and their chromosomal counterparts. To further examine the resulting AEK301/pYK3021ΔPhl isolates, plasmid DNA was isolated from several such isolates and subjected to restriction analysis. In each case, plasmid DNA was recovered but the restriction profile revealed the loss of the terminal *Bam*HI and *Eco*RI restriction sites (not shown) and loss of about 5 kb of

DNA from the *phlX* region of pYK3021. The loss of DNA in this region effectively explains the loss of phenol hydroxylase activity in these isolates. A representative isolate was then selected for further analysis.

To test the stability of phenol hydroxylase activity in the plasmid free strain AEP6, this strain was also inoculated in MMO broth containing the appropriate antibiotics, sodium citrate and phenol. This culture grew well within 24 hours of incubation at 30°C (with an optical density at 425 nm of 1.26), and isolates from this broth culture retained both antibiotic resistance (Sp^r) and phenol hydroxylase activity based on replica plating assays. A representative isolate was then selected for further analysis.

To determine if the capacity to degrade TCE was retained by any of these isolates subjected to phenol challenge, an AEK301/pYK3021ΔPhl representative and an AEP6 isolate were each tested for their ability to degrade TCE. With an initial concentration of 80 μM TCE, the concentration of TCE remaining after two hours of incubation was 62.4 μM TCE for AEP6 and 78.6 μM TCE for AEK301/pYK3021ΔPhl. These data were then compared to similar TCE degradation assays conducted on AEK301/pYK3021 and AEP6 original isolates (Figure 25). These data indicate that phenol hydroxylase activity expressed by AEP6 is stable compared to AEK301/pYK3021 following substrate challenge with phenol. Although the rate of TCE degradation by AEP6 is less than AEK301/pYK3021, the increased stability and retention of phenol hydroxylase activity following substrate challenge may prove a beneficial feature when considering applications of this recombinant construct in bioremediation of contaminated sites.

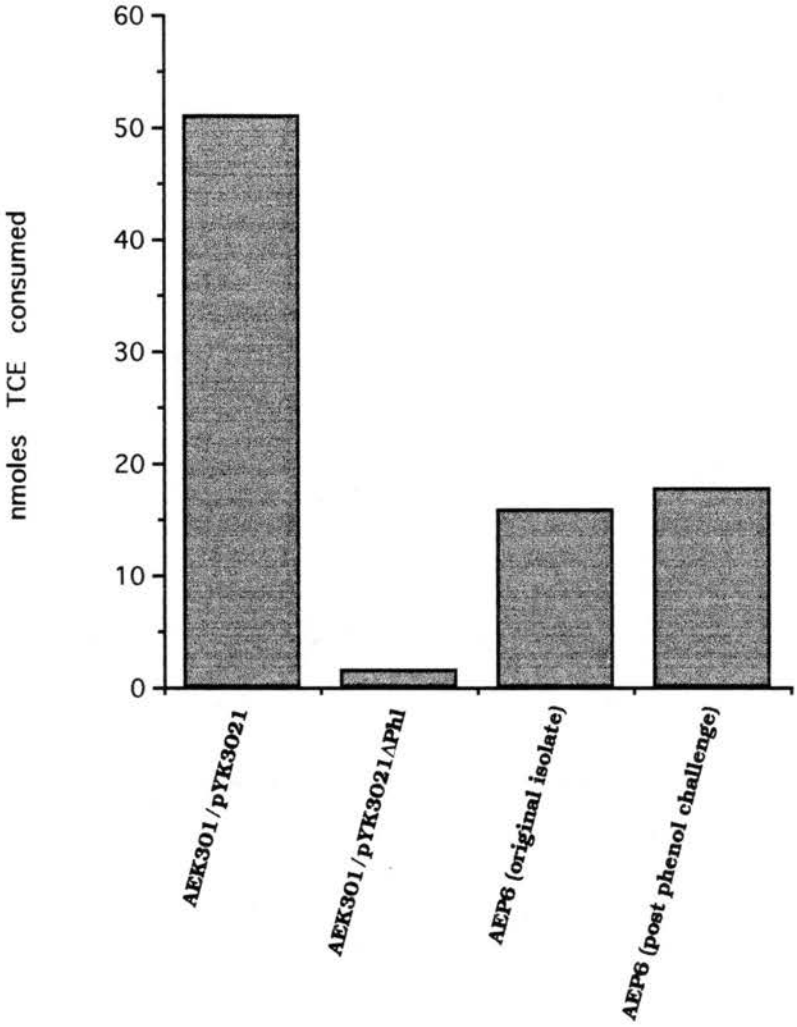

Figure 25. Phenol hydroxylase activity of AEK301/pYK3021 and AEP6 isolates before and after incubation in MMO containing sodium citrate, phenol and appropriate antibiotics. For this assay, each strain was incubated at 30°C with an initial concentration of 80 μM TCE and the amount of TCE remaining was determined after two hours.

Conclusions

In this study, we sought to improve the overall stability of phenol hydroxylase activity and TCE degradation located on a recombinant plasmid in AEK301/pYK3021. A transposon-delivery system was examined as a method to insert the genes responsible for TCE degradation into the chromosome of AEK301 to construct a strain with improved stability and overall usefulness. This approach has resulted in a Tn*5*-mediated chromosomal insertion of a portion of the phenol hydroxylase gene cluster including the *phlX* open reading frame and the *Tac* promoter sequences from the pMMB67EH vector in AEK301. This construct, termed AEP6, was able to degrade TCE in the absence of aromatic induction but at a rate approximately 4 to 5 times less than that of AEK301/pYK3021. This observed difference in TCE degradation rates is most likely due to differences in gene copy number between these two recombinant strains. Although the rate of TCE degradation was less in AEP6, the genes responsible for this activity appear to be more stable in AEP6 than in AEK301/pYK3021. Consistent with earlier conclusions, TCE is able to act as an efficient inducer of the phenol hydroxylase catabolic genes in AEK301/pYK3021 and AEP6. Constitutive expression of the *phlX* open reading frame from the plasmid encoded *Tac* promoter appears to play an important role in this TCE-mediated induction. AEP6 and AEK301/pYK3021 should be tested in bench-scale reactors where their ability to remove TCE in continuous culture could be examined and compared and the overall usefulness of this new construct in the efficient removal of TCE from contaminated waters could be determined.

CHAPTER VI

CONCLUSIONS

This study began as an effort to characterize the degradation of TCE by an *Alcaligenes eutrophus* JMP134 derivative previously constructed in our laboratory through recombinant DNA techniques to efficiently degrade TCE in the absence of any aromatic induction (48, 49). While several TCE-degrading bacteria have been isolated, this isolate is unique based on several merits. The data presented here on the whole cell kinetics of TCE degradation by AEK301/pYK3021 show that, compared to other TCE degrading bacteria (26, 37, 54, 113), this strain is able to co-metabolize TCE at a rapid and sustained rate even at relatively high concentrations of TCE with a V_{max} of 22.6 nmoles/min/mg of total protein observed at 800 μM of TCE with no apparent TCE mediated toxicity. These results are promising when considering applications to TCE bioremediation from contaminated ground water.

The second part of this study involved DNA sequence analysis of the phenol hydroxylase gene cluster from *Alcaligenes eutrophus* AEK301/pYK3021. The catabolic genes encoded on pYK3021 comprise an operon and are similar to other well characterized multicomponent toluene and phenol monooxygenases. The operon for the catabolic genes includes an open reading frame for its cognate regulatory gene (PhlR) which is a member of the NtrC family of transcriptional activators. This genetic organization allows effector molecules to activate the synthesis not only of phenol hydroxylase but also of its respective regulatory

gene, PhlR. A gap of about 230 bp exists between the *phlP* and *phlR* genes in this operon and may lend itself to a yet undetermined regulatory scheme that cannot be overlooked. A more complete transcriptional analysis of this interesting operon is needed to assist in characterizing the regulatory mechanisms involved. These studies have shown that phenol and trichloroethylene are able to serve as effector molecules to activate transcription of these genes. Previous studies have indicated that degradation of TCE by AEK301/pYK3021 is further enhanced by prior induction with phenol, indicating the responsiveness of PhlR to phenol is greater (49). A more complete study of effector specificity and responsiveness would be interesting to assess the range of compounds able to activate this operon.

It is also interesting that these genes are more similar to toluene monoxygenases than other phenol hydroxylases even though JMP134 and AEK301/pYK3021 are unable to grow on toluene as a sole source of carbon and energy. The basis for this apparent contradiction may relate to differences in the catabolic peptides, regulatory protein(s) and/or substrate transport. Amino acid residues that are highly conserved among members of a gene family indicate residues essential for function. Studies such as those involving mutational analysis of such conserved residues or the construction of gene fusions resulting in the synthesis of hybrid catabolic or regulatory protein products may provide valuable insights to explain the substrate range of JMP134 whole cells. Perhaps the basis for these differences is also related to the selective transport of substrate into cells. Toluene degradation assays using crude extracts from phenol or TCE induced cells or the introduction of a toluene specific transport facilitator gene such as *todX* into JMP134 or AEK301/pYK3021 would assist in addressing this issue. It is apparent that the constitutive expression of *phlX* by AEK301/pYK3021 plays a key role in permitting TCE-mediated induction of the

phenol hydroxylase genes. This also implies that wild type *phlX* is not effectively induced by TCE and perhaps induction limitations of this crucial gene have metabolic consequences. The native *phlX* promoter and its regulatory elements should be studied to further enhance our understanding of this cluster of genes.

Finally, we sought to develop a plasmid-free derivative of AEK301/pYK3021 using a mini-Tn*5*-based transposon-delivery system. This approach led to insertion of a portion of the phenol hydroxylase genes including *phlX::Tac* into the AEK301 chromosome. While the desired TCE degradation activity was maintained and appears to be more stable in this construct (AEP6), the reduction in gene copy number most likely resulted in reduced TCE degradation rates. Long term studies of TCE degradation in continuous culture would assist in determining whether the enhanced stability of TCE degradation activity in AEP6 provides an overall benefit in TCE degradation when compared to AEK301/pYK3021.

LITERATURE CITED

1. Abril, M. A., C. Michan, K. N. Timmis, and J. L. Ramos. 1989. Regulator and enzyme specificities of the TOL plasmid-encoded upper pathway for degradation of aromatic hydrocarbons and expansion of the substrate range of the pathway. J. Bacteriol. 171:6782-6790.

2. Alexander, M. 1991. Research needs in bioremediation. Environ. Sci. Technol. 25:1972-1973.

3. Arciero, D., T. Vannelli, M. Logan, and A. B. Hooper. 1989. Degradation of trchloroethylene by the ammonia-oxidizing bacterium *Nitrosomonas euroaea*. Biochem. Biophys. Res. Commun. 159:640-643.

4. Ausubel, F. M., R. Brent, R. E. Kingston, D. D. Moore, J. G. Seidman, J. A. Smith, and K. Struhl. 1989. Current protocols in molecular biology. John Wiley & Sons, Inc., New York.

5. Birnboim, H. C., and J. Doly. 1979. A rapid alkaline extraction procedure for screening recombinant plasmid DNA. Nucleic Acids Res. 7:1513-1523.

6. Bowman, J. P., L. Jimenez, I. Rosario, T. C. Hazen, and G. S. Sayler. 1993. Characterization of the methanotrophic bacterial community present in a trichloroethylene-contaminated subsurface groundwater site. Appl Environ Microbiol. 59:2380-7.

7. Burnap, R., H. Kioke, G. Sotiropoulou, L. A. Sherman, and Y. Inoue. 1989. Oxygen evolving membranes and particles from the transformable cyanobacterium *Synechocystis* sp. PCC6803. Photosynthesis Research. 22:123-130.

8. Byrne, A. M., J. J. Kukor, and R. H. Olsen. 1995. Sequence analysis of the gene cluster encoding toluene-3-monooxygenase from *Pseudomonas pickettii* PKO1. Gene. 154:65-70.

9. Byrne, A. M., and R. H. Olsen. 1996. Cascade regulation of the toluene-3-monooxygenase operon (*tbu*A1UBVA2C) of *Burkholderia pickettii* PKO1: role of the *tbu*A1 promoter (PtbuA1) in the expression of its cognate activator, TbuT. J Bacteriol. 178:6327-37.

10. Byrne, A. M., and R. H. Olsen. 1997. Evidence for the evolution of a single component phenol/cresol hydroxylase from a multicomponent toluene

monooxygenase. Presented at the American Society for Microbiology 97th General Meeting, May 4-8, 1997.

11. Byrne, A. M., and R. H. Olsen. 1996. Nucleotide sequence analysis of *tbuX*, a gene encoding a putative membrane-associated protein from *Burkholderia pickettii* PKO1. Presented at the American Society for Microbiology 96th General Meeting, May 19-23, 1996.

12. Chaudhry, G. R., and S. Chapalamadugu. 1991. Biodegradation of halogenated organic compounds. Microbiol. Reviews. 55:59-79.

13. Craig, N. L., and H. A. Nash. 1984. *E. coli* integration host factor binds to specific sites in DNA. Cell. 39:707-716.

14. de Lorenzo, V., M. Herrero, U. Jakubzik, and K. N. Timmis. 1990. Mini-Tn5 transposon derivatives for insertion mutagenesis, promoter probing, and chromosomal insertion of cloned DNA in gram-negative eubacteria. J Bacteriol. 172:6568-6572.

15. de Lorenzo, V., M. Herrero, M. Metzke, and K. N. Timmis. 1991. An upstream XylR and IHF-induced nucleoprotein complex regulates the σ^{54}-dependent P*u* promoter of TOL plasmid. EMBO. 10:1159-1167.

16. Delgado, A., and J. L. Ramos. 1994. Genetic evidence for activation of the positive transcriptional regulator XylR, a member of the NtrC family of regulators, by effector binding. J. Biol. Chem. 269:8059-8062.

17. Don, R. H., and J. M. Pemberton. 1985. Properties of six pesticide degradation plasmids isolated from *Alcaligenes paradoxus* and *Alcaligenes eutrophus*. J. Bacteriol. 145:681-686.

18. Dong, F. M., L. L. Wang, C. M. Wang, J. P. Cheng, Z. Q. He, Z. J. Sheng, and R. Q. Shen. 1992. Molecular cloning and mapping of phenol degradation genes from *Bacillus stearothermophilus* FDTP-3 and their expression in *Escherichia coli*. Appl Environ Microbiol. 58:2531-5.

19. Drummond, M., W. P., and J. Wootton. 1986. Sequence domain relationships of *ntr*C and *nif*A from *Klebsiella pneumonia*: homologies to other regulatory proteins. EMBO J. 5:441-447.

20. Ehrt, S., F. Schirmer, and W. Hillen. 1995. Genetic organization, nucleotide sequence and regulation of expression of genes encoding phenol hydroxylase and catechol 1,2-dioxygenase in *Acinetobacter calcoaceticus* NCIB8250. Mol Microbiol. 18:13-20.

21. Ensley, B. D. 1991. Biochemical diversity of trichloroethylene metabolism. Annu Rev Microbiol. 45:283-99.

22. Ewers, J., D. Freier-Schroder, and H. J. Knackmuss. 1990. Selection of trichloroethene (TCE) degrading bacteria that resist inactivation by TCE. Arch Microbiol. 154:410-3.

23. Fewson, C. A. 1981. Biodegradation of aromatics with industrial relevance, p. 141-179. *In* T. Leisinger, A. M. Cook, R. Hutter, and J. Nuesch (ed.), Microbial degradation of xenobiotics and recalcitrant compounds. Academic Press, Ltd., London.

24. Fischer, A. J., E. A. Rowan, and R. F. Spalding. 1987. VOC's in groundwater influenced by large scale withdrawals. Ground water. 25:407-413.

25. Folsom, B. R., and P. J. Chapman. 1991. Performance characterization of a model bioreactor for the biodegradation of trichloroethylene by *Pseudomonas cepacia* G4. Appl Environ Microbiol. 57:1602-8.

26. Folsom, B. R., P. J. Chapman, and P. H. Pritchard. 1990. Phenol and trichloroethylene degradation by *Pseudomonas cepacia* G4: kinetics and interactions between substrates. Appl Environ Microbiol. 56:1279-85.

27. Fontecave, M., P. Nordlund, P. Eklund, and P. Reichard. 1992. The redox centers of ribonucleotide reductase of *Escherichia coli*. Adv. Enzymol. Relat. Areas Mol. Biol. 65:147-183.

28. Fujita, M., M. Ike, J. Hioki, K. Kataoka, and M. Takeo. 1995. Trichloroethylene degradation of genetically engineered bacteria carrying cloned phenol catabolic genes. J Ferm Bioeng. 79:100-106.

29. Furste, J. P., W. Pansegrau, R. Frank, H. Blocker, P. Scholz, M. Bagdasarian, and E. Lanka. 1986. Molecular cloning of the RP4 DNA primase region in a multi-host-range *tac*P expression vector. Gene. 48.

30. Gibson, T. L., A. S. Abdul, and R. O. Olsen. 1988. Microbial degradation of aromatic hydrocarbons in hydrogeologic material: microcosm studies. Presented at the Proceedings of the Second Groundwater and Geophysical Methods, Dublin, Ohio.

31. Gossett, J. M. 1987. Measurement of Henry's law constants for C_1 and C_2 chlorinated hydrocarbons. Environ. Sci. Technol. 21:202-208.

32. Habe, H., K. Kasuga, H. Nojiri, Y. H., and T. Omori. 1996. Analysis of cumene (isopropylbenzene) degradation genes from *Pseudomonas fluorescens* IP01. Appl Environ Microbiol. 62:4471-4477.

33. Haigler, B. E., C. A. Pettigrew, and J. C. Spain. 1992. Biodegradation of mixtures of substituted benzenes by *Pseudomonas* sp. strain JS150. Appl Environ Microbiol. 58:2237-44.

34. Hanahan, D. 1983. Studies on transformation of *Escherichia coli* with plasmids. J. Mol. Biol. 166:557-580.

35. Harker, A. R., and Y. Kim. 1990. Trichloroethylene degradation by two independent aromatic-degrading pathways in *Alcaligenes eutrophus* JMP134. Appl Environ Microbiol. 56:1179-81.

36. Harker, A. R., R. H. Olsen, and R. J. Seidler. 1989. Phenoxyacetic acid degradation by the 2,4-dichlorophenoxyacetic acid pathway of the plasmid pJP4: mapping and characterization of the 2,4-D regulatory gene, *tfd*R. J. Bacteriol. 171:314-320.

37. Heald, S., and R. O. Jenkins. 1994. Trichloroethylene removal and oxidation toxicity mediated by toluene dioxygenase of *Pseudomonas putida*. Appl Environ Microbiol. 60:4634-7.

38. Henschler, D., W. R. Hoos, H. Fetz, E. Dallmeier, and M. Metzler. 1979. Reactions of trichloroethylene oxidation by aquifer methanotrophs. Microb. Ecol. 20:151-169.

39. Herrero, M., V. de Lorenzo, and K. N. Timmis. 1990. Transposon vectors containing non-antibiotic resistance selection markers for cloning and stable chromosomal inserion of forgein genes in gram-negative bacteria. J Bacteriol. 172:6557-6567.

40. Herrmann, H., C. Muller, I. Schmidt, J. Mahnke, L. Petruschka, and K. Hahnke. 1995. Localization and organization of phenol degradation genes of *Pseudomonas putida* strain H. Mol Gen Genet. 247:240-6.

41. Inoue, H., H. Nojima, and H. Okayama. 1990. High efficiency transformation of *Escherichia coli* with plasmids. Gene. 96:23-28.

42. Inouye, S., A. Nakazawa, and T. Nakazawa. 1988. Nucleotide sequence of the regulatory gene *xylR* of the TOL plasmid from *Pseudomonas putida*. Gene. 66:301-306.

43. Jiang, H., R. E. Parales, N. A. Lynch, and D. T. Gibson. 1996. Site-directed mutagenesis of conserved amino acids in the alpha subunit of toluene dioxygenase: potential mononuclear non-heme iron coordination sites. J. Bacteriol. 178:3133-3139.

44. Johnson, G. R., and R. H. Olsen. 1995. Nucleotide sequence analysis of genes encoding a toluene/benzene-2-monooxygenase from *Pseudomonas* sp. strain JS150. Appl Environ Microbiol. 61:3336-46.

45. Kalin, M., H. Y. Neujahr, R. N. Weissmahr, T. Sejlitz, R. Johl, A. Fiechter, and J. Reiser. 1992. Phenol hydroxylase from *Trichosporon cutaneum*: gene cloning, sequence analysis, and functional expression in *Escherichia coli*. J Bacteriol. 174:7112-20.

46. Keith, L. H., and W. A. Telliard. 1979. Priority pollutants I - a perspective view. Environ. Sci. Technol. 13:416-423.

47. Kim, I. C., and P. J. Oriel. 1995. Characterization of the *Bacillus stearothermophilus* BR219 phenol hydroxylase gene. Appl Environ Microbiol. 61:1252-6.

48. Kim, Y., P. Ayoubi, and A. Harker. 1996. Constitutive expression of the cloned phenol hydroxylase gene(s) from *Alcaligenes eutrophus* JMP134 and concomitant trichloroethylene oxidation. Appl Environ Microbiol. 62:3227-3233.

49. Kim, Y. 1993. A recombinant approach to the isolation and characterization of a primary degrader of trichloroethylene. Ph. D. Oklahoma State University, Stillwater.

50. Kitayama, A., E. Suzuki, Y. Kawakami, and T. Nagamune. 1996. Genetic organization and low regiospecificity in aromatic-ring hydroxylation of a benzene monooxygenase of *Pseudomonas aeruginosa* JI104. J. Ferment. Bioeng. 82:421-425.

51. Knauf, V. C., and E. W. Nester. 1982. Wide host range cloning vectors: a cosmid clone bank of an *Agrobacterium* Ti plasmid. Plamid. 8:45-54.

52. Knox, R. C., and L. W. Canter. 1996. Prioritization of ground water contaminants and sources. Water, air, and soil pollution. 88:205-226.

53. Kukor, J. J., and R. H. Olsen. 1992. Complete nucleotide sequence of *tbuD*, the gene encoding phenol/cresol hydroxylase from *Pseudomonas pickettii* PKO1, and functional analysis of the encoded enzyme. J Bacteriol. 174:6518-26.

54. Landa, A. S., E. M. Sipkema, J. Weijma, A. A. Beenackers, J. Dolfing, and D. B. Janssen. 1994. Cometabolic degradation of trichloroethylene by *Pseudomonas cepacia* G4 in a chemostat with toluene as the primary substrate. Appl Environ Microbiol. 60:3368-74.

55. Leahy, J. G., A. M. Byrne, and R. H. Olsen. 1996. Comparison of factors influencing trichloroethylene degradation by toluene-oxidizing bacteria. Appl Environ Microbiol. 62:825-33.

56. Li, J. K., and A. E. Humphrey. 1989. Kinetic and fluorometric behaviour of a phenol fermentation. Biotechnol lett. 11:177-182.

57. Lipscomb, J. D. 1994. Biochemistry of the soluble methane monooxygenase. Annu Rev Microbiol. 48:371-399.

58. Little, C. D., A. V. Palumbo, S. E. Herbes, M. E. Lidstrom, R. L. Tyndall, and P. J. Gilmer. 1988. Trichloroethylene biodegradation by a methane-oxidizing bacterium. Appl Environ Microbiol. 54:951-956.

59. Lowry, O. H., S. O. Rosebrough, A. L. Farr, and R. J. Randall. 1951. Protein measurement with the Folin phenol reagent. J. Biol. Chem. 193:265-275.

60. Luu, P. P., C. W. Yung, A. K. Sun, and T. K. Wood. 1995. Monitoring trichloroethylene mineralization by *Pseudomonas cepacia* G4 PR1. Appl. Microbiol. Biotechnol. 44:259-264.

61. Maniatis, T., F. E. F., and J. Sambrook. 1982. Molecular cloning: a laboratory manual. Cold Springs Harbor, NY.

62. Mars, A. E., J. Houwing, J. Dolfing, and D. B. Janssen. 1996. Degradation of toluene and trichloroethylene by *Berkholderia cepacia* G4 in growth-limited fed-batch culture. Appl Environ Microbiol. 62:886-891.

63. Mason, J. R., and R. Cammack. 1992. The electron-transport proteins of hydroxylating bacterial dioxygenases. Annu. Rev. Microbiol. 46:277-305.

64. Matin, A., C. D. Little, C. D. Fraley, and M. Keyhan. 1995. Use of starvation promoters to limit growth and select for trichloroethylene and phenol transformation activity in recombinant *Escherichia coli*. Appl Environ Microbiol. 61:3323-8.

65. McClay, K., S. H. Streger, and R. J. Steffan. 1995. Induction of toluene oxidation activity in *Pseudomonas mendocina* KR1 and *Pseudomonas* sp. strain ENVPC5 by chlorinated solvents and alkanes. Appl Environ Microbiol. 61:3479-81.

66. Miller, R. E., and F. P. Guengerich. 1982. Oxidation of trichloroethylene by liver microsomal cytochrome P450: evidence for chlorine migration in a transition state not involving trichloroethylene oxide. Biochemistry. 21:1090-1097.

67. Morett, E., and L. Segovia. 1993. The σ^{54} bacterial enhanser-binding protein family: mechanism of action and phylogenic relationships of their functional domains. J. Bacteriol. 175:6067-6074.

68. Muller, C., L. Petruschka, H. Cuypers, G. Burchhardt, and H. Herrmann. 1996. Carbon catabolite repression of phenol degradation in *Pseudomonas putida* is mediated by the inhibition of the activator protein PhlR. J. Bacteriol. 178:2030-2036.

69. Nakamura, K., and H. Ishida. 1996. Development of a genetically engineered microorganism for trichloroethylene degradation by

homologous recombination and analysis of its gene expression. Proc. Environ. Engineering Research. 33:165-175.

70. Neidle, E. L., C. Hartnett, L. N. Ornston, A. Bairoch, M. Rekik, and S. Harayama. 1991. Nucleotide sequences of the *Acinetobacter calcoaceticus benABC* genes for benzoate 1,2-dioxygenase reveal evolutionary relationships among multicomponent oxygenases. J Bacteriol. 173:5385-95.

71. Nelson, M. J., S. O. Montgomery, W. R. Mahaffey, and P. H. Pritchard. 1987. Biodegradation of trichloroethylene and involvement of an aromatic biodegradative pathway. Appl Environ Microbiol. 53:949-54.

72. Neujahr, H. Y., and A. Gaal. 1973. Phenol hydroxylase from yeast. Purification and properties of the enzyme from *Trichosporon cutaneum.* Eur. J. Biochem. 35:386-400.

73. Neujahr, H. Y., S. Lindsjo, and J. M. Vargo. 1974. Oxidation of phenols by cells and cell-free enzymes from *Candida tropicalis.* J. Microbiol. 40:209-216.

74. Newman, L. M., and L. P. Wackett. 1997. Trichloroethylene oxidation by purified toluene-2-monooxygenase: products, kinetics, and turnover-dependent inactivation. J. Bac. 179:90-96.

75. Ng, L. C., C. L. Poh, and V. Shingler. 1995. Aromatic effector activation of the NtrC-like transcriptional regulator PhhR limits the catabolic potential of the (methyl)phenol degradation pathway it controls. J. Bacteriol. 177:1485-1490.

76. Ng, L. C., V. Shingler, C. C. Sze, and C. L. Poh. 1994. Cloning and sequences of the first eight genes of the chromosomally encoded (methyl) phenol degradation pathway from *Pseudomonas putida* P35X. Gene. 151:29-36.

77. Nordlund, I., J. Powlowski, and V. Shingler. 1990. Complete nucleotide sequence and polypeptide analysis of multicomponent phenol hydroxylase from *Pseudomonas* sp. strain CF600. J Bacteriol. 172:6826-33.

78. Nurk, A., L. Kasak, and M. Kivisaar. 1991. Sequence of the gene (pheA) encoding phenol monooxygenase from *Pseudomonas* sp. EST1001: expression in *Escherichia coli* and *Pseudomonas putida.* Gene. 102:13-8.

79. Oldenhuis, R., J. Y. Oedzes, d. W. J. J. van, and D. B. Janssen. 1991. Kinetics of chlorinated hydrocarbon degradation by *Methylosinus trichosporium* OB3b and toxicity of trichloroethylene. Appl Environ Microbiol. 57:7-14.

80. Oldenhuis, R., R. L. Vink, D. B. Janssen, and B. Witholt. 1989. Degradation of chlorinated aliphatic hydrocarbons by *Methylosinus trichosporium* OB3b expressing soluble methane monooxygenase. Appl Environ Microbiol. 55:2819-26.

81. Olsen, R. H., and J. Hansen. 1976. Evolution and utility of a *Pseudomonas aeruginosa* drug resistance factor. J. Bacteriol. 125:837-844.

82. Olsen, R. H., J. J. Kukor, and B. Kaphammer. 1994. A novel toluene-3-monooxygenase pathway cloned from *Pseudomonas pickettii* PKO1. J Bacteriol. 176:3749-56.

83. Perez-Martin, J., J. Rojo, and V. de Lorenzo. 1994. Promoters responsive to DNA bending: a common theme in prokayotic gene expression. Microbiol. Rev. 58:268-290.

84. Pieper, D. H., K. H. Engesser, and H. J. Knackmuss. 1989. Regulation of catabolic pathways of phenoxyacetic acids and phenols in *Alcaligenes eutrophus* JMP134. Arch. Microbiol. 151:356-371.

85. Pieper, D. H., W. Reineke, K. Engesser, and H. Knackmuss. 1988. Metabolism of 2,4-dichlorophenoxyacatic acid, 4-chloro-2-methylphenoxyacetic acid and 2-methylphenolyacetic acid by *Alcaligenes eutrophus* JMP134. Arch Microbiol. 150:6834-6840.

86. Pikus, J. D., J. M. Studts, C. Achim, K. E. Kauffmann, E. Munck, R. J. Steffan, K. McClay, and B. G. Fox. 1996. Recombinant toluene-4-monooxygenase: catalytic and Mossbauer studies of the purified diiron and Rieske components of a four-protein complex. Biochemistry. 35:9106-19.

87. Powlowski, J., J. Sealy, V. Shingler, and E. Cadieux. 1997. On the role of DmpK, an auxiliary protein associated with multicomponent phenol hydroxylase from *Pseudomonas* sp. strain CF600. J. Biol. Chem. 272:945-951.

88. Powlowski, J., and V. Shingler. 1994. Genetics and biochemistry of phenol degradation by *Pseudomonas* sp. CF600. Biodegradation. 5:219-36.

89. Rajagopal, R. 1986. Conceptual design for a groundwater quality monitoring strategy. Environ. Prof. 8:244-264.

90. Ramos, J. L., A. Stolz, W. Reineke, and K. N. Timmis. 1986. Altered effector specificities in regulators of gene expression: TOL plasmid *xylS* mutants and their use to engineer expansion of the range of aromatics degraded by bacteria. Proc Natl Acad Sci U S A. 83:8467-71.

91. Rasche, M. E., M. R. Hyman, and D. J. Arp. 1991. Factors limiting aliphatic chlorocarbon degradation by *Nitrosomonas europaea*: cometabolic inactivation of ammonia monooxygenase and substrate specificity. Appl. Environ. Microbiol. 57:2956-2994.

92. Reij, M. W., J. Kieboom, B. J. A. de, and S. Hartmans. 1995. Continuous degradation of trichloroethylene by *Xanthobacter* sp. strain Py2 during growth on propene. Appl Environ Microbiol. 61:2936-42.

93. Rieske, J. S., D. H. MacLennan, and R. Coleman. 1964. Isolation and properties of an iron-protein from the (reduced coenzyme Q)-cytochrome C reductase complex of the respiratory chain. Biochem. Biophys. Res. Commun,. 15:338-344.

94. Sanger, F., S. Nicklen, and A. R. Coulson. 1977. DNA sequencing with chain-terminating inhibitors. Proc. Natl. Acad. Sci. USA. 74:5463-5467.

95. Schirmer, F., S. Ehrt, and W. Hillen. 1997. Expression, inducer spectrum, domain structure, and function of MopR, the regulator of phenol degradation in *Acintobacter calcoaceticus* NCBI8250. J. Bacteriol. 179:1329-1336.

96. Shanklin, J., E. Whittle, and B. G. Fox. 1994. Eight histidine residues are catalytically essential in a membrane-associated iron enzyme, stearoyl-CoA desaturase, and are conserved in alkane hydroxylase and xylene monooxygenase. Biochemistry. 33:12787-12794.

97. Shields, M. S., S. O. Montgomery, P. J. Chapman, S. M. Cuskey, and P. H. Prichard. 1989. Novel pathway of toluene catabolism in the trichloroethylene-degrading bacterium G4. Appl. Environ. Microbiol. 55:1624-1629.

98. Shingler, V. 1996. Signal sensing by σ^{54}-dependent regulators: de-repression as a control mechanism. Mol Microbiol. 19:409-416.

99. Shingler, V., M. Bartilson, and T. Moore. 1993. Cloning and nucleotide sequence of the gene encoding the positive regulator (DmpR) of the phenol catabolic pathway encoded by pVI150 and identification of DmpR as a member of the NtrC family of transcriptional activators. J. Bacteriol. 175:1596-1604.

100. Shingler, V., F. C. Franklin, M. Tsuda, D. Holroyd, and M. Bagdasarian. 1989. Molecular analysis of a plasmid-encoded phenol hydroxylase from *Pseudomonas* CF600. J Gen Microbiol. 135:1083-92.

101. Shingler, V., and T. Moore. 1994. Sensing of aromatic compounds by the DmpR transcritional activating of phenol-catabolizing *Pseudomonas* sp. strain CF600. J. Bacteriol. 176:1555-1560.

102. Shingler, V., and H. Pavel. 1995. Direct activation of the ATPase activity of the transcriptional activator DmpR by aromatic compounds. Mol. Microbiol. 17:505-513.

103. Shingler, V., J. Powlowski, and U. Marklund. 1992. Nucleotide sequence and functional analysis of the complete phenol/3,4-dimethylphenol catabolic pathway of *Pseudomonas* sp. strain CF600. J Bacteriol. 174:711-24.

104. Simon, R., U. Priefer, and A. Puhler. 1983. A broad host-range mobilization system for *in vivo* genetic engineering transposon mutagenesis in Gram-negative bacteria. Bio/Technology. 1:784-791.

105. Spain, J. C., and D. T. Gibson. 1988. Oxidation of substituted phenols by *Pseudomonas putida* F1 and *Pseudomonas* sp. strain JS6. Appl Environ Microbiol. 54:1399-404.

106. Spiegle, S. J. 1988. In situ biological treatment of ground water, p. 304-316. *In* O'Brian and Gere (ed.), Hazardous Waste Site Remediation, New York.

107. Stanier, R. Y., N. Palleroni, and M. Doudorff. 1966. The aerobic pseudomonads: a taxonomic study. J Gen Microbiol. 43:159-271.

108. Suzuki, M., T. Hayakawa, J. P. Shaw, M. Rekik, and S. Harayama. 1991. Primary structure of xylene monooxygenase: similarities to and differences from the alkane hydroxylation system. J. Bacteriol. 173:1690-1695.

109. Takeo, M. 1995. Cloning and sequencing of the regulation gene of the phenol degradative genes from *Pseudomonas putida* BH. (DDBJ, EMBL and GenBank accession number D28864).

110. Takeo, M., Y. Maeda, H. Okada, K. Miyama, K. Mori, M. Ike, and M. Fajita. 1995. Molecular cloning and sequencing of the phenol hydroxylase gene from *Pseudomonas putida* BH. J Ferm Bioeng. 79:485-488.

111. Tsien, H. C., G. A. Brusseau, R. S. Hanson, and L. P. Waclett. 1989. Biodegradation of trichloroethylene by *Methylosinus trichosporium* OB3b. Appl Environ Microbiol. 55:3155-61.

112. Vogel, T. M., and P. L. McCarty. 1985. Biotransformation of tetrachloroethylene to trichloroethylene, dichloroethylene, vinyl chloride, and carbon dioxide under methanogenic conditions. Appl Environ Microbiol. 49:1080-3.

113. Wackett, L. P., and D. T. Gibson. 1988. Degradation of trichloroethylene by toluene dioxygenase in whole-cell studies with *Pseudomonas putida* F1. Appl Environ Microbiol. 54:1703-8.

114. Wackett, L. P., and S. R. Householder. 1989. Toxicity of trichloroethylene to *Pseudomonas putida* F1 is mediated by toluene dioxygenase. Appl. Environ. Microbiol. 55:2723-2725.

115. Wang, Y., M. Rawlings, D. T. Gibson, D. Labbe, H. Bergeron, R. Brousseau, and P. C. Lau. 1995. Identification of a membrane protein and a truncated LysR-type regulator associated with the toluene degradation pathway in *Pseudomonas putida* F1. Mol Gen Genet. 246:570-579.

116. Whited, G. M., and D. T. Gibson. 1991. Toluene-4-monooxygenase, a three-component enzyme system that catalyzes the oxidation of toluene to p-cresol in *Pseudomonas mendocina* KR1. J Bacteriol. 173:3010-6.

117. Williams, P. A. 1997. *Xyl*UW, two genes at the start of the upper pathway operon of TOL plasmid pWW0, appear to play no essential part in determining its catabolic phenotype. Microbiol. 143:101-107.

118. Yen, K. M., and M. R. Karl. 1992. Identification of a new gene, *tmo*F, in the *Pseudomonas mendocina* KR1 gene cluster encoding toluene-4-monooxygenase. J Bacteriol. 174:7253-61.

119. Yen, K. M., M. R. Karl, L. M. Blatt, M. J. Simon, R. B. Winter, P. R. Fausset, H. S. Lu, A. A. Harcourt, and K. K. Chen. 1991. Cloning and characterization of a *Pseudomonas mendocina* KR1 gene cluster encoding toluene-4-monooxygenase. J Bacteriol. 173:5315-27.

120. Zylstra, G. J., L. P. Wackett, and D. T. Gibson. 1989. Trichloroethylene degradation by *Escherichia coli* containing the cloned *Pseudomonas putida* F1 toluene dioxygenase genes. Appl Environ Microbiol. 55:3162-6.

VITA

Patricia J. Ayoubi

Candidate for the Degree of

Doctor of Philosophy

Thesis: CHARACTERIZATION OF TRICHLOROETHYLENE DEGRADATION BY RECOMBINANT PHENOL HYDROXYLASE IN AN *ALCALIGENES EUTROPHUS* JMP134 DERIVATIVE

Major Field: Microbiology, Cell and Molecular Biology

Biographical:

Personal Data: Born in Spokane, Washington, October 1, 1964, the daughter of James C. Cockrell.

Education: Graduated from Waukomis High School, Waukomis, Oklahoma in May 1982; received Bachelor of Science degree in Medical Technology and a Master of Science degree in Microbiology from Oklahoma State University in July, 1986 and December, 1990, respectively. Completed the requirements for the Doctor of Philosophy degree at Oklahoma State University in July, 1997.

Experience: Medical Technologist, Dodge City Medical Center, Dodge City, Kansas, August 1987 to August 1988. Teaching and Research Assistant, Department of Microbiology and Molecular Genetics, Oklahoma State University, Stillwater, Oklahoma, August 1988 to December 1996.

Fellowships: Edward Grula Distinguished Graduate Fellowship, 1991-1992.

Membership: American Society for Microbiology, American Association for the Advancement of Science, Society for Industrial Microbiology, American Society or Clinical Pathology.